



<https://theses.gla.ac.uk/>

Theses Digitisation:

<https://www.gla.ac.uk/myglasgow/research/enlighten/theses/digitisation/>

This is a digitised version of the original print thesis.

Copyright and moral rights for this work are retained by the author

A copy can be downloaded for personal non-commercial research or study, without prior permission or charge

This work cannot be reproduced or quoted extensively from without first obtaining permission in writing from the author

The content must not be changed in any way or sold commercially in any format or medium without the formal permission of the author

When referring to this work, full bibliographic details including the author, title, awarding institution and date of the thesis must be given

Enlighten: Theses

<https://theses.gla.ac.uk/>  
[research-enlighten@glasgow.ac.uk](mailto:research-enlighten@glasgow.ac.uk)

THE DYNAMICS  
OF  
THE ENCLOSED LAMINAR DIFFUSION FLAME

by

LESTER D. SAVAGE, Jr., B.S., M.S.M.E.

University of Minnesota, U.S.A.

Thesis submitted for the Degree of Ph.D.  
to the University of Glasgow.

May, 1962

ProQuest Number: 10656280

All rights reserved

INFORMATION TO ALL USERS

The quality of this reproduction is dependent upon the quality of the copy submitted.

In the unlikely event that the author did not send a complete manuscript and there are missing pages, these will be noted. Also, if material had to be removed, a note will indicate the deletion.



ProQuest 10656280

Published by ProQuest LLC (2017). Copyright of the Dissertation is held by the Author.

All rights reserved.

This work is protected against unauthorized copying under Title 17, United States Code  
Microform Edition © ProQuest LLC.

ProQuest LLC.  
789 East Eisenhower Parkway  
P.O. Box 1346  
Ann Arbor, MI 48106 – 1346

## ACKNOWLEDGEMENTS

The author is grateful to Professor James Small, Director of the Engineering Laboratories, for encouragement and support of this study; to Dr. B.E.L. Deckker for ready advice and discussion; to the Metropolitan-Vickers Electrical Company for financial support; to the staff of the computing centre of the University for assistance in using the computer; and to the British Hydrocarbon Chemical Company, Ltd. for providing the methane and ethane used in this study.

CONTENTS

		<u>Page</u>
TITLE		
ACKNOWLEDGEMENTS		
CONTENTS		
CHAPTER 1	Introduction	1
CHAPTER 2	Preliminary Experimental Studies	13
CHAPTER 3	Burner Design and Test	20
CHAPTER 4	Momentum Exchange Studies	30
CHAPTER 5	Instrumentation and Design of Experiments	41
CHAPTER 6	Flame Maps	50
CHAPTER 7	Floating Flames	64
CHAPTER 8	Dynamic Parameters of Flame Height	73
CHAPTER 9	Multiple Species Interdiffusion	92
CHAPTER 10	Conclusions	103
BIBLIOGRAPHY		107
APPENDIX I		108
APPENDIX II		Printer Paper

CHAPTER 1

INTRODUCTION

In the last half century research on the problem of combustion has split into many branches. Among these the laboratory flames supported on streams of flowing gases have been divided into those where the fuel and oxidant are mixed prior to the reaction and those where the mixing and the reaction occur simultaneously.

The term 'diffusion' flame was firmly established for this latter type of flame in 1928 when Burke and Schumann<sup>(1)\*</sup> demonstrated that a particular concentration contour from a solution of the Ficks law diffusion equation for a simplified enclosed flow configuration displayed qualitative agreement with experimental flame profiles in an enclosed flow system.

Observations by later investigators of open diffusion flames prompted the assumption that both the open and the enclosed diffusion flames would have the same quantitative description. Barr<sup>(2)</sup> questioned this assumption, and Goudie<sup>(3)</sup>, in an unpublished work, demonstrated that the behaviour of enclosed diffusion flames was different from the behaviour of open diffusion flames as reported in the literature.

The present study is limited to the axially symmetrical case since it is possible experimentally to obtain axial symmetry which is comparable to a two dimensional analysis without qualification. The

\*Superscript numbers refer to the appended bibliography.

enclosed laminar diffusion system studied is, thus, an axially symmetrical flow system bounded by a tube of constant radius within which the fuel and oxidant (for convenience in this study the oxidant is air) are initially separated, one being concentrically within the other. The condition of laminarity specifies that the random motion in the gas streams is of a molecular scale so that mixing only takes place by means of molecular diffusion.

Diffusion flames, whether open or enclosed, always occur in a region where the flow is undergoing a transition from some initial velocity distribution to a stable, or fully developed, velocity distribution. In the laminar enclosed flow system the final state is the Hagen-Poiseuille velocity distribution, whereas in the open diffusion flame, whether laminar or turbulent, the ultimate state is the zero velocity of the quiescent surrounding atmosphere.

The transition in the bounded flow system is dominated by the conservation of mass, which requires that the mass flux through any plane normal to the axis of flow must be equal to the mass flux through the plane normal to the axis at the origin of the transition. The momentum flux varies throughout the transition region in order to satisfy this condition.

In the case of open jet mixing, however, the mass flux in the direction of the flow varies throughout the transition region, and this problem is generally treated by assuming that the momentum flux is constant throughout this region.

The analysis presented by Burke and Schumann provides a starting point for further theories of enclosed laminar diffusion flames, which, in order more accurately to represent real flames, introduce complications into those assumptions employed by Burke and Schumann. It is pertinent at this stage, therefore, to state the assumptions employed by Burke and Schumann and to present a criticism of these in the light of more recent developments.

1. The flow velocity, in the direction of  $z$ , is constant over all  $z$  and all  $r$ .
2. The coefficient of diffusion is constant in both the  $r$  and  $z$  directions.
3. The diffusion process is between two gases.
4. The reaction surface is described by the surface of stoichiometric concentration of the two gases.
5. The processes are radial, only.
6. The rate of chemical reaction is much higher than the rate at which the diffusion process provides material to this reaction.

The major part of the discussion in the literature is directed to the assumption of a constant coefficient of diffusion. Hawthorne and Hottel<sup>(4)</sup> and Wohl, Gazley and Kapp<sup>(5)</sup> point out that, as fuel is consumed, heat is released to the fixed mass flow of the bounded system raising the average temperature of the total mass flow. The coefficient of diffusion is temperature dependent, so that the increase of the average

temperature will result in an increase in the average coefficient of diffusion in the direction of flow. This argument was used by these authors to explain the non-linear relationship of flame height to fuel flow which was observed for open diffusion flames and which contradicted the linear relationship predicted by their theories. The theory of Hawthorne and Hottel was developed from jet mixing considerations, and the theory of Wohl, Gazley and Kapp was developed by considering an unbounded system in which the constant velocity of Burke and Schumann's approach extended to infinity in the radial direction.

Gaydon and Wolfhard<sup>(6)</sup> point out the following interesting anomaly concerning the assumption of a constant coefficient of diffusion. The reaction occurs at a unique radius for each axial position and the temperature decreases as the radius is traversed in either direction from the point of reaction, hence the temperature dependence of the coefficient of diffusion will introduce a gradient of the coefficient in the radial direction.

This criticism may be extended as follows: at any axial position the radial temperature profile will be approximately the same as the radial concentration profile of the products of the reaction; and at those radii where there are no products from the reaction, the concentration gradients of the fuel, or the oxidant, will be zero, so that the value of the coefficient of diffusion in these regions will be of no significance in the descriptive equations. If, now, an average coefficient of diffusion is determined at each axial position only for those radii where it has significance, then, the average for the various axial positions

will be essentially constant until the products from the reaction reach the bounding wall. Thus, particularly in the case of the open diffusion flame in which there is always a region where the products of the reaction have not penetrated, the effect of the radial thermal gradients lends credence to the assumption of a constant coefficient of diffusion.

A more extensive discussion of the implications of a radially variable coefficient of diffusion is presented in a later section of this thesis.

The assumption of a constant velocity, although rarely discussed in the literature, is as unrealistic as the assumption of a radially constant coefficient of diffusion. In real flow systems, increasing the temperature of the gases decreases their density and increases their flow velocity, so that any existing thermal gradient will introduce, in addition to the radial gradient of the coefficient of diffusion, a radial velocity gradient. There is an additional effect introduced by the viscous forces in the fluid developing radial velocity gradients, the velocity at the solid boundaries, of necessity, being zero. Even when nozzles are used experimentally to provide an approximately constant velocity across the cross section at the initial plane of the transition, there is a thin film adjacent to the wall of the nozzle in which the fluid assumes all velocities between this constant velocity and zero. The use of the term 'boundary layer' to describe this region has been carefully avoided as Shapiro<sup>(7)</sup> has shown recently that the mathematical approach which is implied by this term is not necessarily

valid for bounded flow systems. The use of a nozzle to obtain velocity profiles that are nearly constant requires more stringent precautions than is often assumed. For example in the literature on combustion, it is not at all uncommon to find nozzles being used with as much as ten throat diameters of straight section following the throat of the nozzle. If these are used at a Reynolds number of 1000 or less there is no portion of the velocity profile which is constant at the exit of the straight portion. If there is only one throat diameter of straight section following the throat, the velocity profile will be continually changing at the exit for Reynolds numbers less than 100. Thus, if a nozzle is used for the purpose of obtaining an essentially constant velocity profile, the nozzle must be terminated at the throat.

Barr<sup>(2)</sup> has suggested that the difference between the actual experimental velocity profiles and the idealized velocity profile is a major factor in the disparity between experimental diffusion flames and Burke and Schumann's theory.

The assumption of a two gas system has not been seriously questioned and can be justified on the grounds that Ficks law is written in terms of the concentration in a binary system; on the oxidant side of the flame boundary the two gases can be oxidant and products, the products being at the same concentration the fuel would have assumed had it been able to pass through the flame boundary. The same argument applies to the fuel side of the flame boundary.

The assumption of the reaction surface being defined by the surface of stoichiometric concentration of the two gases is intimately

connected to the assumption and the implications of a two gas system and, therefore cannot be criticised separately.

The assumption of the processes being only radial has been accepted generally, although it has been questioned by Barr on the basis of experiments which Burke and Schumann originally suggested would be outwith the scope of the assumption. The writer has tested this assumption and has found a slight departure from this condition for all real enclosed flames.

From the form of their solution Burke and Schumann selected as the critical test of their theory the relationship of the flame height as a function of the fuel flow. Their theory predicted that this relationship should be linear. The fact that this relationship is approximately satisfied experimentally has led workers in this field to accept the behaviour of these flames as being described by Ficks Law. However, in a system where the molecular transport effects of specie diffusion, viscosity and thermal diffusion occur, the choice of any one of these effects as being descriptive of the entire process appears to be unjustified.

In any bounded, constant area, homogeneous, laminar system undergoing transition from a given initial velocity distribution to the Hagen-Poiseuille velocity distribution, the relationship of the velocity and pressure distributions over any plane along the transition to the initial distributions of these variables is defined by the value of  $z/R(Re)$ . In this notation ( $z$ ) is the distance along the axis of flow

*Japan?*

*$R_0(r)$*

from the initial distribution to the plane of concern,  $(R)$  is the radius which will generate the constant area, and  $(Re)$  is the Reynolds number based on the mean fluid properties, the mean velocity and the length  $2R$  at the initial plane of the system.

The Reynolds number still forms the group  $z/R(Re)$  with the distance along the transition in the equations of conservation of mass, momentum and energy as the conditions of constant area and homogeneity are relaxed provided the properties and dimensions at an intermediate section are expressed relative to those at the initial section.

Relaxation of homogeneity, however, is feasible only if it is assumed that molecular interchange along a stream tube has a second order effect upon the distributions, which is essentially the same as assuming that the processes are only radial.

The viscosity of a fluid is the dynamic manifestation of the self diffusion of that fluid, the constant of proportionality between the coefficient of self diffusion and the coefficient of viscosity as obtained from the Kinetic Theory of Gases, and multiple correlation for a few typical gases, is 1.4.<sup>(8)</sup> Thus in the homogeneous system the value of  $z/R(Re)$  will define the distribution of a group of initially labeled molecules as well as velocity and pressure distributions. Similarly, for the case of a non-homogeneous laminar system the specie, velocity, and pressure distributions will be defined by the value of  $z/R(Re)$ , the geometry of the system and the initial velocity and specie distributions.

The localized energy release from the combustion reaction does not alter the form of the conservation of energy equation, but introduces the local temperature into the problem. (Rigorously, the local temperature changes in the constant area, homogeneous, non-energy releasing system due to the viscous friction losses, but the temperature changes are so small that they do not affect the fluid properties). The heat transfer equations that are thus introduced are of the same form as the diffusion equation, and the conservation of momentum equations. The local temperature at the reaction will be defined by the value of  $z/R(Re)$ , since this term defines the local distribution of reagents and diluents, thus, when heat transfer in the direction of flow may be ignored, the temperature distribution at any position along the system is defined by the value of  $z/R(Re)$ . Therefore, all of the property distributions will be defined by the value of  $z/R(Re)$ .

It follows, that a theoretical solution of any or all of the controlling equations for a bounded system will have axial lengths occurring in groups which will form the variable  $z/R(Re)$ , unless the treatment is so complete as to include axial molecular transport effects.

This set of arguments does not apply to the unbounded (open jet) flow system, however, as in these systems the Reynolds number must be a function of the distance from the origin to the plane of concern in order to be representative of the phenomena involved.

Typically, flame height is described as a particular distribution state, namely, either that point where the fuel concentration at the centreline is zero or that point where the oxygen concentration at the wall is zero. Thus in any series of experiments where the initial

conditions are dynamically and speciewise similar the flame height will be defined by a particular value of  $z/R(\text{Re})$ . When the system is limited to a particular burner the flame height will be proportional to the Reynolds number. To maintain the condition of dynamic similarity the diameter ratio of the two tubes, the ratio of air flow to fuel flow and the shape of the velocity profiles of both the air stream and the fuel stream must be held constant. In any set of dynamically similar experiments, the fuel stream Reynolds number at the entrance to the system will have, therefore, a fixed relationship to the air stream Reynolds number and a fixed relationship to the mean entering Reynolds number of the combined flows.

Any experimental disagreement with the  $z/R(\text{Re})$  relationship for a bounded system must of necessity arise from one of two sources:

1. The results being compared are not from dynamically similar experiments.
2. Axial molecular transport phenomena are significant in what are otherwise dynamically similar experiments.

Therefore, in order to verify that a set of equations, which are solved for some linear coefficient of the relative flame height Reynolds number relationship, are descriptive of the phenomena within the flame there must be quantitative agreement between this coefficient and the results from experiments where the assumption of purely radial processes are approximately valid. The solution by Burke and Schumann does not display this quantitative agreement, the flame heights predicted being five to twenty times the experimentally observed flame heights. To

surmount this difficulty, Burke and Schumann proposed an 'apparent coefficient of diffusion' as a name for the experimentally determined coefficient of this relationship. Since this relationship could as well be deduced from any of the equations of the transition it could, according to the equation employed, be called the apparent coefficient of energy release or the apparent coefficient of momentum exchange with, consequently, quite different interferences as to the mechanism of the processes involved.

Since a number of interrelated mechanisms are involved, and the complete set of descriptive equations is intractable with present day mathematical techniques, the investigator is faced with the problem of experimentally separating the variables of the process, and determining, if possible, the influence of each variable on the behaviour of the system.

As has been already pointed out, the fluid dynamical variables of the flame transition region are: the fuel Reynolds number, the diameter ratio of the two tubes, the ratio of the mass flows in the two streams, and the relative velocity profiles of the two streams. This last item, which includes the actual shape of the velocity profiles as well as the magnitudes of the velocities, is not amenable to symbolic representation. However, when the flows involved are axially symmetrical and fully developed this condition is represented by the ratio of the mass flows of the two streams and the ratio of the densities of the two gases.

These dynamic variables are complex combinations of the directly

controlled variables which are: the fuel supply tube diameter, the outer tube diameter, the air flow, the fuel flow, and the fuel employed. The change of a single directly controlled variable will affect more than one dynamic variable as follows:

Changing the air flow while holding all other directly controlled variables constant will alter the ratio of mass flows of the two gases and the relative velocity profiles.

Changing the diameter of the outer tube while holding all other directly controlled variables constant will alter the diameter ratio and the relative velocity profiles.

Changing the diameter of the fuel supply tube while holding all other directly controlled variables constant will alter the diameter ratio, the relative velocities and the fuel Reynolds number.

Changing the fuel flow while holding all other directly controlled variables constant will alter the fuel Reynolds Number, the air-fuel ratio and the relative velocities.

Changing the fuel while holding the fuel mass flow and all other directly controlled variables constant will alter the fuel Reynolds number, the relative velocities and the chemistry of the flame.

In the subsequent experimental studies it has been attempted to determine the influence that each dynamic variable has upon the flame.

CHAPTER 2

PRELIMINARY EXPERIMENTAL STUDIES

There are two transition regions to be considered in the geometry of the enclosed laminar diffusion flame, namely, that transition region in which the flame exists; and the transition regions between the points of introduction of the fuel and air and the terminal plane of the inner tube. The latter will be referred to as the approach transition region in order to avoid confusion.

Since the dimensions of the approach transition region are fixed in any particular burner, there are only two possible velocity profiles for the initial plane of the flame transition region which will satisfy the condition of dynamic similarity at all flows. One possibility is the constant velocity profile, which can only be approximated by using two concentric nozzles whose throats are in the same plane. The design of such an approach flow system is extremely challenging and even when this is satisfied, the velocity profile is still only approximate. In such a system, if the design velocity profile can be attained at the lowest flows anticipated, then it will be also attained for all larger flows. The second possible system of velocity profiles is the Hagen-Poiseuille velocity profile in the inner tube and in the annulus. This set of profiles can nominally be attained by making the approach transition lengths sufficiently long so that the profiles are attained for the highest flows anticipated, whence they also will be attained for all lower flows.

The set of Hagen-Poiseuille velocity profiles is an obvious choice from the standpoint of the possibility of an exact analytical

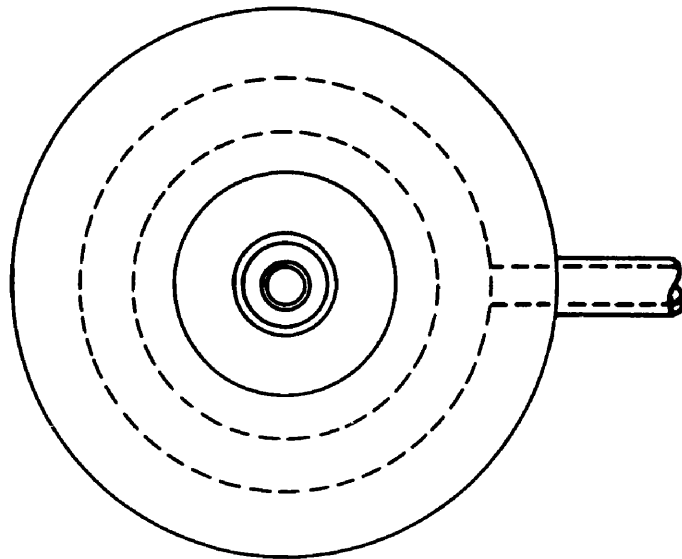
description and ease of design.

It was intended that the initial experiments should be comparable with the experimental results obtained by Barr and the analysis of Burke and Schumann. The experimental results from Barr, upon reduction, indicated that the observations would be complicated by soot issuing from the tip of the flame at a nearly constant air-fuel ratio of 25, so that an air-fuel ratio of 100 was selected as an ideal value for experimental studies and the corresponding diameter ratio of 10 (the ratio of the outer bounding tube diameter to the inner fuel supply tube diameter) was selected for evaluating the solution by Burke and Schumann.

It was possible to use the same fuel that had been used by Barr in his studies. This fuel was nominally butane, but was in fact 30% isobutane, 20% normal butane, 47% butenes, and the remainder lower order hydrocarbons. The dynamic properties of the fuel were assumed to be the same as those of isobutane. Later determinations of these dynamic properties using the dynamic properties of 96% pure ethane as a reference indicated that this assumption was valid.

At the time of these experiments a burner of the design illustrated in Figure 1 was available. The design of this burner is such that the velocity profile of the fuel at the initial plane of the flame transition is the Hagen-Poiseuille profile, but only at the very lowest flows is this the case for the air flow in the annulus.

Two sets of experiments were conducted in the burner of this design. In one set a 0.83 cm. bore fuel supply tube was mounted within a 2.1 cm. bore pyrex tube with the flow system shown. The second set was conducted



TOP VIEW SHOWING AIR  
DISTRIBUTION ANNULUS

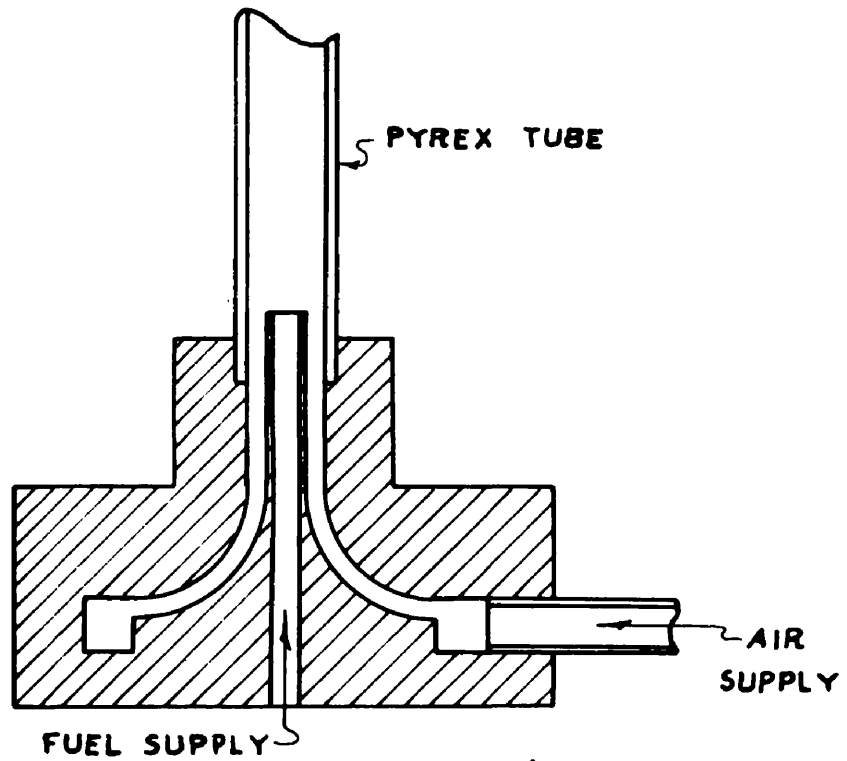


FIGURE 1

with a 0.28 cm. bore fuel supply tube mounted within the 2.1 cm. bore pyrex tube.

In order to approximate the Hagen-Poiseuille velocity profile in the second set of experiments a group of small concentric tubes of 0.01 cm. wall thickness was inserted in the air supply annulus, the length and spacing of the tubes being so designed that the flow in the annulus between any two tubes would become fully developed within the length of the annulus. The lengths of the tubes were increased from the centre of the air supply annulus towards the two walls in such a fashion that the pressure drop for a given flow in the outer annuli was four times the pressure drop for that same flow in the centremost annulus. This arrangement forced a major portion of the flow to pass through the centremost portion of the air supply annulus thus providing an approximately fully developed velocity profile. The very close agreement between the results obtained with this configuration and those obtained by Barr, who used concentric tubes one meter long to assure the development of the velocity profiles, was considered to be verification of the attainment of the desired air flow velocity profile.

A copy of the paper which currently is being published in COMBUSTION AND FLAME presenting the results of these experiments is included as Appendix II.

The main results of these experiments are:

The height of all possible stable reclosed (i.e. those flames terminating at the centreline) flames for dynamically similar flows in a given burner can be defined by determining the two parametric curves of flame height as a function of fuel Reynolds number at a given air-fuel

ratio, and flame height as a function of air-fuel ratio at a given fuel Reynolds number.

There are first order departures from the conditions of a purely radial phenomenon in real laminar diffusion flames.

The extensive experimental results of Barr can be represented by a single complex equation, expressing the flame height in terms of the Reynolds number, the diameter ratio and the air-fuel ratio. The principle term of this equation containing only fluid dynamic variables is the linear coefficient of the Reynolds number, which is representative of the whole of the radial molecular transport processes. This single equation points out the artificial nature of the previous use of the 'device' of an apparent coefficient of diffusion expressed as a function of the directly controlled variables of the system.

In reporting these results very little space was given to the discussion of the results from the 0.83 cm. burner since they were obtained without the use of the concentric tubes for shaping the air flow velocity profile which, as a consequence, was not even approximately fully developed. The flames in these experiments were consistently longer than those obtained by Barr for the same diameters of burner and outer tube.

The most striking feature of these experiments, however, was not the difference in the flame lengths, but the manner in which the flame 'lifted' from the burner; the very low fuel Reynolds number as which this occurred; and the sharp reduction in the flame height - fuel Reynolds number relationship for the incompletely anchored flames. In

the process of 'lifting' a small portion of the anchoring ring of the flame was raised about half a burner diameter above the remainder, very much like lifting a fabric skirt by gripping a single point on the hem. This 'lifting' always occurred at the same point on the circumference of the burner, and a review of the results obtained from the 0.28 cm. fuel supply tube indicated that the less spectacular 'lifting' of these flames occurred at the same point relative to the air supply system.

Upon investigation of the air supply system, attention was drawn to the introduction of the air at a single point to a constant area distribution annulus, which is known in fluid dynamics to cause a distortion to the distribution leaving the annulus, a disproportionate part of the mass flow being delivered from that portion of the annulus directly opposite the point of introduction. This high flow was coincident with the point of 'lifting'.

An interesting feature of the fully anchored flames studied with these two burners was that they did not show any signs of axial asymmetry except at the 'lifting' of the anchoring ring and also near the point where soot issued from the tip of the flame even though calculations indicated that there was at least a 20% variation in the velocity of the air stream around the annulus.

The excellent agreement between the results from the 0.28 cm. diameter burner and the results obtained by Barr for the same diametral dimensions, coupled with the known imperfections of the flow system for the 0.28 cm. diameter burner, necessitated an investigation into the dynamic conditions of the flows used by Barr. In some of the experiments

presented in his map of possible flames in an enclosed system (reproduced in Figure 14) the Reynolds number in the air supply annulus exceeded 3500 although a Reynolds number of 2300 is nominally associated with a change in the mechanisms of random transport in the flow stream from laminar processes to turbulent processes. For the same air flow, the Reynolds number just above the tip of the fuel supply tube (where the only constraint on the system is the outer tube) is in excess of 9000. Thus, subject to further investigation, there was no assurance that the random processes of the flame transition were still in the laminar domain.

The existence of both uncontrolled variables and uncertainties as to the dynamic conditions was considered to be unsuitable for the study of the effects of dynamic variables and prompted the need,

- (a) to design a flow system in which these uncontrolled variables would be eliminated, or at least be reduced in magnitude, and
- (b) to verify that equipment constructed to this design satisfied the design objectives.

CHAPTER 3

BURNER DESIGN AND TEST

On the basis of the preliminary experiments and taking into account the scope of the dynamic variables studied by Barr the following requirements were set down for the design of the burner.

The flow in the air supply annulus must be laminar, fully developed, and axially symmetrical for all Reynolds numbers less than 5,000. The flow in the fuel supply tube must conform to these conditions for all Reynolds numbers less than 1,000. Further, several outer tubes and fuel supply tubes were to be provided so that they could be paired together to provide either a range of diameter ratios at a given scale or a constant diameter ratio at different scales.

The burner design originally used by Barr was discarded for two reasons. First, the length required to attain full development at large flows in the proposed scale would have made it necessary to obtain straight runs of unjoined tubing 16 meters long and to provide vertical space for such a burner. Secondly, Barr was faced with the problem of keeping the fuel supply tube concentric within the outer tube which formed the annulus. To accomplish this he placed a 'spider' consisting of several radial spacers, made to an aerodynamic shape, between the two tubes at some convenient point along the tube. This 'spider' must cause several low velocity nodes in the air flow velocity profile around the annulus, consequently introducing axial asymmetry.

Several investigators have found experimentally that laminar flow in tubes can be attained for Reynolds numbers in excess of 100,000

while turbulent flow in tubes can be maintained for Reynolds numbers less than 1500. These results for laminar flow have been explained on the principle that if the magnitude of the random disturbances in the flow approaching a tube are sufficiently small for a given Reynolds number in the tube, then the fully developed viscous velocity profile can be established. This profile will then be maintained for any additional length of the tube.

A corollary to this principle was set forth as a hypothesis for the design of the air supply annulus, thus:

If all the random variations in a flow stream can be removed by developing a viscous velocity profile in a region of low Reynolds number, the geometry of the system can be altered, within limits, in such a manner that the Reynolds number is increased without destroying the viscous profile or without introducing random disturbances.

If this hypothesis is valid it should be possible to pass the flow from a very narrow annulus of large mean diameter where the Reynolds numbers are low, through a conical annulus, into a wide straight annulus of small mean diameter, thereby increasing the Reynolds number many times while the laminarity of the flow is maintained.

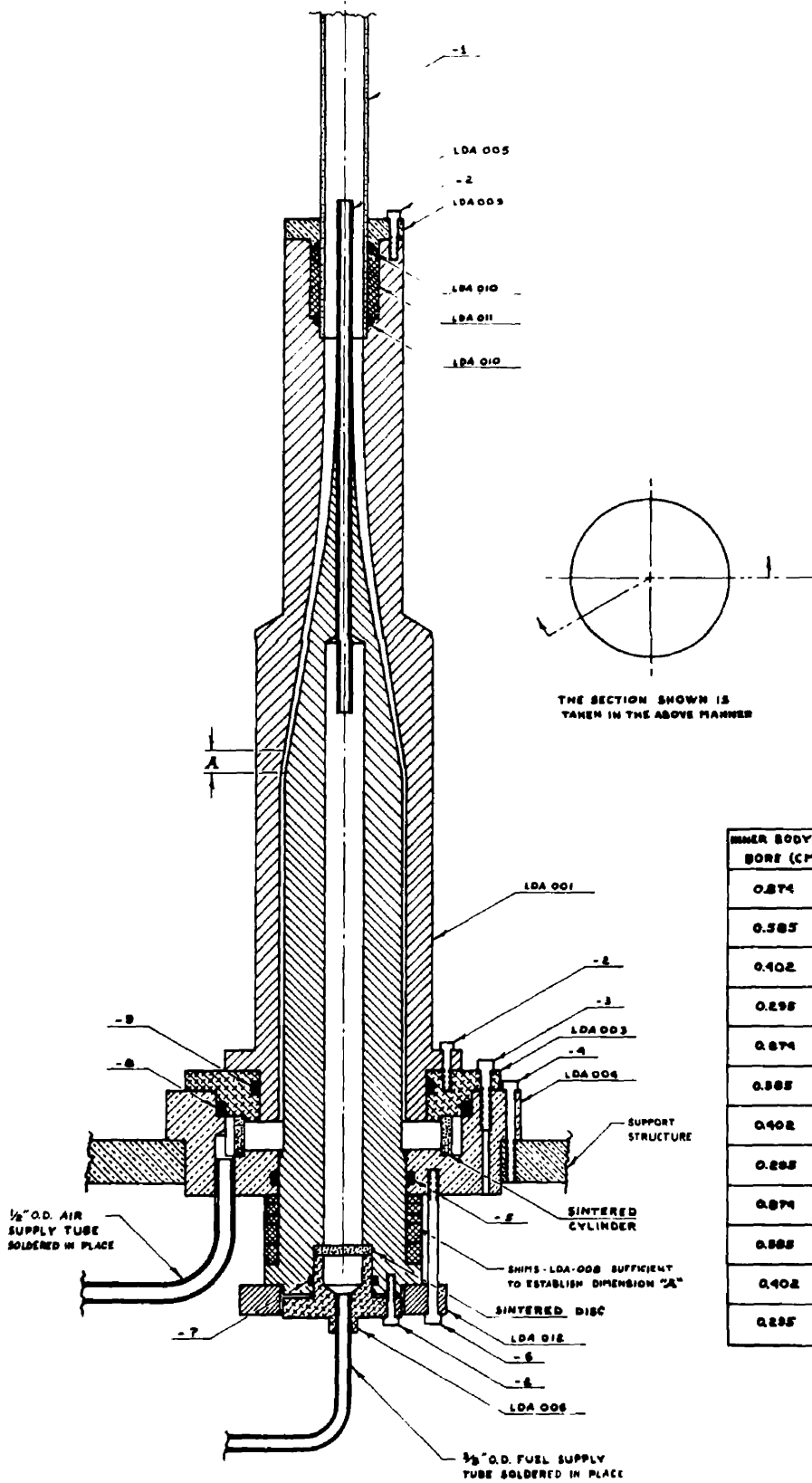
Two restrictions were set down as probably limits to the manner in which the flow path could be altered with the maintenance of the laminar condition. First, the cross sectional area along the path of flow was to be held approximately constant. The condition of constant

area could not be exactly satisfied due to the difficulty of manufacturing the complex contours demanded by this condition, and also the need to have a contour which could be used interchangeably with various pairs of tubes. The purpose of this condition was to hold the magnitude of the velocity vector constant at any particular fraction of the distance across the annulus. Secondly, the turning angle of the flow was to be held within the limits of separation for divergent flow.

In the completed design as shown in Figure 2, sintered elements were placed in the entrances to the approach transition regions in order to provide uniform velocity distributions with a minimum of random disturbances. In the original design it was considered acceptable to introduce the air at a single point into a constant cross section annulus surrounding the sintered cylinder, since the large pressure drop through the sintered cylinder was expected to equalize any tendency towards asymmetry in the flows from the annulus. It was further assumed that any axial asymmetry which might be present after the sintered cylinder would be redistributed during the restrictive development in the narrow approach-transition region.

A total pressure probe was designed at the same time with two directions of micrometer adjustment in the plane of Figure 2. This probe was to be used with an Ascott-Casella micromanometer to investigate the actual velocity distributions obtained with this design.

While this equipment was being constructed, an investigation into the fluid dynamic equations applicable to the flame transition region was undertaken. A numerical method for the solution of these equations was devised for the special condition of no radial pressure gradients. Originally it was the intention to compare the results of the calculations



INNER BODY BORE (CM)	OUTER BODY BORE (CM)	DIMENSION "A"
0.874	2.400	0.373"
0.585	2.400	0.420"
0.402	2.400	0.437"
0.298	2.400	0.448"
0.874	1.600	0.144"
0.585	1.600	0.196"
0.402	1.600	0.208"
0.298	1.600	0.215"
0.874	3.600	0.873"
0.585	3.600	0.921"
0.402	3.600	0.939"
0.298	3.600	0.943"

FIGURE 2

by this method with published results, if any, for the 'simple' case of transition from an initial constant velocity profile to the Hagen-Poiseuille velocity profile for a constant density fluid flowing in a tube of constant area. However, an investigation into the literature disclosed that at the present there is no analytic solution for this 'simple' case. The numerical method was followed, therefore, for this 'simple' case to a point where comparison of the computer results with published experimental measurements of transition variables for this case indicated that the method was successful. At this point it was found that the time required to complete this 'simple' case with the computer available would have been prohibitive and, further, the initial experimental results from the new burner indicated that the assumption of their being no radial pressure gradients was not applicable to the flame transition region. Details of the numerical method are presented in Appendix I. Another computer has now been offered in the United States for the completion of this investigation of the transition from a uniform initial velocity.

Upon the completion of the experimental equipment a burner was assembled with a fuel supply tube of 0.874 cm. bore and an outer constraining tube of 2.400 cm. bore. The Pyrex tube used as a constraint was a precision bore tube. The tube used for the purposes of probing the velocity field extended 6.5 cm. above the tip of the fuel supply tube. Air was metered to both the air supply annulus and the fuel supply tube. The air flow of 1350 ml/sec. delivered to the annulus was the maximum the equipment at that time would permit. Later alterations to the flow

metering system and use of the pressure drop characteristics of the sintered cylinder and the development annulus permitted increasing this maximum to 5,000 ml/sec.

The first problem encountered in the experiments was the response characteristics of the total pressure measuring system. Details of the probe are shown in Figure 3. The internal volume of the micromanometer and the connecting tubing was about 150 ml. which, coupled with the small bore at the tip of the probe, resulted in a time constant for the system of about 20 minutes, or a settling time for a single reading of about two hours. To overcome this problem a curve of the settling characteristics of the system was constructed, giving the interval between the observed pressure and the final pressure as a function of the pressure change over a period of ten minutes. This curve was determined experimentally and it was found that the settling characteristics were the same when the pressure in the enclosed volume was greater or less than the pressure at the tip of the probe.

Total pressures were measured along three different diameters equally spaced about the annulus 0.15 cm. below the tip of the fuel supply tube. A uniformly varying maximum velocity was observed around the annulus, the difference between the minimum and maximum of the velocities being about 15% of the maximum velocity. It was established that this variation was not being introduced by the probe carriage by reversing the probe system. The minimum and maximum points in the velocity distribution occurred respectively directly above and directly

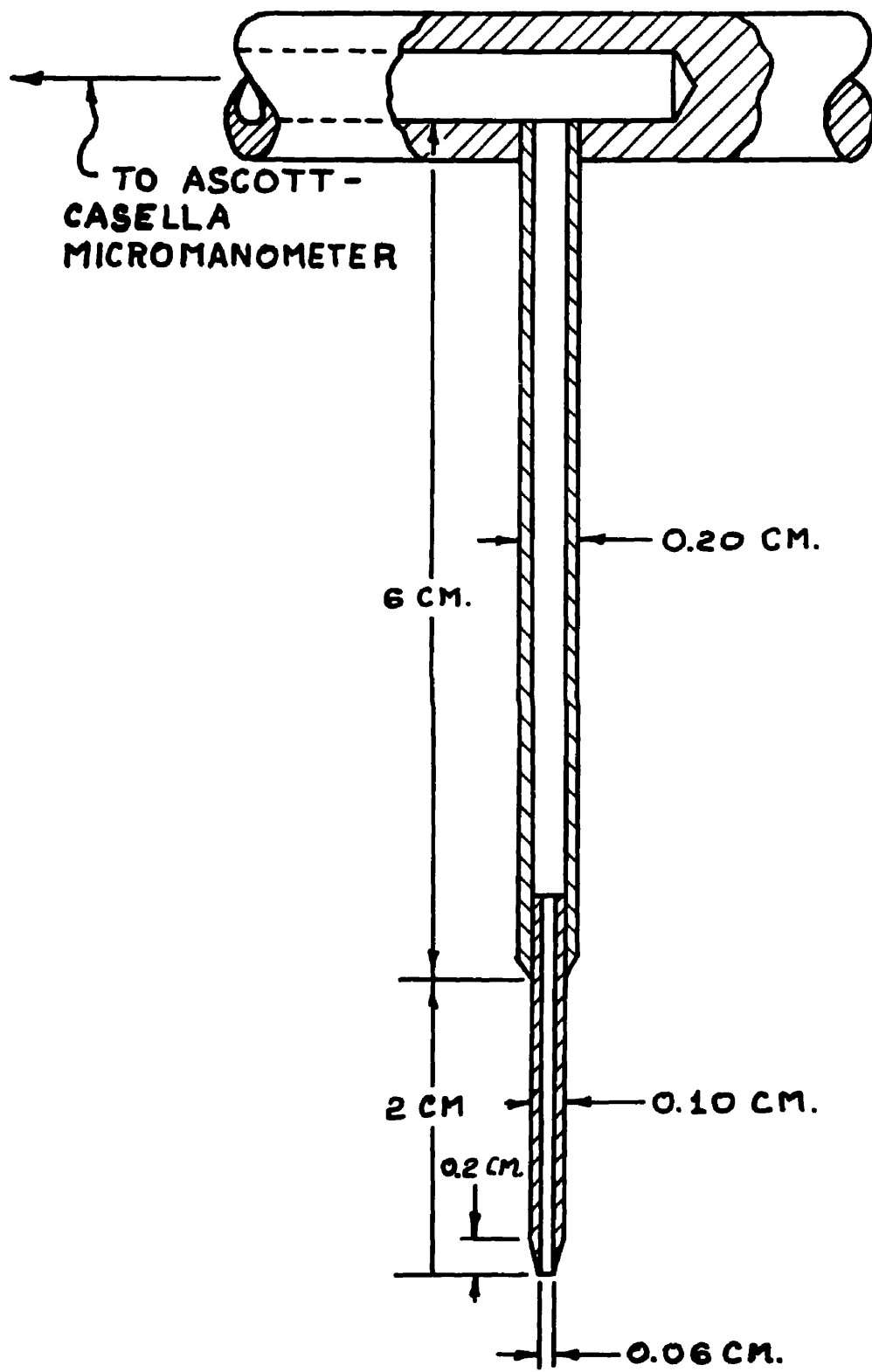


FIGURE 3

opposite the point of introduction of the air into the annulus surrounding the sintered cylinder, which is the position they would assume if they were due to the point-introduction of the air.

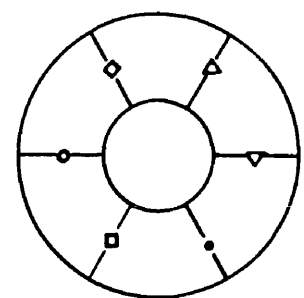
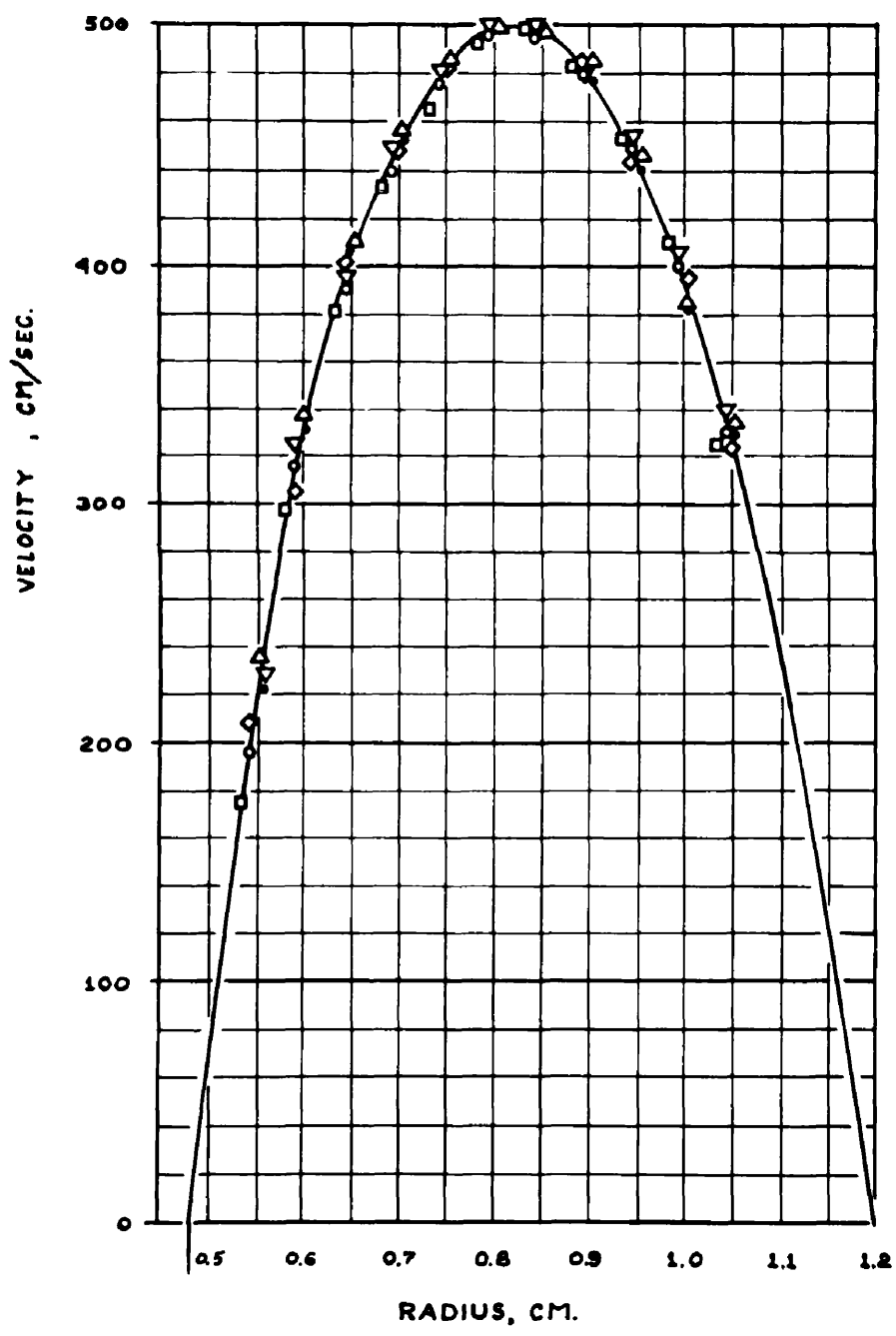
This asymmetry was reduced to approximately 6% by changing the form of the air distribution annulus outside the sintered cylinder so that the cross sectional area of flow was continually reduced as the fluid progressed around the annulus from the point of introduction of the air. This reduction in the asymmetry of the velocity profiles indicates that the single point introduction of the air into a constant area distribution annulus was a major factor in the asymmetrical distribution. This effect also indicates that the circumferential pressure gradients in the development annulus are not sufficiently large to redistribute the mass flow in the annulus and that the pressure drop through the sintered cylinder is less than the pressure drop for the distribution of the air in the constant area annulus outside the sintered cylinder.

The remaining asymmetry of the velocity distribution in the annulus was traced to the machined surfaces of the mounting structure for the two tubes being slightly out of parallel, which resulted in the tip of the inner tube being 0.02 cm. eccentric within the outer tube even though the base of the inner tube was concentric within the outer tube to 0.0005 cm. The effect of this very slight eccentricity points out the extreme difficulty of satisfying the analytical condition of axial symmetry in an experimental apparatus.

The extremely fine tolerances involved made it impossible to correct completely this condition of eccentricity, as in the final state

the maximum velocity point could be moved about the annulus at will simply by altering the loading of the assembly bolts. In this final state the velocity profiles at the six radii selected are in agreement to within 1% as shown by the aggregate of the results presented in Figure 4, and agree with the Hagen-Poiseuille velocity profile for this annulus.

The nearly identical fully developed viscous velocity profiles at all radii in the annulus approaching the tip of the fuel supply tube indicate that the design objectives of axially symmetrical fully developed flows at the initial point of the flame transition region had been attained. These profiles do not, however, substantiate or negate the design hypothesis, since the velocity profile developed in the narrow initial annulus could be altered slightly in the conical section and then could be re-established in the straight final annulus. Such an effect must be very slight, however, since the Reynolds number in the upper annulus is 1350 at these flows, and the development length for these conditions is 71.2 cm. while the actual length of final straight section is only 10 cm. Thus, with slight reservations, the flow in the approach transition region does ~~behave~~ in the manner set forth in the design hypothesis.



RADIAL PATH AND ASSOCIATED SYMBOL

FIGURE 4

CHAPTER 4

MOMENTUM EXCHANGE STUDIES

It was possible to investigate the effect of momentum exchange between two concentric fully developed air streams over a limited length of the flame transition region with the total head pressure probe. However, the design of the probe, intended for studying the velocity profiles in the air supply annulus at the tip of the fuel supply tube, restricted the investigation to the initial stages of the transition.

It has been suggested<sup>(3)</sup> that the mechanism of vortex shedding occurs above the tip of the fuel supply tube, similar to that occurring behind a bluff body in a free stream. However, it is also feasible for a laminar system to pass through a series of velocity profiles without the introduction of such vortices provided the direction of the velocity vectors is not severely altered. Vortex shedding should be more difficult for this flow arrangement than it is for a bluff body obstruction in a free stream for two reasons. First, the presence of fluid streaming from the fuel supply tube should prevent the velocity vector at the circumference of the fuel supply tube from undergoing as severe a turning as it would have if the fuel supply tube were a solid body. Secondly, if the flow is axially symmetrical, a turning of this velocity vector beyond some limiting value should result in a stable toroid at the exit of the fuel supply tube, which can only shed when there is some asymmetry in the flow.

It is possible to determine whether vortex shedding or laminar development occurs beyond the tip of the fuel supply tube, even though the

total head measurements have a long time constant and thus only provide the local average velocity over a long period, since the developing velocity profiles for these two mechanisms are quite different. The comparative shapes of such average velocity profiles at a short distance above the tip of the fuel supply tube are shown in Figure 5, where it is shown that a region of apparent constant velocity will occur above the wall of the fuel supply tube as a consequence of any vortex shedding.

Velocity profiles were studied at two values of the ratio of the mass flow in the annulus to the mass flow in the fuel supply tube, namely 100 and 6,680. These values were considered to be representative of the range of this parameter which would be encountered in the study of flames. At both of these mass flow ratios, the mass flow of air in the annulus of 1350 ml/sec. fixed the Reynolds number for the total flow above the tip of the fuel supply tube at 4,800. This Reynolds number is ideal for any study which would differentiate between laminar processes and processes of vortex shedding since it is large enough that any instabilities in the flow system will persist, and any subsequent vortices will be amplified as they travel with the flow rather than being suppressed.

In the early stages of the measurement of the total heads for the purpose of determining the velocity, total pressures less than atmospheric were encountered in the region above the centre of the fuel supply tube where there was no reason to expect reverse flows. This situation made it necessary to actually probe for the static pressures rather than assume that the static pressure was constant and equal to

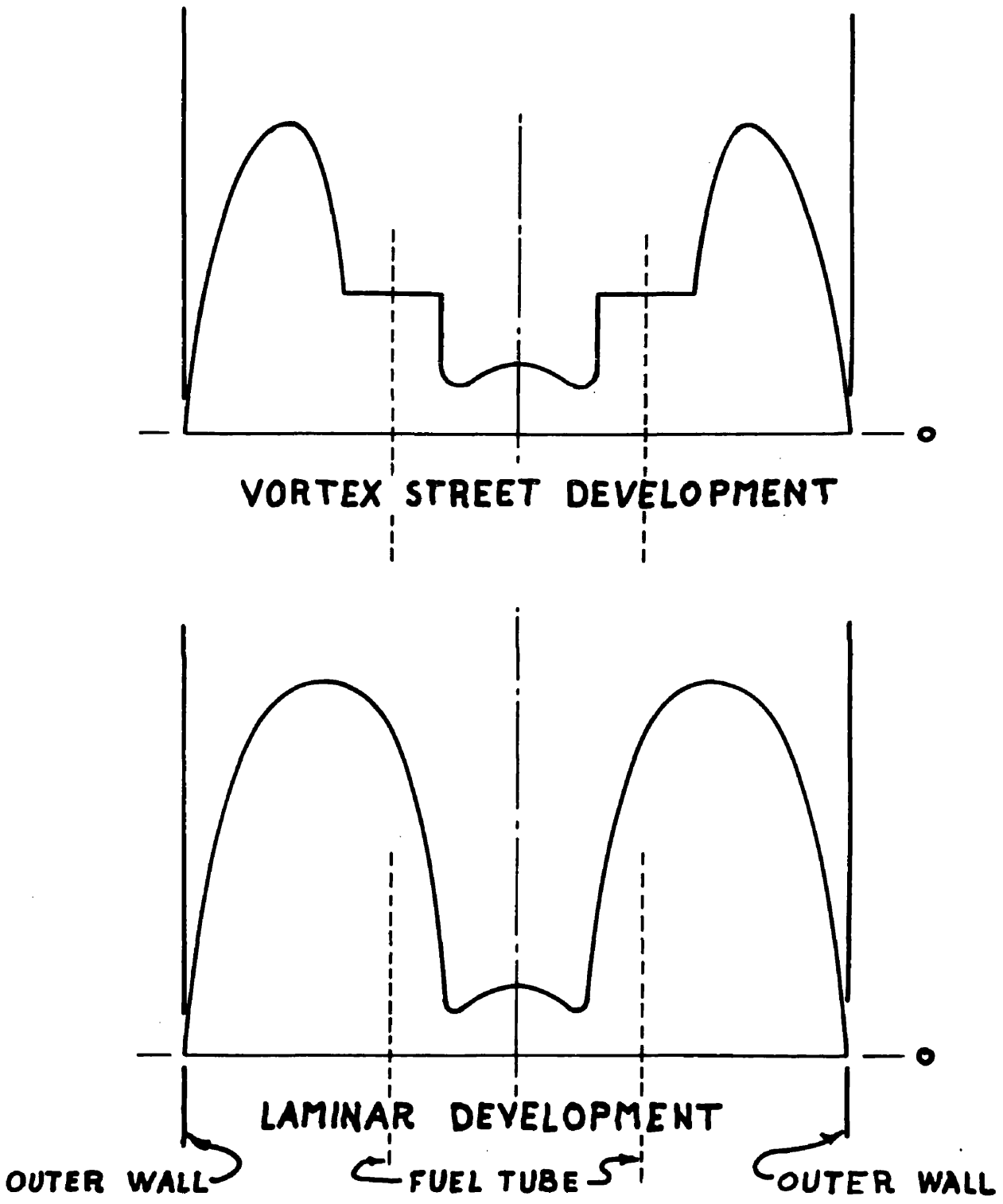


FIGURE 5

the atmospheric pressure throughout the transition region. The flow system was sufficiently stable that a given flow condition could be maintained for several days, so that it was possible to adapt the total head probe as a static pressure probe, and by locating this probe with an external cathetometer, to measure the local static pressure at the same points where total head measurements had been taken. Details of the static pressure adapter are shown in Figure 6. The adapter was mounted on the probe carriage in such a fashion that the static taps were at right angles to the radius which was being traversed so that non-axial velocity vectors would not introduce very great errors in the measured static pressures. However, slight errors did occur in the measured static pressures as a result of the radial components of the velocity vectors within the transition region, the error being the greatest at the centreline.

The static pressure fields for the two mass flow ratios studied are presented in Figures 7 and 8, where the units of pressure are 0.001 cm. of water with reference to atmospheric pressure.

The most significant feature of these static pressure distributions is that the pressure is not constant across the cross section as is the case in the development from the uniform initial velocity case. Another feature is that the magnitude of the local pressures, and the nature of the pressure distributions, is dependent upon the ratio of the mass flows rather than the total mass flow in the system.

These complex static pressure fields indicate that such

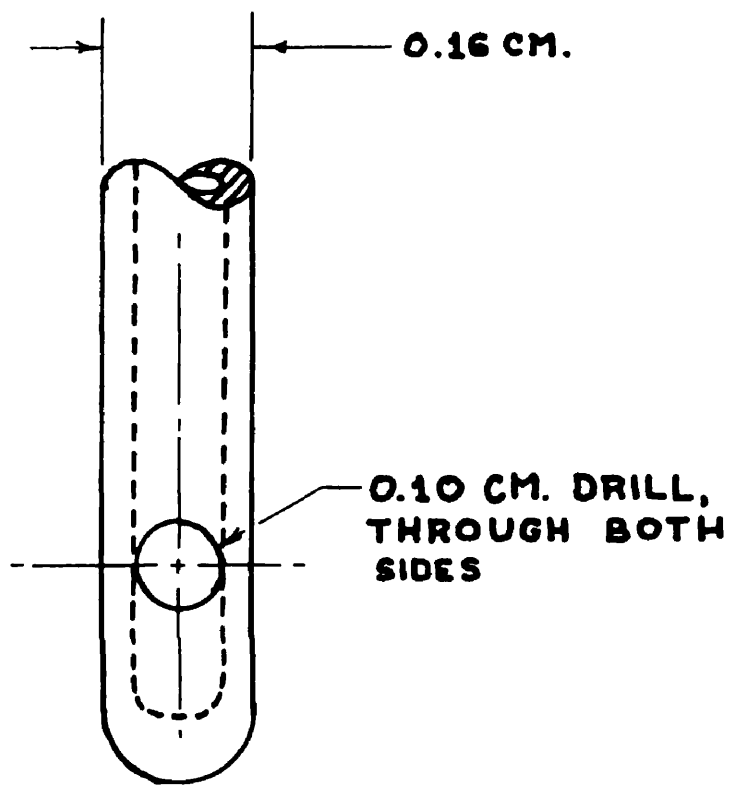
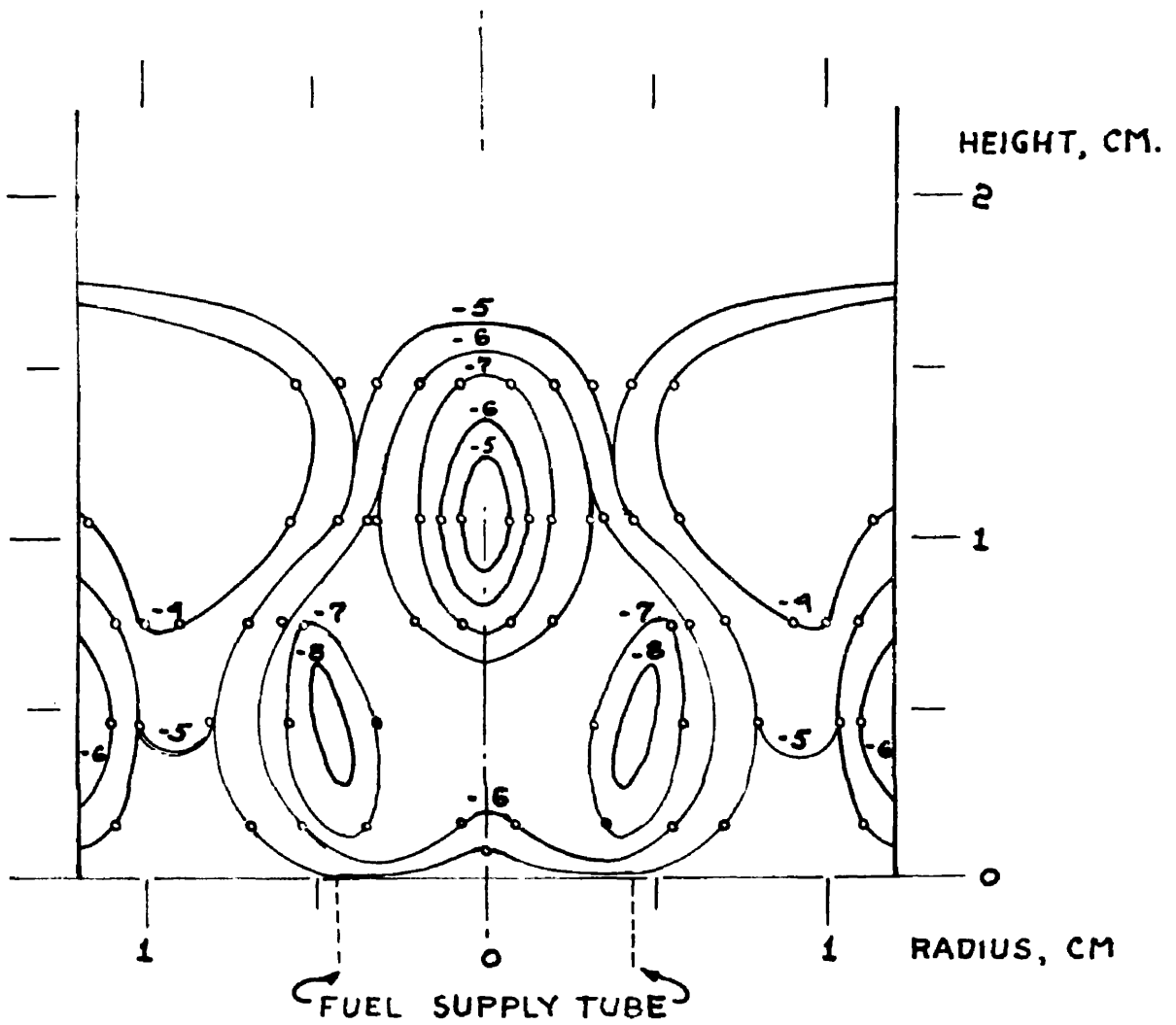
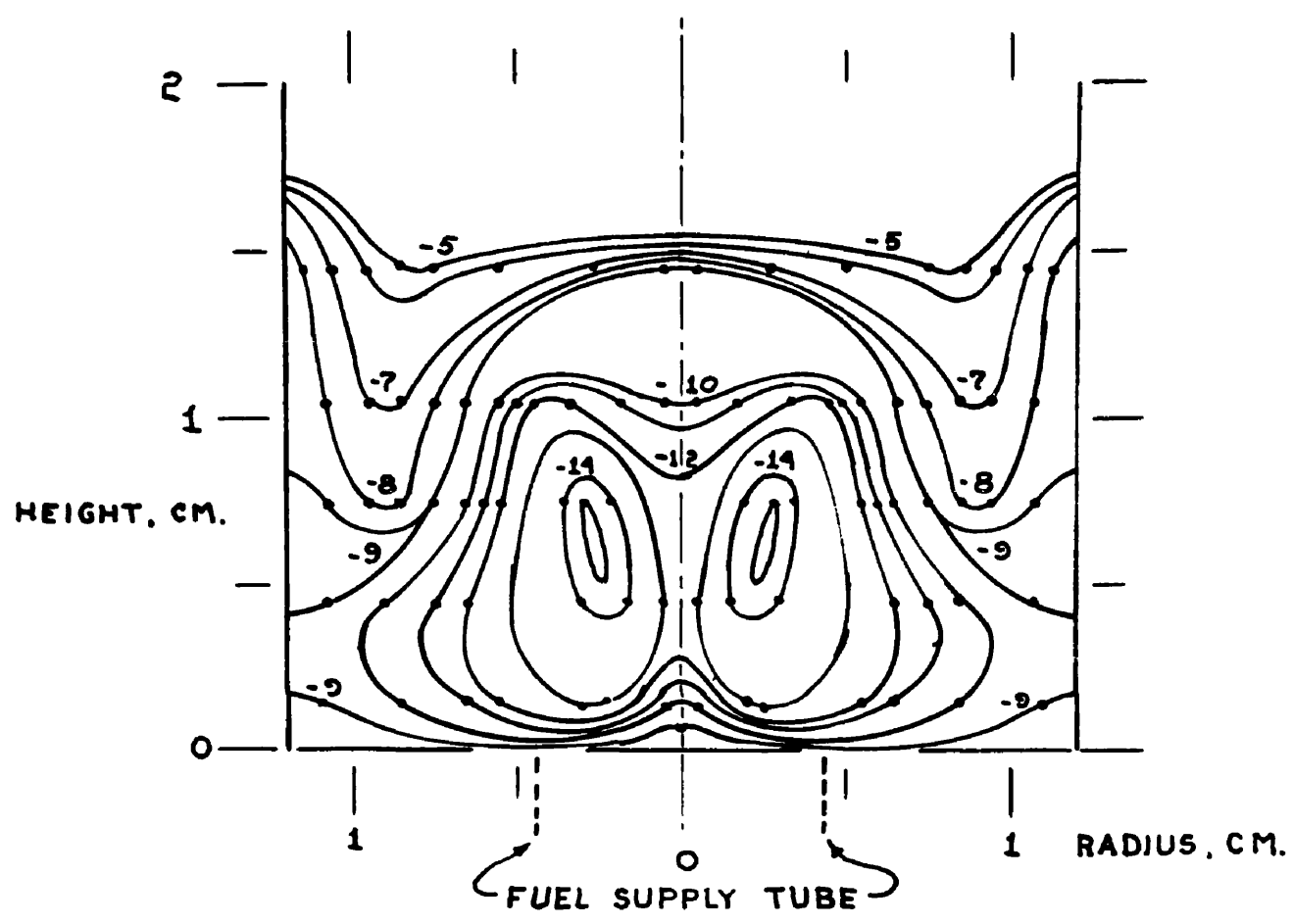


FIGURE 6



STATIC PRESSURE FIELD  
MASS FLOW RATIO ,  
OUTER / INNER  
100 / 1

FIGURE 7



STATIC PRESSURE FIELD  
MASS FLOW RATIO,  
OUTER/INNER  
6,680/1

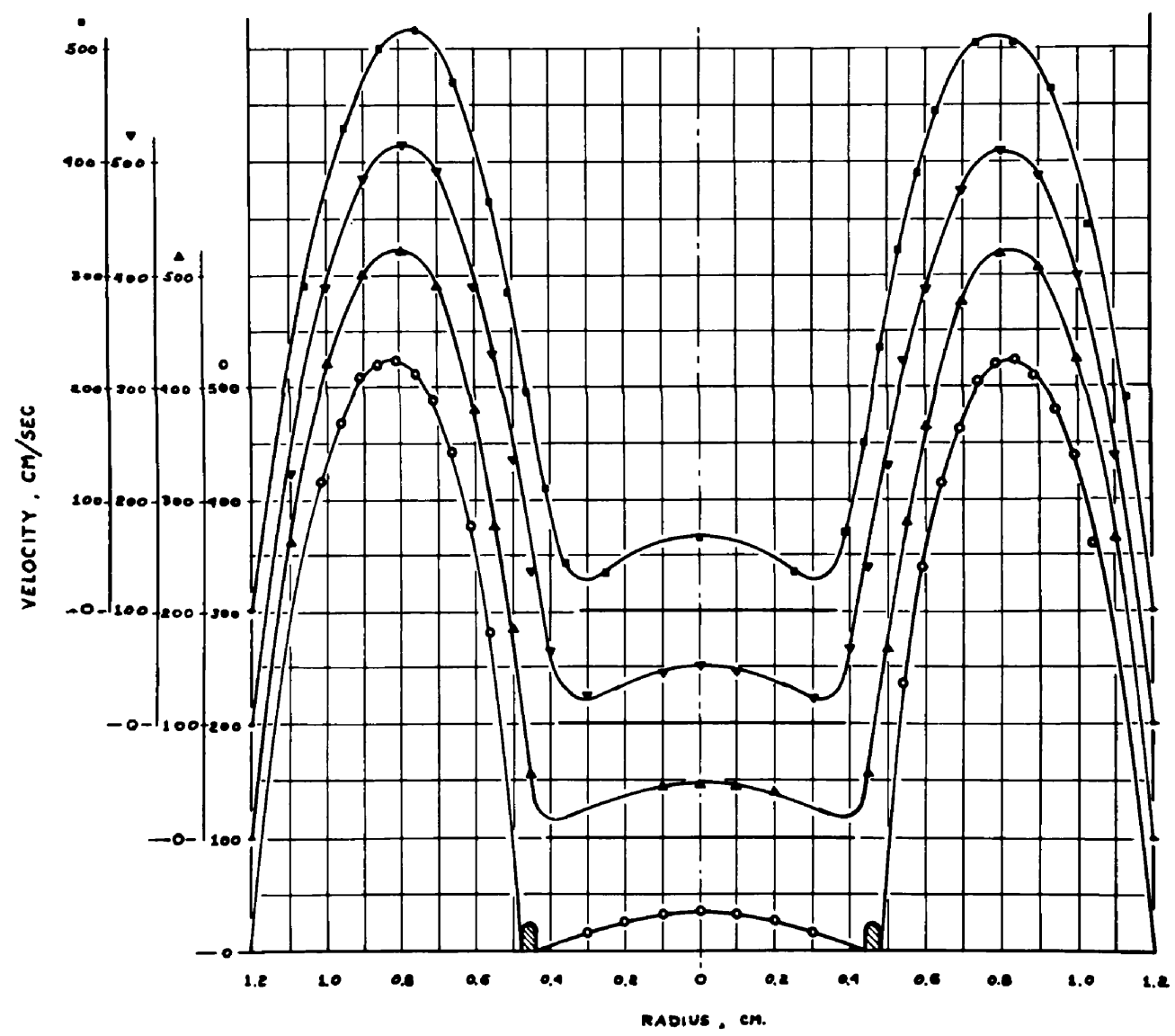
FIGURE 8

measurements are necessary in order to determine the actual velocity heads at any given point within transition regions of this type. The actual velocity profiles at several positions along the transition path are presented in Figures 9 and 10 for the two mass flow ratios studied. Both of these flow configurations show a development of the laminar form without any indication of vortex shedding, although the results for the mass ratio of 6,680 indicate flow reversal at a position of 1.05 cm. above the tip of the fuel supply tube.

For the reasons discussed in Chapter 2 a mass flow ratio of 100 was established as a reference condition in the preliminary experiments, so that the momentum exchange under these conditions is of particular significance. The velocity profiles in Figure 9 indicate that the development for these conditions is of a smooth regular form. This result at the Reynolds number of 4,800 was very gratifying, since it had been hoped that the care taken to ensure laminar fully developed approach flow might make laminar transitions in the flame region possible even at these high Reynolds numbers. There had been considerable uncertainty about this possibility since the literature on the subject indicates that the discontinuity presented by the tip of the fuel supply tube might induce transition to turbulent flow at Reynolds numbers less than 2000.

Prior to these experiments the question had been raised as to whether the viscous forces or the conservation of mass dominated the transition. If the viscous forces dominated the transition there would be a minimum of the velocity profile at the centreline, whereas, if

SYMBOL	HEIGHT ABOVE TIP OF FUEL SUPPLY TUBE
○	0.15 CM
△	0.15 CM
▽	1.05 CM
●	1.45 CM



VELOCITY FIELDS      MASS FLOW RATIO = 100

FIGURE 9

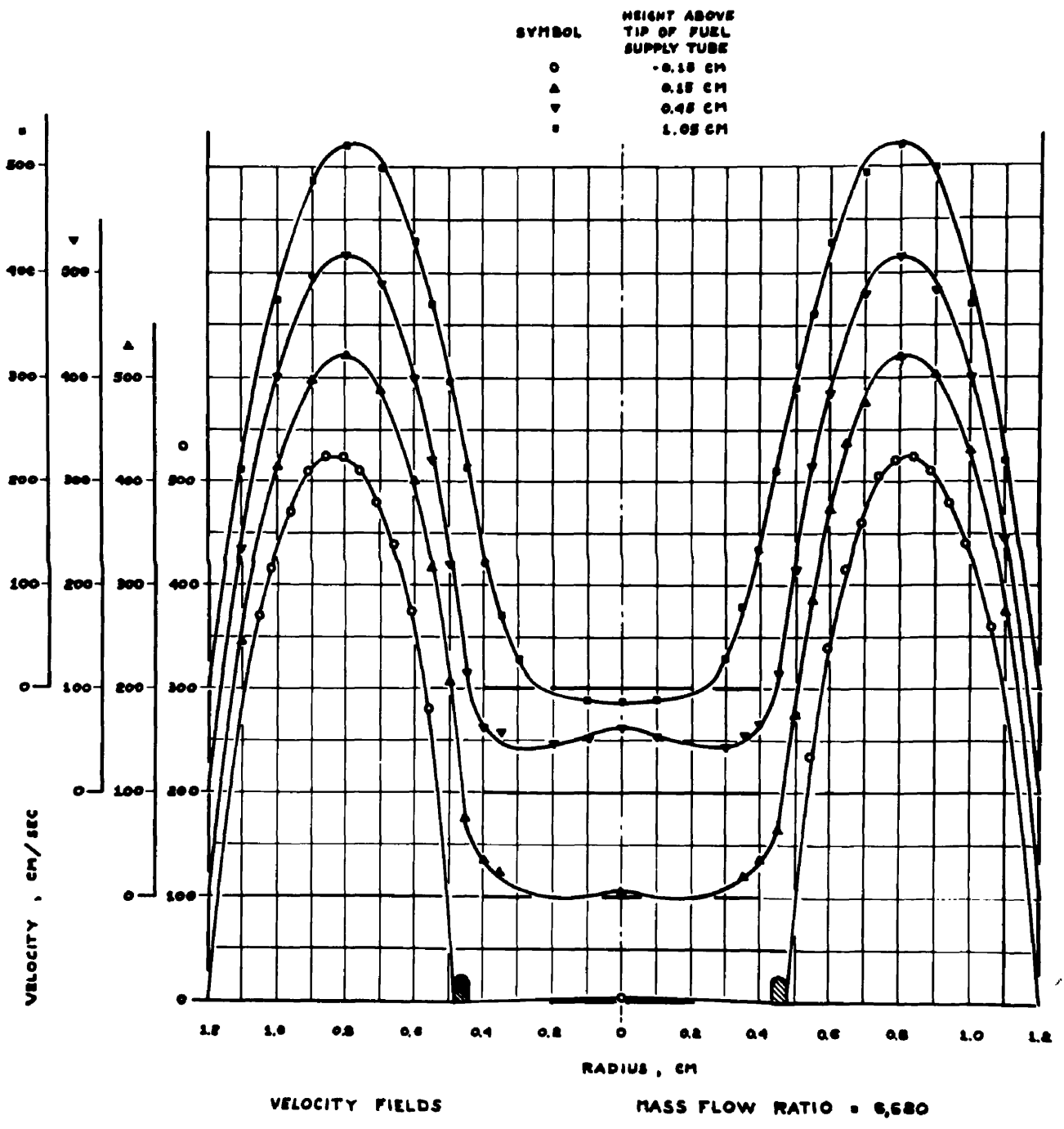


FIGURE 10

the conservation of mass dominated the transition there would be minima some distance away from the centreline, with a residual of the initial parabolic profile of the central flow between these minima and the centreline. The results obtained from these investigations indicate that the latter is the operative mechanism.

In the results for the larger mass flow ratio of 6,680, severe changes in the velocity profiles were observed within the small portion of the transition region investigated. The apparent reverse flow at the centreline 1.05 cm. above the tip of the fuel supply tube suggests the possibility that a stable toroidal flow pattern has been established in the flow stream. If such a flow pattern exists, the direction of rotation in the toroid is the same as that which would be established in a vortex at the tip of the fuel supply tube, and at least the lower portion of the toroid is in a laminar flow region.

An extensive investigation into these processes was precluded by the slow responses of the instrumentation and the limited length of the transition region which could be studied. However, the observed departures from the conventional concepts concerning the momentum exchange processes in a tube indicate that instrumentation designed to study these processes in the flow system which is studied here might provide further insight into the behaviour of laminar systems.

CHAPTER 5

INSTRUMENTATION AND DESIGN OF EXPERIMENTS

The velocity profile studies indicated that the components of the air flow control system limited the air flow to a value considerably less than that obtained by Barr; that oil and water were being carried over into the air flow system from the air compressor; and that the pressure drop in the tubing used to mount the capillary flow meters would be in excess of the one metre of water which was the limit of the manometers installed for pressure drop measurements when the largest flows desired were established.

Figure 11 is a schematic diagram of the final arrangement of air and fuel supply systems which was necessary to overcome the difficulties mentioned above. The design of the 'moisture' separator is of a conventional form consisting of large diameter cylindrical pressure vessel into which the air is admitted through a small diameter tube extending about half way down the vertical axis of the pressure vessel and is withdrawn through a large diameter port in the top of the vessel; the outlet for the extracted oil and water is through a drain cock in the bottom of the vessel. The separator which was located between the air compressor and the air pressure regulator was operated with the drain cock partially open at all times in order to improve the separation performance and to prevent the air compressor pressure-switch from operating. Occasionally it was necessary to use the separator after the pressure regulator in the same manner, when the air flows being used were

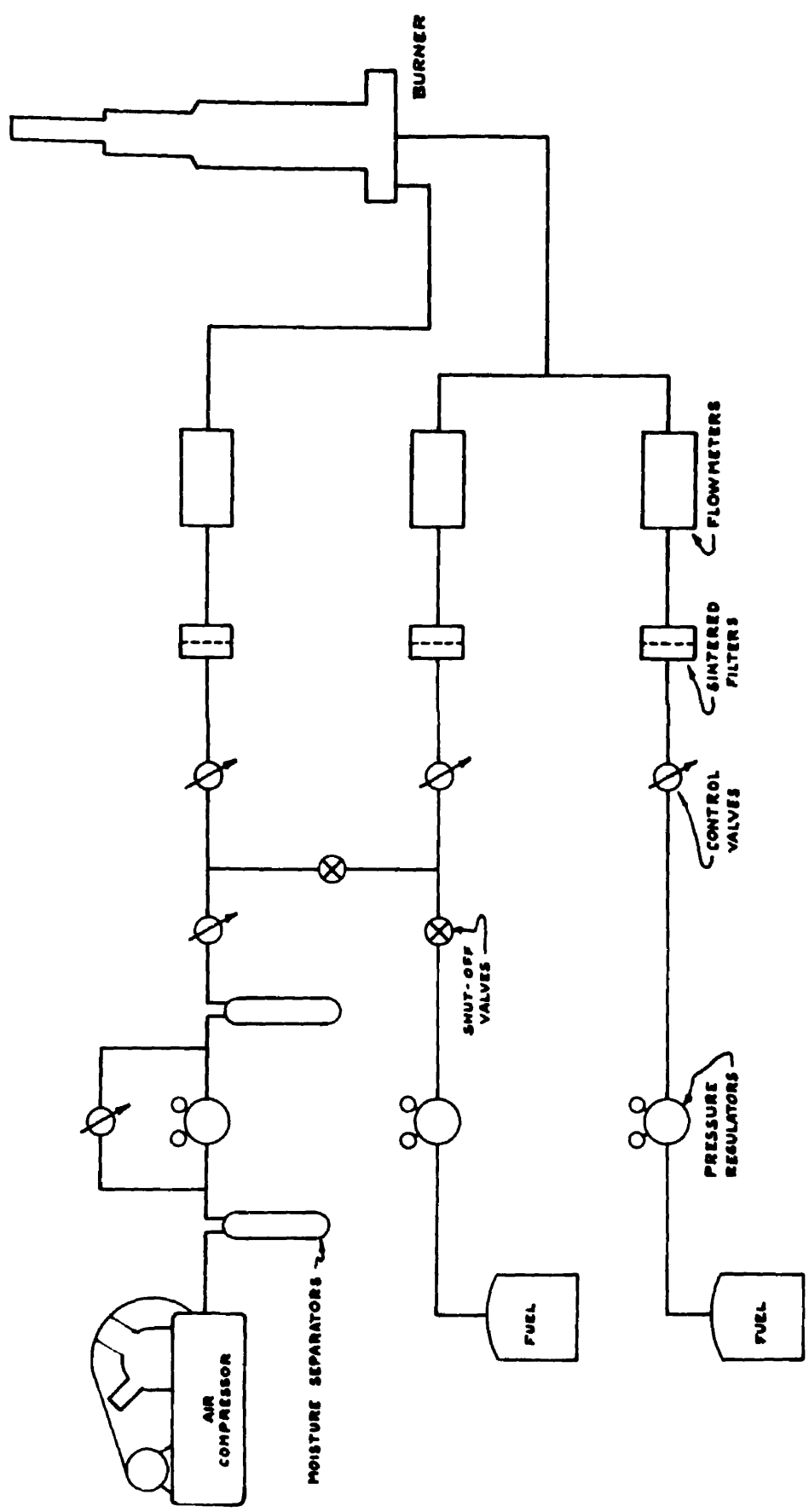


FIGURE 11

less than the through leakage of the pressure regulator. As the air flow was increased the successive limiting restrictions to flow were moved back towards the air supply. First, fittings of full tube bore were substituted for the two series needle valves in turn: finally, for air flows in excess of 2000 ml/sec., a special shut-off control valve which, when fully open provided a through passage of the same bore as the tubing, was employed to by-pass the pressure regulator. (The largest air flow employed in these studies was 4360 ml/sec.)

The largest air flow which could be measured by a pressure drop of 100 cm. of water across a capillary of 0.585 cm. bore was 1700 ml/sec. Measurement of higher flows was accomplished by calibrating the back pressure of the flow into the annulus. Since the back pressure was actually measured at the outlet of the capillary flow meter it was composed of two terms, the turbulent pressure drop in the tube connecting the flow meter to the air flow annulus, and the laminar pressure drop of the sintered cylinder and the air flow annulus. The pressure drop for the turbulent flow in the tube is proportional to the square of the volume flow; and the laminar pressure drop of the sintered cylinder and the air flow annulus is proportional to the volume flow, thus, the equation for the back pressure is of the form  $ax + bx^2$ . There was a sufficient range of back pressures through which flows were measured by the capillary flow meters to establish the two coefficients in this equation.

The equipment and interconnections for a dual fuel system were incorporated so that if the subsequent experiments indicated a striking difference in the behaviour of the various fuels which were to be studied,

an "artificial" intermediate fuel could be devised by mixing two of the fuel studied.

Since (a) the dynamic properties of density and viscosity are dependent upon the nature of the fuel employed, (b) the exact determination of these properties for an unknown gas is a research problem in itself, and (c) the studies anticipated are dependent upon the dynamic properties of the fuel; a series of straight chain hydrocarbons which separately were nearly pure single gases was obtained for these studies. These fuels were methane, ethane, propane and butane of the following analysis:

METHANE

Methane	93.8%
Hydrogen	3.8%
Ethane and Ethylene	2.4%

PROPANE

Propane	95.0%
Propylene	4.5%
Ethane	0.8%
Butenes	1.7%

ETHANE

Ethane	95.8%
Ethylene	0.4%
Propane and Propylene	3.8%

BUTANE

Iso Butane	49.8%
n-Butane	37.2%
Propane	11.0%
Iso Butene	1.1%
Trans Butene	0.5%
Cis Butene	0.4%

For convenience the specific gravity of each of these fuels, relative to air, was assumed to be equal to that of the pure fuel. Even at the level of purity indicated by the above analysis, this assumption introduces an error into the calculated air-fuel ratios of the same

magnituae as the error in the specific gravities. Table 1 presents a comparison of the published values of the specific gravities of the pure fuels with the specific gravities of the fuels used which were calculated by mixing rules from the above analysis.

TABLE 1

Fuel	Specific Gravity	
	Pure	Experimental fuel
Methane	0.554	0.547
Ethane	1.049	1.070
Propane	1.554	1.554
Butane	2.07	2.01

However, the effect of the error introduced by this assumption is negligible since (a) in the presentation of the results from stability studies the errors in the air-fuel ratio will be of the same order of magnitude as the resolution of the graphs and (b) the preliminary experiments indicated a 3% error in the air-fuel ratio used for the measurements of flame heights will only result in an 0.03% error in the measured flame height.

Since (a) the viscosity data on these fuels is less reliable than the density data, (b) the calculation of the viscosities of mixtures by conventional mixing rules has not been well verified, and (c) the characteristics of flames of different fuels were to be studied at a given Reynolds number, a method of determining the flows at which a particular Reynolds number occurred for the different fuels was devised

using the characteristics of a particular capillary flow meter.

A typical set of calibration curves for the fuel flow meters is presented in Figure 12. The curve for flow meter (N), which was chosen for this method of determining a characteristic Reynolds number of the fuel, is of a multiple-function form; at the lower flows, the pressure drop is proportional to the flow; at the higher flows, the pressure drop is proportional to the square of the flow and at the junction of these two curves there is a small region where the flow can take on several values for the same pressure drop. This curve is very repeatable for a given fuel, both for increasing and decreasing flows. The behaviour of the development of the flow in a particular tube is defined by the Reynolds number of the flow, so that this point of inflection on the calibration curve of flow meter (N) will always occur at a particular Reynolds number independent of the fuel. From this property and from determinations of the flow at which this inflection occurs for each fuel it is possible to establish the dynamic properties of the remaining fuels relative to the dynamic properties of any chosen fuel. Ethane was chosen as the reference fuel since it was the fuel with the highest concentration of a single component, and since the published values for its viscosity appear to have the highest reliability. The Reynolds number as a function of the volume flow was calculated for ethane flowing in the 0.874 cm. bore fuel supply tube and all fuel flow Reynolds numbers were correlated to this value. The following coefficients of the Reynolds number as a function of the volume flow of fuel in this tube were determined by this correlation method: Methane, 10.10; Ethane, 22.0 (calculated); Propane, 34.8; Butane, 45.7; Barr's fuel, 50.9.

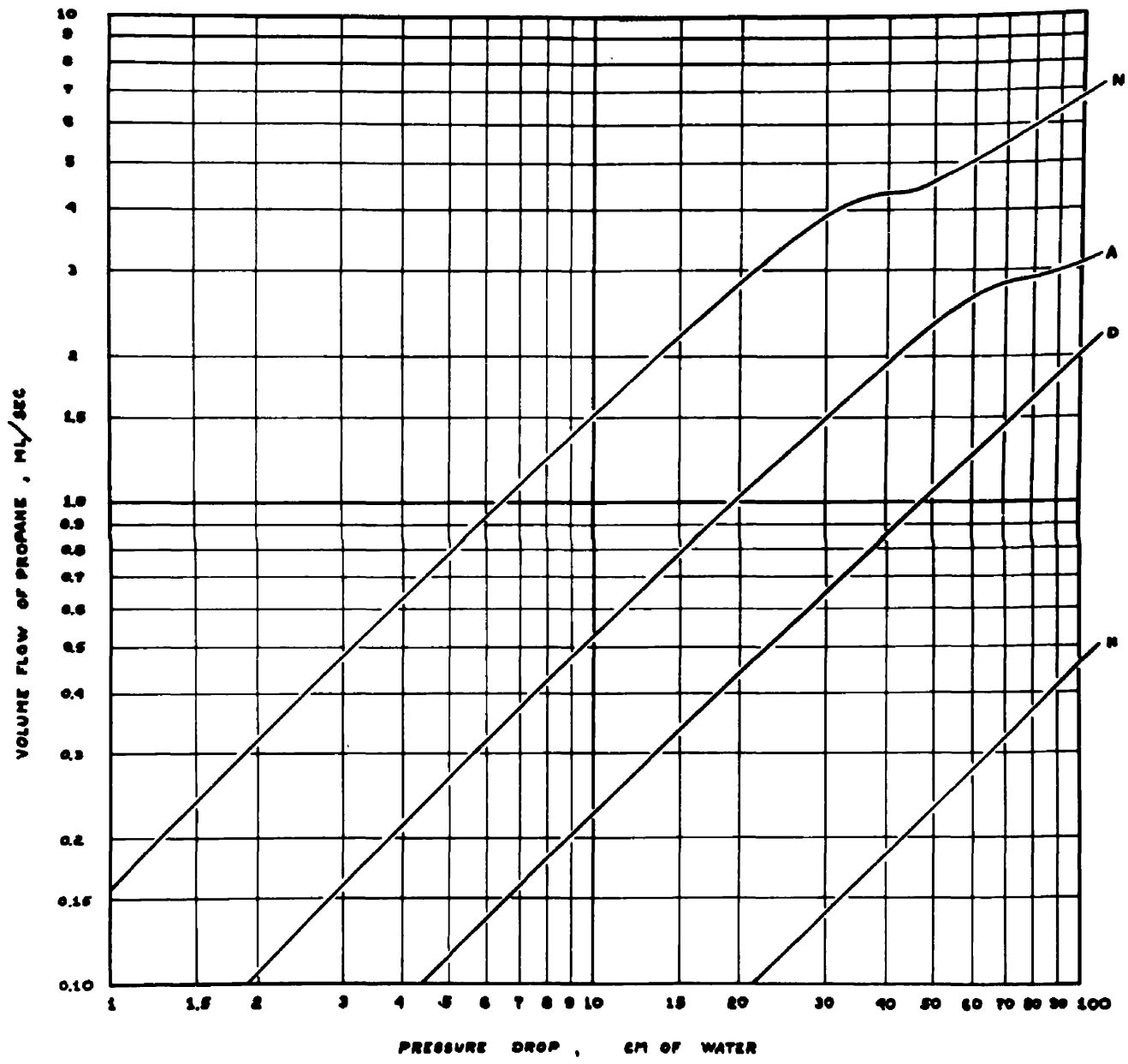


FIGURE 12

The published values for the properties of iso-butane, which were used in calculating the Reynolds numbers for the conversion of Barr's flame maps to the author's dimensionless co-ordinates yield a value for this factor of 51.9 which is in fair agreement with this determination. The values for the viscosity of normal butane which were used to calculate the Reynolds numbers in the preliminary experiments were not very reliable, and as a result the Reynolds numbers were 20% below the correlation values.

The fuel flow meters, and the air flow meters for the lowest flows were calibrated against bubble flow meters. For the intermediate flows the capillary flow meters were calibrated against one another in series.

Flame height was measured with a cathetometer which has a resolution of 0.005 cm. which is two to three times the accuracy of the decision as to the locus of the terminal point of the flame.

The experiments were conducted in an air tight, dust free laboratory whose temperature was nominally maintained at  $20^{\circ}\text{C.} \pm 0.5^{\circ}\text{C.}$  Although the room was well ventilated with a large flow of filtered air there was a  $1^{\circ}\text{C.}$  difference in the temperature at various points throughout the room, this distribution remaining quite stable independent of the mean temperature of the room.

Photographs were taken with an optical bench system for mounting the lens and the film holder so that any desired degree of magnification could be repeatedly established. The film used for the photographs was a very slow film, sensitive to the blue and ultraviolet region of the

spectrum only. The speed of the film was such that the exposure time for the carbon radiating flames was 25 seconds and the exposure time for the non-carbon radiating flames was of the order of 40 seconds, so that the distinct photographs provide an indication of the stability of the flames.

CHAPTER 6

FLAME MAPS

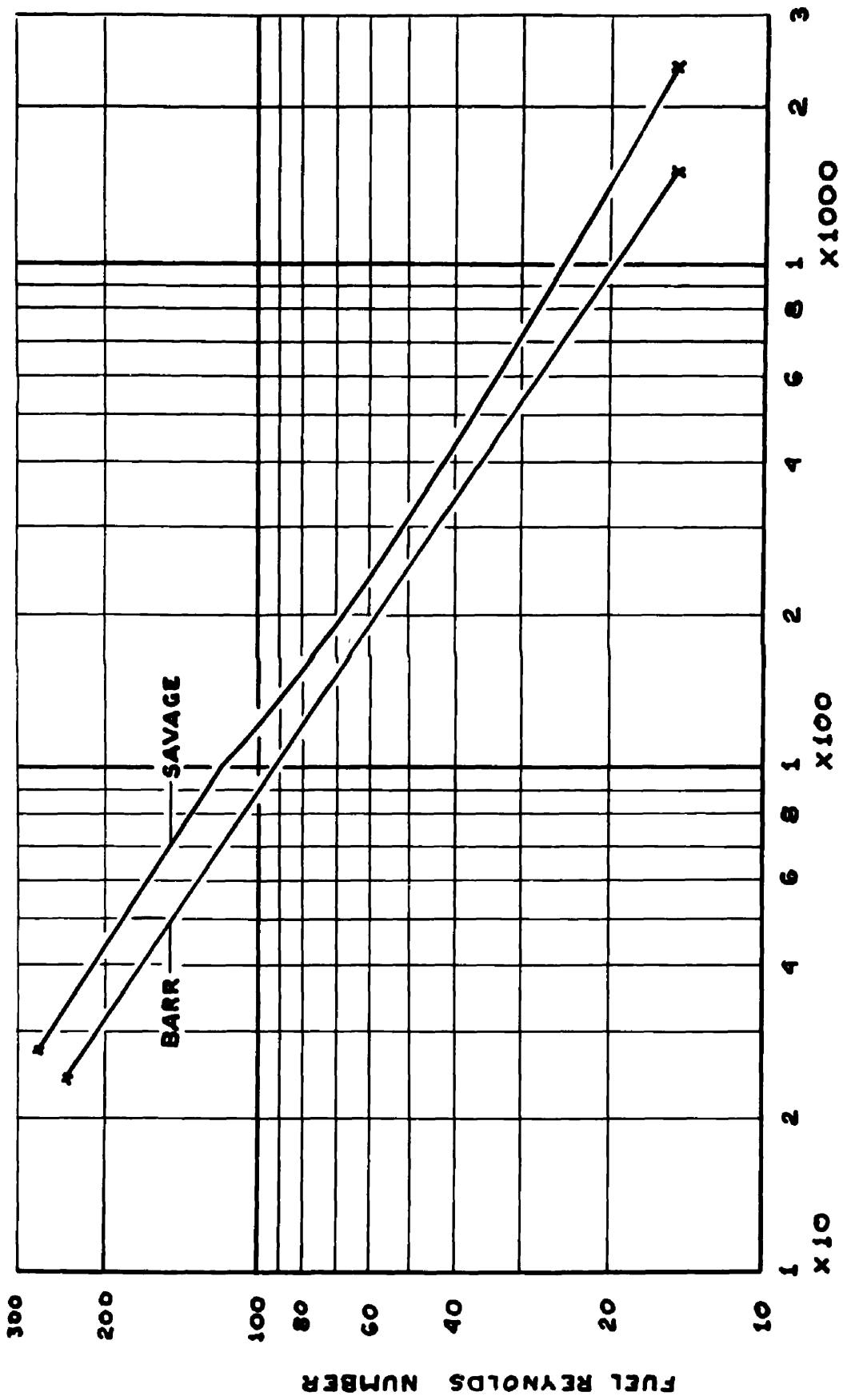
The literature indicates that the so called 'stability boundary' will be the most sensitive test of the nature of the velocity profiles of the gas streams which support a flame. The concept of the 'stability boundary' was developed from observations of open premixed and diffusion flames where it was found that open flames were extinguished when the velocity gradient at the wall of the burner exceeded a particular value dependent upon the fuel, or fuel mixture, and the dimensions of the burner. These open flames were of the same form over a wide range of flows until this 'stability boundary' was reached. These concepts were applied also to the enclosed flame, although, as the scope of study of the enclosed diffusion flame was extended it was found that the boundary of extinction of these flames was not a single valued function of the velocity gradients at the wall of the fuel supply tube, and that the form of the flame at extinction was dependent upon the flow of the two gases involved. Hattori, Takeuchi, Yoshiyawa, Hitamoto and Hoshino<sup>(9)</sup> modified the concept of the 'stability boundary' for enclosed diffusion flames by defining the 'stability boundary' as that point where there was a distinct departure from the conventional diffusion flame which was completely anchored. These authors then demonstrated that this 'stability boundary' exhibited a dependence upon the velocity gradients at the wall of the fuel supply tube similar to that observed for the open flames. The 'stability boundary' for an enclosed diffusion flame, therefore, may reflect transitions between two stable forms of flames as well as extinction

of the flame. One such transition that already has been mentioned is the 'lifting' of the anchoring ring described in Chapter 2.

Therefore, by comparing the 'stability boundary' determined by Barr to the 'stability boundary' obtained from investigations with the known profiles of the newly constructed burner, it would be possible to determine if the velocity profiles of the flow system used by Barr satisfied the condition of fully developed axially symmetrical laminar flow. The dimensional configuration used by Barr, namely, a 0.846 cm. bore fuel supply tube within a 2.2 cm. bore constraint tube, does not match the new 0.874 cm. bore fuel supply tube within a 2.400 cm. constraint tube, but the diameter ratios of these two burners are nearly matched so that results in terms of the dynamic variables of fuel Reynolds number and air-fuel ratio should be comparable.

A comparison of the 'stability boundaries' from these two series of experiments is presented in Figure 13. The difference between the boundaries indicates that the velocity gradients at the wall of the fuel supply tube must be different for the two configurations. Since fully anchored flames can be maintained at higher air-fuel ratios with the fully developed flow burner than could be maintained by Barr for all fuel Reynolds numbers, it can be deduced that the velocity gradients in the air stream at the wall of the fuel supply tube must be greater in Barr's experiments. The fact that the eccentricity of the fuel supply tube in Barr's experiments could have been as much as 0.02 cm. may be a significant contribution to this difference in the velocity profiles.

The study of the 'stability boundaries' was extended to cover the range of flame transitions at the high flows studied by Barr to



AIR-FUEL RATIO  
FIGURE 13

ascertain if the difference in the velocity profiles affected any of his other observations. In these experiments, whenever possible, the transition was approached by increasing the air flow at a constant fuel flow. There were two cases where this was not feasible, namely: the smoke point; and that region where the air-fuel ratios at a given fuel Reynolds number were separated by a region of extinction, and in both of these cases the boundary was approached by decreasing the air flow at a constant fuel flow.

Figure 14a is a reproduction of the results obtained by Barr which have been converted to the coordinates of fuel Reynolds number and air-fuel ratio. The boundary shown by the broken line on this map is the extinction boundary from the results presented in Figure 14b which is the map of the transition boundaries determined, in the present study, for 'pure' butane. The solid boundaries of Figure 14b correspond to the boundaries of the map by Barr, the broken boundaries being transitions which Barr did not define.

The difference which is apparent in the shapes of the boundaries, and the existence of flames at higher Reynolds numbers and air-fuel ratios for the 'perfect' flows indicate that the differences in the velocity profiles affect the loci of the transitions of enclosed diffusion flames. A rather surprising result of the comparison of these two maps is the fact that Barr was able to maintain flames at much lower fuel Reynolds numbers and higher air-fuel ratios than was possible with the 'perfect' velocity profiles. This might be the result of a stabilizing influence introduced by the low velocity nodes produced by the locating

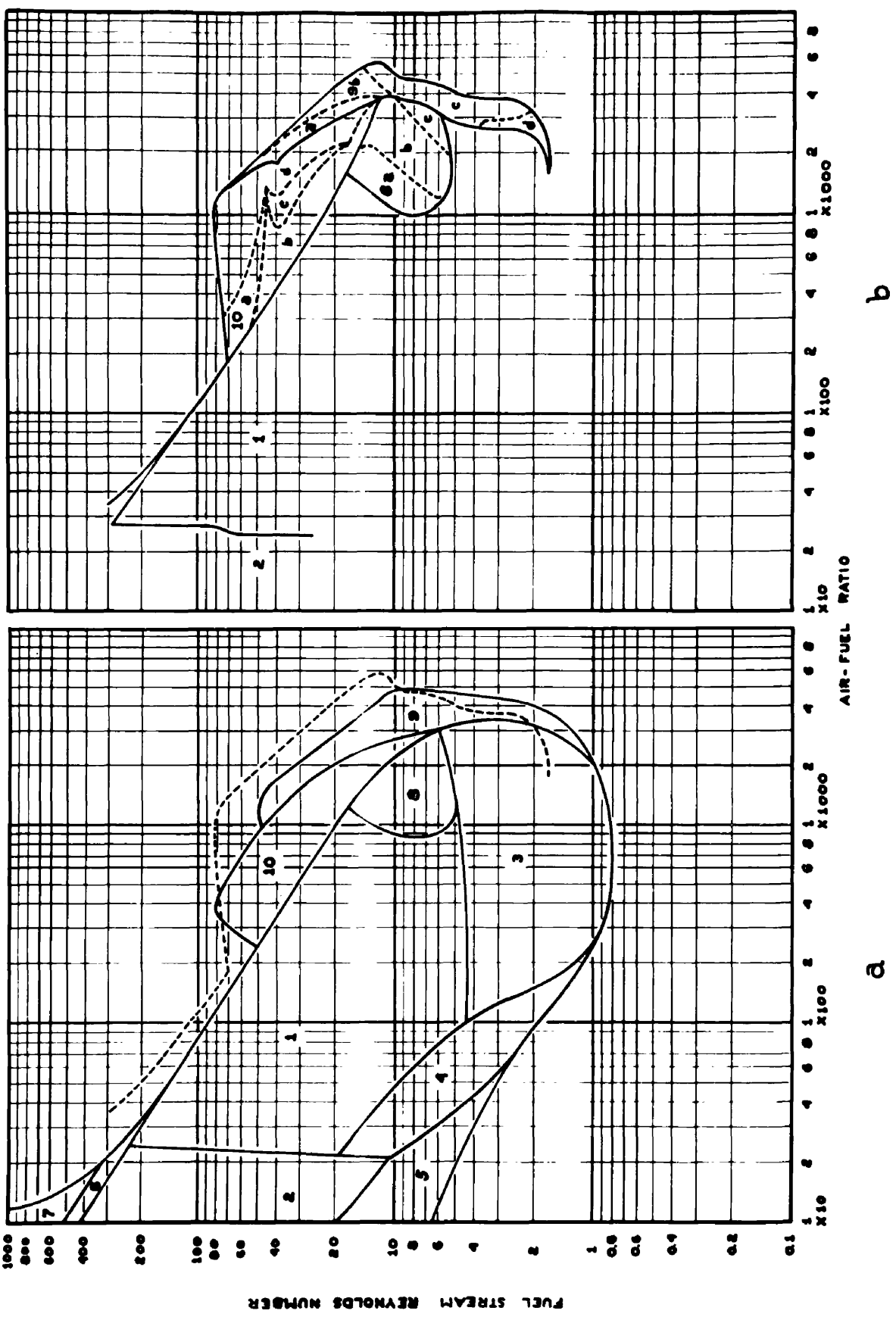


FIGURE 14

'spider' for the fuel supply tube.

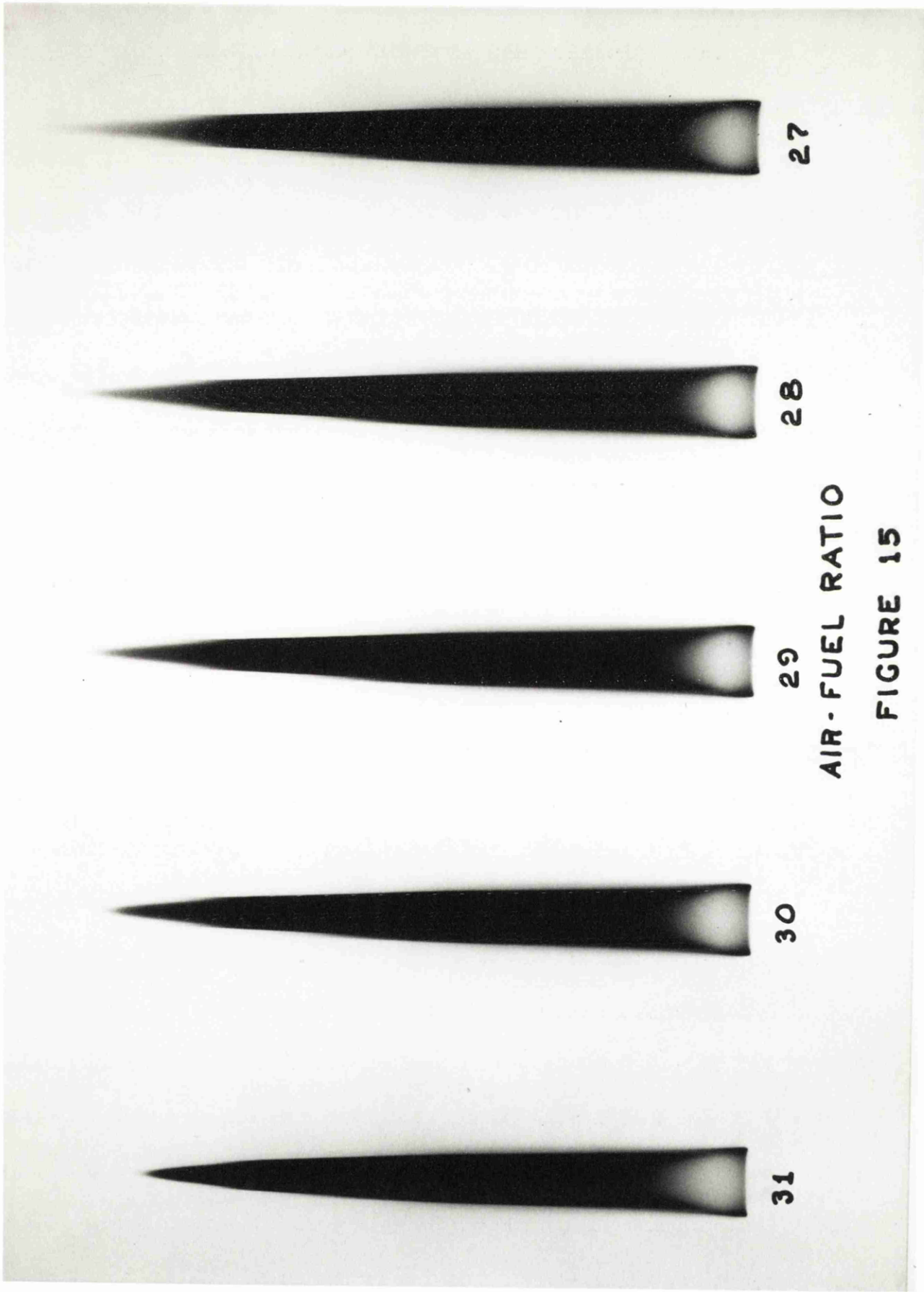
The identification of the regions of Figure 14a are those set down by Barr, in reference 2a, in his detailed description of the types of flames. Since the same types of flames occur in both maps, the names given to the flames occurring within these regions and, where pertinent, the definitions of these flames will be outlined.

- Region 1: The reclosed, or overventilated, laminar diffusion flame. This flame has been considered as the 'standard' flame in this study.
- Region 2: The open, or underventilated, diffusion flame.
- Region 3: The meniscus flame. This flame is defined as a 'standard' hydrocarbon diffusion flame without any carbon radiation.
- Region 4: The lambent flame. This flame is defined as a 'standard' flame where the tip of the flame moves freely within the constraint tube.
- Region 5: The rich tilted flame.
- Region 6: The incipient lifted flame. This flame results from the 'lifting' described in Chapter 2.
- Region 7: The turbulent lifted flame.
- Region 8: The vortex flame.
- Region 9: The single weak tilted flame.

Region 10: The multiple weak tilted flame.

The boundary between regions one and two is the 'smoke'point' and is defined as that point where soot first issues from the tip of a reclosed flame as the air flow is reduced. The use of an ignition flame at right angles to the flow, above the tip of the constraint tube, made it possible to observe the distribution of the solid carbon issuing from the tip of the flame as the smoke point was approached. This simple device made it possible to verify an effect which had been observed for all flames in which the flows were fully developed. Figure 15 is a series of full scale photographs of flames at a fuel Reynolds number of 90, in the burner used to obtain the map of Figure 14b, at successively smaller air-fuel ratios in the vicinity of the smoke point. The fact that the radiation at the tip of the flame was almost completely outside the sensitivity spectrum of the film makes it difficult to see the two 'horns' on the flame on either side of the tip of the three flames at the lower air-fuel ratios. These 'horns' are associated with a ring of carbon particles separated from the tip of the flame by a region where no solid carbon is present. The results of the momentum exchange studies presented in Chapter 4 indicate that the minima of the velocity profiles within the transition region occur in the same radial region where there is no solid carbon issuing from the flame.

The boundary between regions 6 and 1, and between regions 10 and 1, is dependent upon the direction of approach, in such a manner that when the air flow is decreased at a constant fuel flow, the air-fuel ratio of the transition is approximately 10% less than that obtained when the air flow is increased at a constant fuel flow.



AIR-FUEL RATIO

FIGURE 15

Many of the flames observed were not obviously stabilised by the fuel supply tube, and thus appeared to be more truly in dynamic equilibrium than the 'standard' flame. Several of the flames of regions 9 and 10 appeared to be 'floating' a short distance above the tip of the fuel supply tube and would be shifted within the constraint tube by the slightest transient disturbance. Thus it was often observed that when a door was opened or closed in some other part of the building the extremely small pressure transient created thereby would cause the flame to shift its position. The standard flame was insensitive to these disturbances except in the neighbourhood of the 'stability boundary' where a premature transition would be caused by such a transient.

Figure 16 is a series of sketches of the various flames observed in regions 8, 9 and 10. In reference 2a Barr has described flames 8a, 8b, 8c, 9d, 10a, 10b and 10c; and in reference 2 he has reported observing a flame of the form of 10d.

The three types of flames of region 8 all appear to be associated with a stable toroidal vortex established at the tip of the fuel supply tube. The various shapes of flames in this region are related to the diameter of the generating circle of the toroid and the rotational velocity within this circle. The boundary between the standard flame and the vortex flame may be defined as the locus of those points where a small peak in the carbon radiation surface is formed at the centreline as the air flow is increased. At these flow conditions an occasional large incandescent carbon particle is formed within the fuel supply stream. When it first appears, such a particle is trapped in a vortex flow pattern of low rotational velocity and almost half the

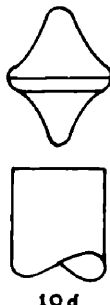
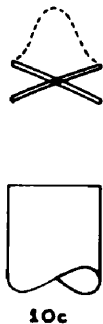
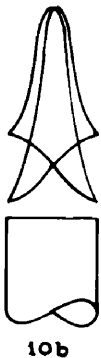
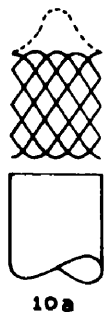
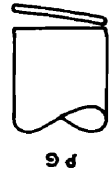
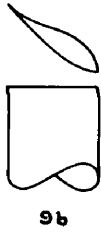


FIGURE 16

width of the fuel supply tube in diameter. When the particle leaves the vortex, it escapes through the peak on the carbon radiation surface. As the air flow is increased the number of incandescent particles increases, and their apparent size decreases. As the air flow is further increased the transition into region 8b is encountered. At this transition the peak to the carbon radiation surface suddenly inverts, forming an apparent hole at the centreline in the flame profile. There is, however, the faint blue radiation of the meniscus flame forming a cover to this 'hole'. There are very few large incandescent carbon particles formed in this region, but those which are formed indicate that the toroid is smaller than that of region 8a and has a higher rotational velocity. As the air flow is further increased the diameter of this toroid decreases until there is no normal carbon radiating surface and the flame takes on the form of 8c. In this region the flame surface is the faint blue radiation of the meniscus flame while a large number of intermediate sized incandescent carbon particles appear to be formed in a circle and then to escape upwards to form an incandescent cylinder. This appears to be the result of the diameter of the generating circle of the toroid being reduced to its limiting value, when the toroid becomes a circle.

The flames of region 9 form two classes. The flames of regions 9b, 9c and 9d form one class and are all anchored at the nominal distance of the standard flame, above the tip of the fuel supply tube; and the asymmetries of the velocity profiles distort the rest of the surface. The flame of region 9c is interesting in that about half of the flame is a conventional meniscus flame while the remaining half of

the flame is distorted by the asymmetry of the velocity profile.

The second class of flames are those of region 9a, which were originally grouped in region 9 since the flames appear as flat discs. They appear to be a variation of the flames of region 10d since they are not anchored and since this form is approached as a limiting form in region 10d as the air flow is increased.

The flames of region 10 also form two classes. Those flames of regions 10a and 10b are basically of the same type as those flames of region 6, except that they are reduced to a single point of anchoring which assumes various positions about the circumference of the fuel supply tube rather than a single point of 'lifting'. At high fuel flows both of these flames exhibit a flame tip similar to that of the standard flame. The terminal height of these flames, like that of the flames of region 6, is less than that of a standard flame at the same fuel flow. For the flame of 10a this luminous tip disappears upon reducing the fuel flow, only to reappear again upon the transition into region 10b. The flame of region 10c belongs to the same class as the flames of regions 10a and 10b, and is a 'floating' variation of the type of region 10b.

The flame of region 10d is unique. Whereas the other flames of region 10 display carbon radiation at some flows, those flames of region 10d always appear as truly premixed flames. The central belt of these flames is a region of intense blue-green radiation, while the upper cone is the faint deep blue of a carbon-monoxide flame and the lower inverted cone is a faint violet colour. Photographs of this type of flame at fuel stream Reynolds numbers of 25, 30, 35 and 40 are shown

in Figure 17, together with a photograph of a standard flame at a fuel stream Reynolds number of 35 to indicate the locus of the tip of the fuel supply tube. These photographs are all at a magnification of two and a half times full size. The upper and lower cones are very faint in these photographs; separate measurements, however, indicate that the heights of these cones above and below the central belt as well as the distance from the tip of the fuel supply tube to the centre of the belt are proportional to the fuel stream Reynolds number. These flames could only be obtained with flow systems where the ratio of the bore of the constraint tube to the bore of the fuel supply tube was less than 4.2. There was an interesting change in the appearance of this type of flame when it was obtained over a fuel supply tube of 0.402 cm. bore within a 1.600 cm. bore constraint tube. At this scale the lower cone of the flame was much more distinct than for the larger scale and the radiation from this cone was of an intense green colour.

The location of these flames at the same air-fuel ratio as the vortex flames, the premixed characteristics of these flames, and the fact that the flow conditions for these flames are near the flow conditions where reversed flows were observed in the momentum exchange studies suggest that these flames may be associated with a stable toroidal vortex located a short distance above the tip of the fuel supply tube. Such a toroid would be larger than those of the vortex flames and its plane of generation would be located at the plane of the central belt of the flame l0d.

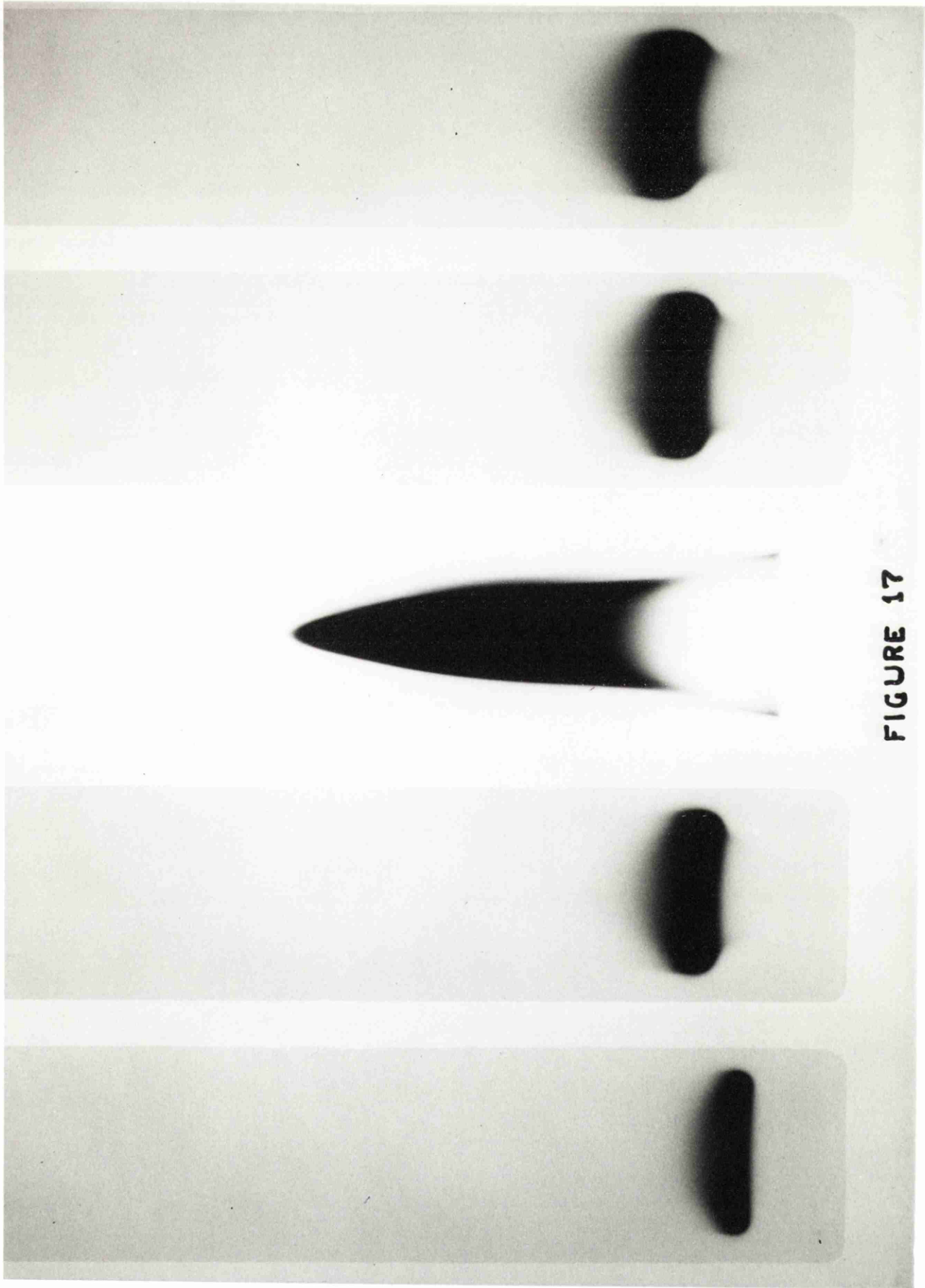


FIGURE 17

CHAPTER 7

FLOATING FLAMES

A distinct family of flames which occur at essentially the same fuel Reynolds number and air-fuel ratio was observed in the course of investigation of flames on an 0.295 cm. bore fuel supply tube mounted within the 2.400 cm. bore constraint tube. The existence of such a family of flames at a single point on the coordinate system of Figure 14 is an anomaly in the concept of the flame map which is based on a unique form of a stable flame at any given point. After the techniques of manipulating these flames had been perfected and successfully employed with several combinations of fuel supply and constraint tubes it was concluded that this family could be obtained for any combination of tubes as long as the approach flows were essentially axially symmetrical fully developed laminar flows and the transition above the fuel supply tube was laminar.

An investigation of the range of variables for which such flames could be maintained was not conducted, but all of the flames investigated were within the region of the standard flames of the map of Figure 14b near an air-fuel ratio of 100 and at a fuel Reynolds number about 10% below that of the 'stability boundary'.

The ignition of the enclosed laminar diffusion flames has always been an interesting process to observe. In the normal ignition procedure the flows of the fuel and air were adjusted so that a small hemispherical flame was attached to the lower side of the ignition flame. Then, when either the fuel flow was increased or the air flow was decreased, this

hemispherical flame would propagate down the constraint tube, and as it approached the position of the standard flame it would take on the shape of the standard flame. Once underway, this propagation occurred so rapidly that it was difficult to attempt to form a mental image of the succession of flames.

However, it was found that by careful manipulation of the flows it was possible to hold any of the flames of this progression at a fixed position within the constraint tube. The procedure for establishing these flames was to adjust the flows so that a flame of the form occurring between the hemispherical flames and the anchored flames was attached to the ignition flame with its base just within the constraint tube. At this point the ignition flame could be removed and the floating flame **would** remain stable. These floating flames could be moved up and down the constraint tube at will, simply by decreasing the air flow slightly to lower the flame, and increasing the air flow to raise the flame. In the quantitative study of these flames a 2% variation in the air flow covers a 30 cm. range in the location of the lowermost point of the flame. At any particular air flow, decreasing the fuel flow would lower the flame, which is the opposite of the effect of decreasing the fuel flow upon the hemispherical flame attached to the ignition flame.

Figure 18 is a series of full scale photographs of several members of this family of flames, including that of the standard flame at the same flow conditions. The 30-second exposure time for these photographs indicates the stability of these flames when there are no external transients. The small wedge which is slightly upturned from the base of the floating flames is the result of the slight residual

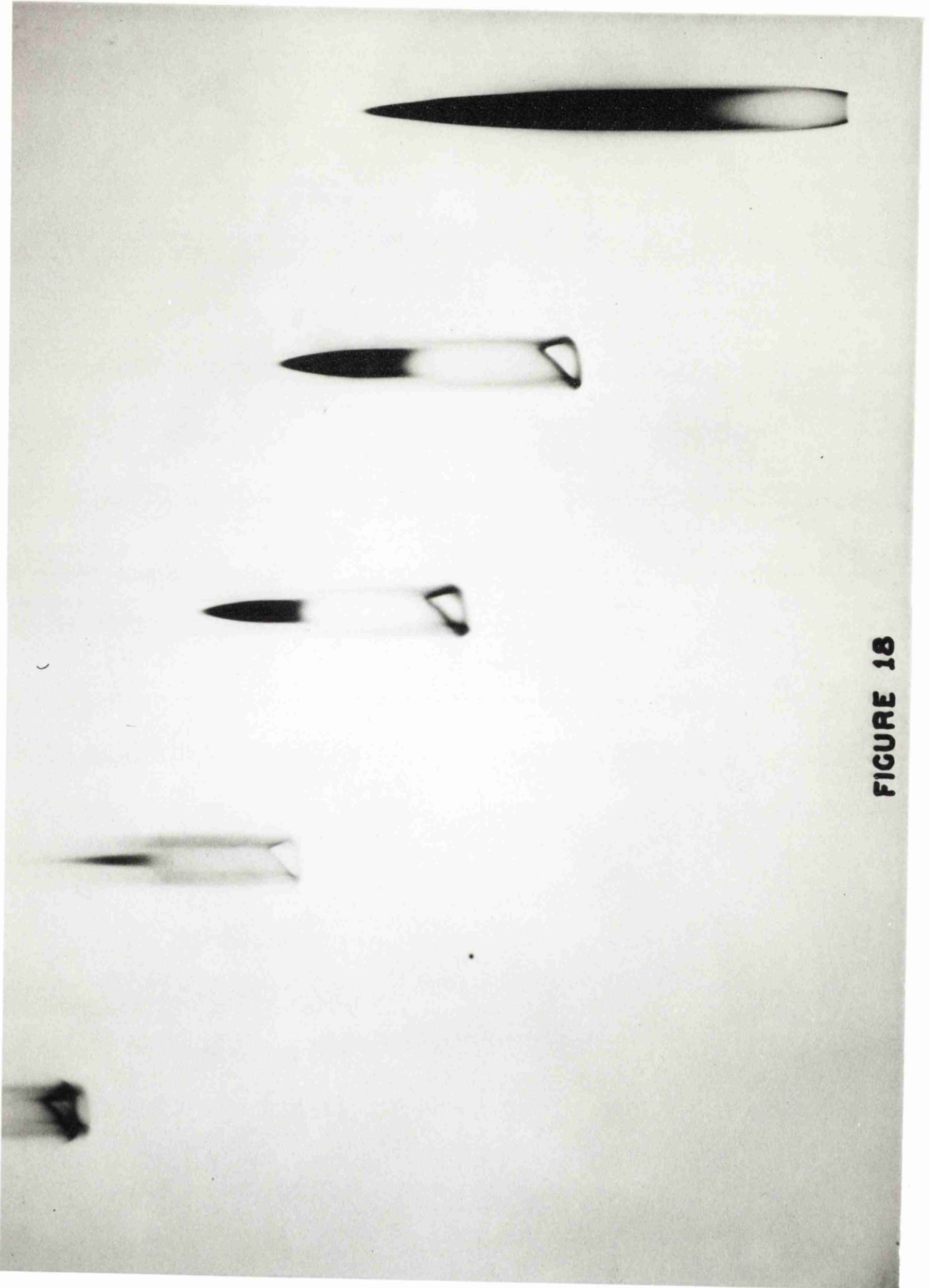


**FIGURE 18**

axial asymmetry in the air flow. This effect disappears as the flame is brought to the stage of having a hemispherical base. The photographs do not bring out certain of the fine details of these flames, and the vertical limitations of the photographic system excluded some of the interesting flames which were located at higher positions within the constraint tube. Sketches of this family, therefore, are presented in Figure 19.

The fuel flow of 1.53 ml/sec. used in the experiments of Figures 18 and 19 was such that all of the flames shown were completely contained within the 50 cm. length of the constraint tube. The Reynolds numbers for the total flow within the constraint tube varied between 1000 and 1070 as the air flow was varied between 294 and 300 ml/sec.

In all of the regions between the tip of the fuel supply tube and the base of these flames the fuel concentrations vary continuously in the radial direction as a result of the diffusion processes, the richest mixture at any axial position always occurring at the centre of the tube. Further, the fuel concentration at the centreline decreases continuously with increasing height.

The first type of flame of this family to be discussed is that of Figure 19a. This is the complete flame, the lower portion of which had been observed in the ignition procedure of the flame map investigations. This type of flame was the most difficult to manipulate and unless moved very slowly would be blown away. The lowest position at which this completely hemispherical base to the flame could be obtained was 30.4 cm. above the tip of the fuel supply tube for the above flow conditions.

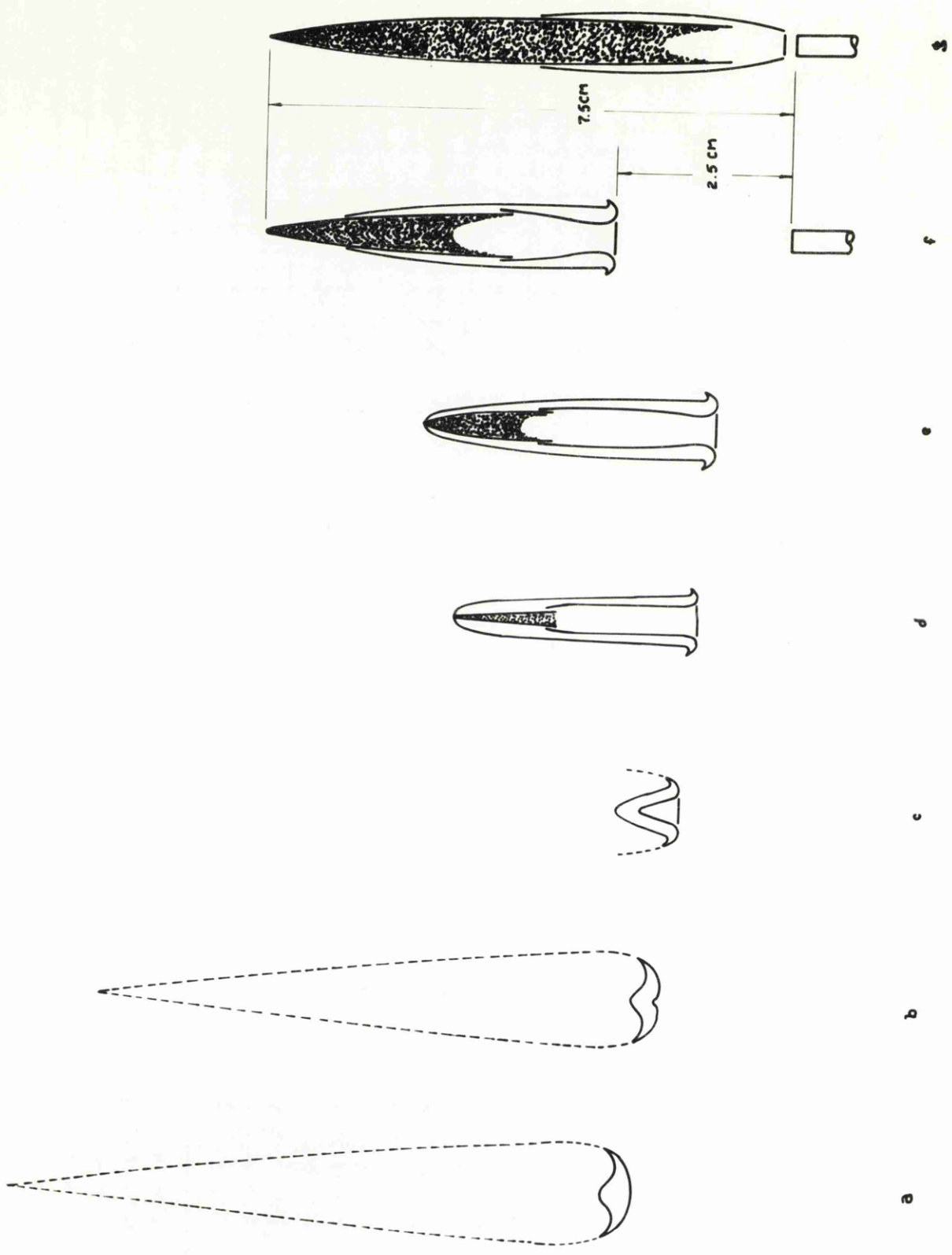


FIGURE 19

The portion of the flame outlined with solid boundaries was a small premixed flame in which reaction appeared to occur throughout the total volume of the flame. That portion of the flame outlined with a broken boundary was a surface of flame only, where the premixed fuel from outside the initial flame was consumed as it diffused into the hot gases above the initial flame.

The second member of this family is the flame shown in sketches 19b and 19c. The highest position at which a distinct flame of this type occurred was 30.1 cm. above the tip of the fuel supply tube. In this flame there is a small cone of an intense blue-green radiation at the centreline and, except for this, the remainder of the flame is identical to that of 19a. At successively lower positions within the range of occurrence of this type of flame the central cone becomes steadily larger, and the surface of flame from the premixed fuel diffusing into the hot gases becomes steadily smaller and merges with the volume of reaction outside the central cone.

The third member of this family consists of flames where luminous carbon occurs at the tip of the inner cone. The highest position of a flame of this type occurs approximately 20 cm. above the tip of the fuel supply tube. In these flames the walls of the inner cone are so nearly vertical that it is difficult to decide whether to call this surface a cone or a cylinder. In this member of the family the outer surface of the flame definitely assumes the characteristics of the carbon-monoxide diffusion flame associated with bunsen flames.

For the flows used in this experiment, when the base of the flame is brought nearer to the tip of the fuel supply tube than 8.5 cm.

the flame assumes the form of the fourth and last member of this family. This type of flame is characterised by the inner reaction surface proceeding from the initial radius of the flame to some minimum radius and then following the surface of a toroid to some larger radius, whence, it forms a surface similar to that of a diffusion flame until it is masked by the radiation from the luminous carbon, the intensity of the radiation from the inner surface decreasing with increasing height along the surface. The whole of this flame is surrounded by a carbon-monoxide diffusion flame. Figure 19f is a dimensioned sketch of this type of flame at the lowest position in which it could be maintained. Any attempt to move the base of this flame to a lower position resulted in the flame immediately assuming the form of the standard flame. The upper reaches of the flame envelope of this lowest member of the family are identical in shape and spatial position to those of the standard flame.

Since all of these flames are stable in space and time, and are stabilised on a premixed flame, the burning velocity at the lowest point of each premixed flame must be equal and opposite in direction to the flow velocity of the gas stream at that point. When the flow velocities are nearly constant in the neighbourhood of the minimum point of the flame profile, the burning velocity at the minimum point of the flame profile must be the maximum of the possible burning velocities in this neighbourhood. The maximum burning velocity for any fuel occurs at a concentration near the stoichiometric air-fuel ratio, the burning velocity becoming progressively lower at leaner and richer mixtures. Thus, if the scope of possible concentrations near the radial locus of the

minima of these flames includes the stoichiometric concentration the minima will occur at this concentration.

One consequence of this condition is that a plot of the minima of the sequence of floating flames will describe the surface of stoichiometric concentration (or near stoichiometric) for the cold interdiffusion process and the base of the lowest flame of the form 19a will occur at the point where the concentration at the centreline is stoichiometric.

The Burke and Schumann solution of the diffusion equation yields exactly the distance from the tip of the fuel supply tube to that point where the concentration at the centreline is stoichiometric when the velocity is constant throughout the transition region. Thus, a comparison of the results of the Burke and Schumann solution with the lowest position of the base of flame type 19a will indicate the effect of the difference in the transition flows. For the Reynolds number of total flow of 1000 and for butane as a fuel, the Burke and Schumann solution indicates that the base of this flame should occur 76 constraint tube diameters above the tip of the fuel supply tube, whereas in this experiment the base of the flame occurs 12.6 constraint tube diameters above the tip of the fuel supply tube. Thus, the form of the velocity profiles in the development region have a very pronounced effect upon the diffusion processes in the cold system.

The experimentally determined height to stoichiometric concentration makes it possible to test the contention that the difference between Burke and Schumann's theory and experiment was due to the difference between the hot and cold coefficients of diffusion. The

coefficient of viscosity of air at 1200°C is 2.8 times the coefficient of viscosity of air at 20°C which will be essentially the ratio of the coefficients of interdiffusion of butane and air at these two temperatures. The value of 1200°C is not the average temperature of the flame, but is nearer the temperature of the reaction surface. If the temperature dependence of this coefficient were the main cause of the difference between the above theory and experiment, then the height to stoichiometric concentration at the centreline could be no greater than 2.8 times the height of the standard flame at the same conditions of flow, whereas the ratio of these two heights from these experiments is 4.0.

The lowermost flame of type 19a is interesting from the aspect of momentum exchange. The maximum burning velocity of butane-air mixtures is approximately 40 cm/sec<sup>(6)</sup> which, then, must be the centreline velocity at the base of this flame. The maximum velocity of the fuel issuing from the supply tube is 45 cm/sec. the maximum velocity in the air stream is approximately 140 cm/sec. and the centreline velocity of the fully developed flow (cold) within the constraint tube is 145 ml/sec. It follows that as the momentum exchange processes have been in action through this region, the centreline velocity has hardly undergone any change; and that this point is still in the intermediate stages of development. The value of  $z/R(\text{Re})$  at this point is 0.024 which is about one fifth the value for full development from an initially constant velocity profile of 0.130<sup>(7)</sup>.

CHAPTER 8

DYNAMIC PARAMETERS OF FLAME HEIGHT

One of the initial objects of this research was to determine the effect upon the flame height of the various dynamic variables, including the form of the velocity profiles.

In the preliminary experiments it was established that the principal variables were the relative flame height, that is, the ratio of the height of the flame to the bore of the fuel supply tube; the fuel Reynolds number based on the bore of the fuel supply tube; and the air-fuel ratio. Of the dynamic variables outlined in Chapter 1, the fuel Reynolds number is the only one which can be readily varied while holding the remaining dynamic variables constant. This is accomplished, for a given fuel supply tube and constraint tube, by altering the fuel flow and the air flow simultaneously in such a manner that the air-fuel ratio is constant. Thus, the influence of the remaining dynamic variables can be examined on the basis of their parametric effect upon the characteristic curve of the relative flame height as a function of the fuel Reynolds number at a constant air-fuel ratio. The reference value of the air-fuel ratio chosen for use in these studies is 100, as was used in the preliminary experiments. Once a reference value for the air-fuel ratio has been chosen it is possible to examine the parametric effect of the dynamic variables upon the characteristic curve of the reduced flame height as a function of the air-fuel ratio. The reduced flame height is defined as the ratio of the height of the observed flame to the height of a flame at the reference air-fuel ratio and at the same fuel Reynolds number. Thus, the product of the reduced flame height and the

characteristic relative flame height will result nominally in the relative flame height at any prescribed point in the fuel Reynolds number - air-fuel ratio space.

As has been indicated in Chapter 3, the diameter ratio can be altered by changing either the fuel supply tube or the constraint tube. Thus, one of these tubes must be considered to control the scale of the experiment and the remaining tube to control the diameter ratio. In correlating the results of the preliminary experiments with those of Barr (Appendix II, Departure from Dynamic Similarity) complete correlation was accomplished by attributing a parametric effect to the diameter ratio when the constraint tube was assumed to determine the scale of the experiment. In the results to be presented in this discussion, the assumption that the constraint tube controls the scale is substantiated.

The 2.400 cm. bore constraint tube was chosen as the reference scale of these studies. Fuel supply tubes of 0.874 cm. bore, 0.585 cm. bore, 0.402 cm. bore and 0.295 cm. bore were successively mounted within this constraint tube to establish the diameter ratios of 2.75, 4.10, 5.96 and 8.14.

The relative flame heights as a function of the fuel Reynolds number of butane from the experiments with these four diameter ratios are presented in the graph of Figure 20. The results are essentially identical up to a Reynolds number of 100, after which there are slight divergences. The divergences for fuel Reynolds numbers greater than 100 appear to be related to the rapid movement of the smoke point at these Reynolds numbers to higher air-fuel ratios as shown in Figure 14b. The results which lead to this deduction will be discussed later.

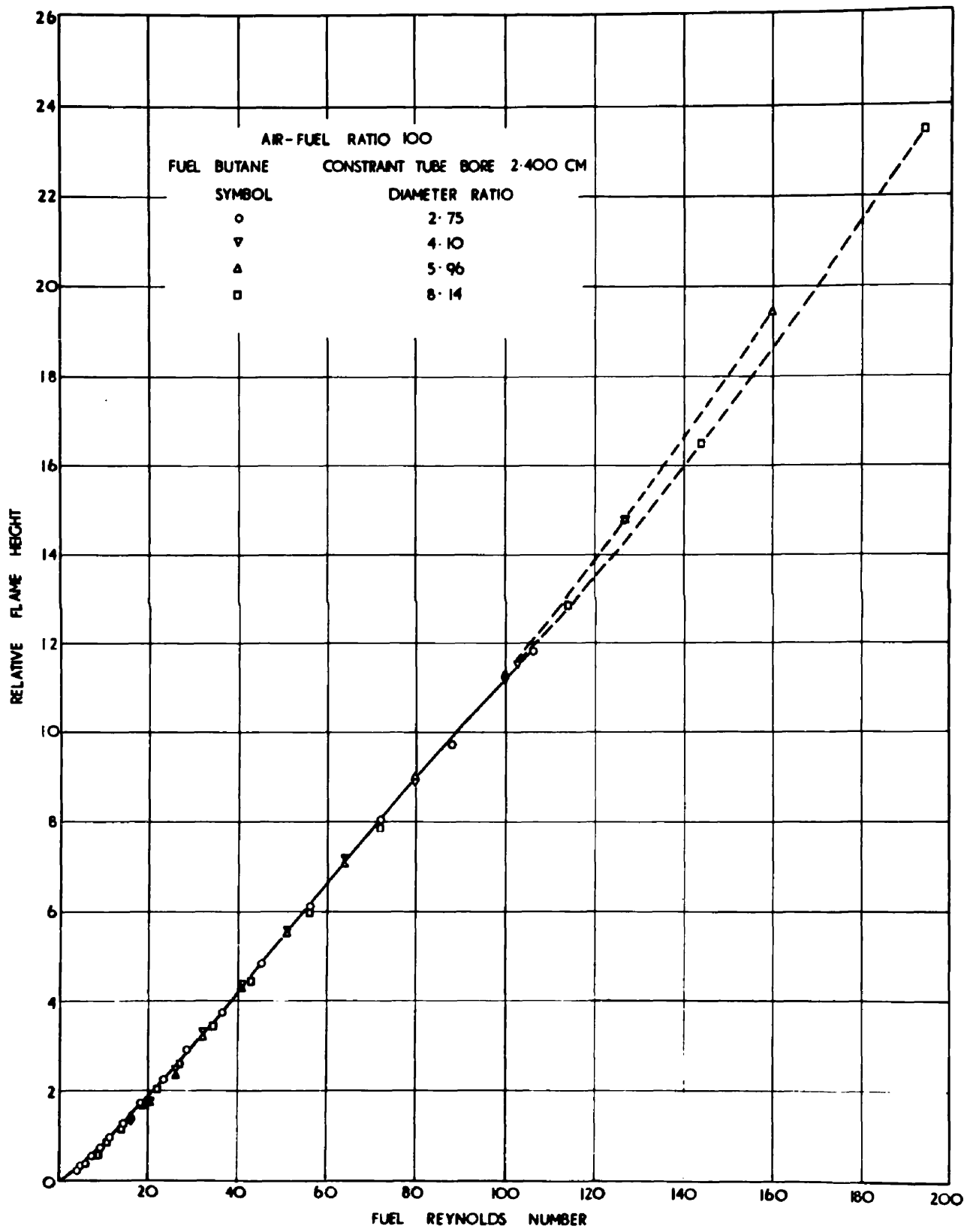


FIGURE 20

That portion of the relative flame height - fuel Reynolds number curve which is common to the four diameter ratios could arise from one of two effects: either both the diameter ratio and the ratio of the average velocities of the two streams do not have an effect upon the characteristic curve, or they have equal and opposite effects. The effect of the velocity ratio was investigated at a single point by adding oxygen free nitrogen to a constant fuel flow. In this way the velocity ratio was altered without altering the chemical ratio of the air and fuel. The only chemical effect of this addition would then be a slight reduction in the flame temperature. When a volume flow of nitrogen 3.1 times that of the fuel was mixed with the fuel the relative flame height was reduced 1%: and when a volume flow of nitrogen 3.98 times that of the fuel was mixed with the fuel the flame height was increased 0.1%. From these experiments it was concluded that the velocity ratio did not have any effect upon the relative flame height. Since the velocity ratio and the diameter ratio have equal and opposite effects upon the relative flame height, and the velocity ratio does not have an effect it follows that the diameter ratio cannot have an effect upon the relative flame height.

The reduced flame heights as a function of the air-fuel ratio for these four diameter ratios at fuel Reynolds numbers of 44 and 50 are presented in Figure 21. These results are derived from the ratio of the two experimental measurements so that errors are cumulative and a 3% error in the air-fuel ratio is possible. These curves by the definition of the reduced flame **height** must pass through unity at an air-fuel ratio of 100. There appears to be a slight dependency upon the diameter ratio

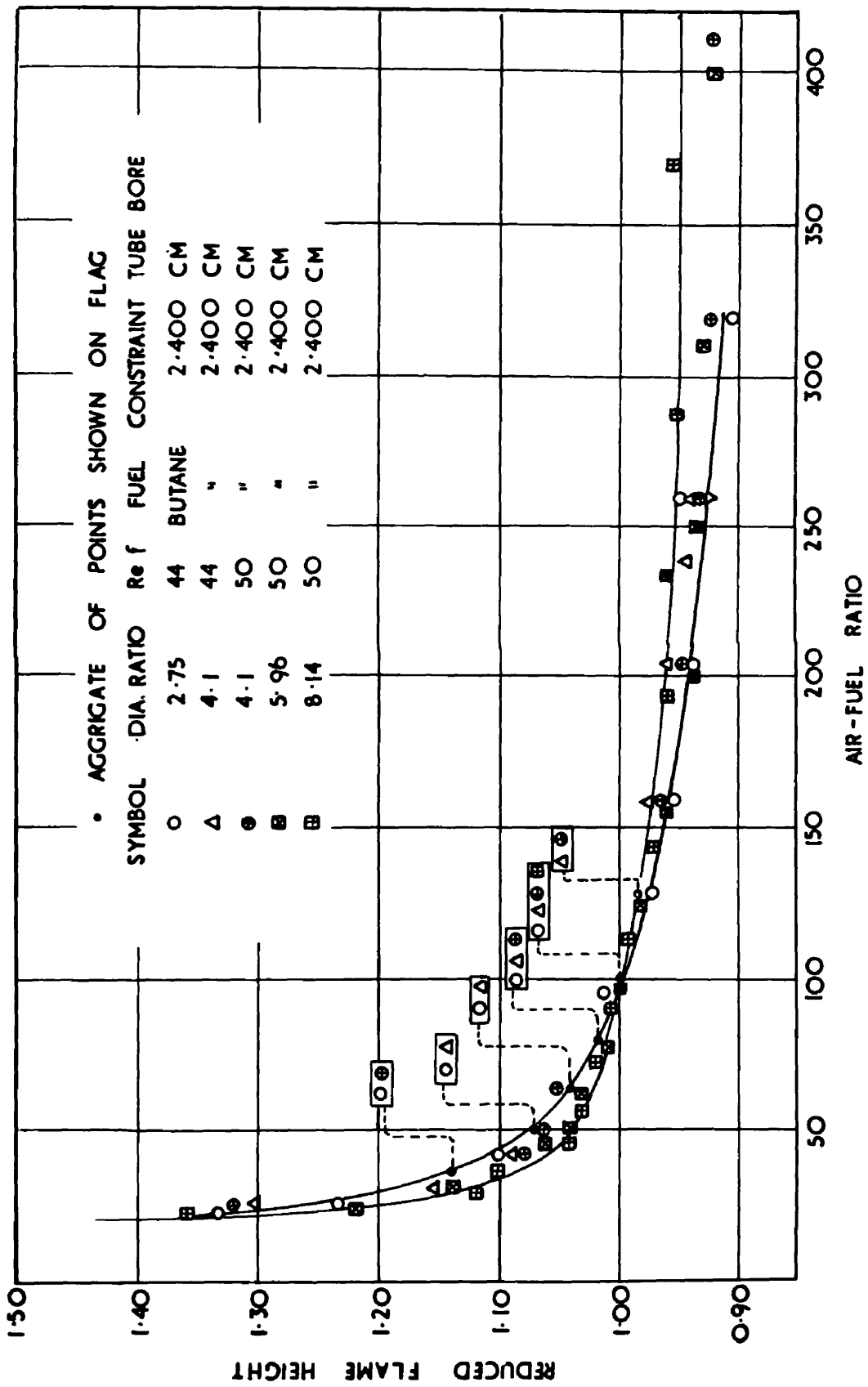


FIGURE 21

for these results in contrast to the lack of this effect upon the relative flame height. Thus, either the diameter ratio or the velocity ratio has a parametric effect upon the characteristic curve of reduced flame height such that the asymptotic value of the reduced flame height is more nearly attained at an air-fuel ratio of 100, the larger the diameter ratio.

In order to further assess the effects of the diameter ratio upon the relative flame height, the four fuel supply tubes were mounted within a 1.600 cm. bore constraint tube, when the diameter ratios of 1.83, 2.75, 3.97 and 5.41 were established.

The relative flame heights as a function of the fuel Reynolds number for these experiments are presented in the graph of Figure 22. Again all of the results lie on a common curve which is, however, about 10% lower than the common curve of Figure 20, shown as a broken line in Figure 22. The diameter ratio of 2.75 is common to both curves, so that for these two particular curves all of the dynamic parameters are identical, the only difference in the two experiments being the scale. Therefore, this 10% difference in the results must be the result of the difference in the scale.

The results from the 0.402 cm. bore and 0.295 cm. bore fuel supply tubes mounted within a 3.600 cm. bore constraint tube, giving diameter ratios of 8.95 and 12.2, presented in Figure 23 further demonstrate the effect of scale. The results for the diameter ratio of 8.14 from Figure 20 are also presented for comparison. The results of the experiments with the 3.600 cm. bore constraint tube form a common curve about 5% above those of the 2.400 cm. bore constraint tube.

AIR-FUEL RATIO = 100  
FUEL - BUTANE CONSTRAINT TUBE BORE 1.600CM  
SYMBOL DIAMETER RATIO  
○ 1.63  
□ 2.75  
△ 3.97  
▽ 5.41

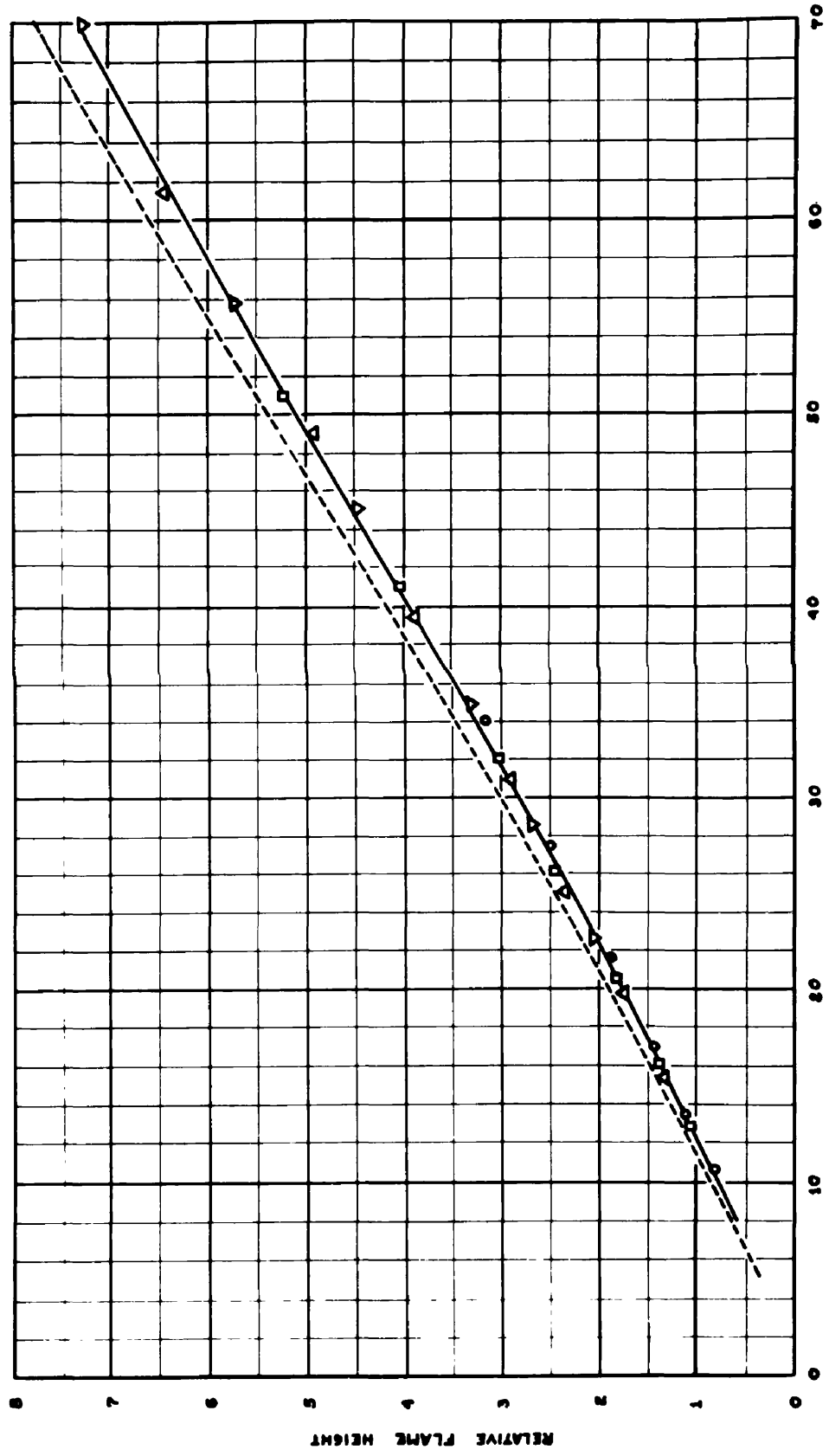


FIGURE 22

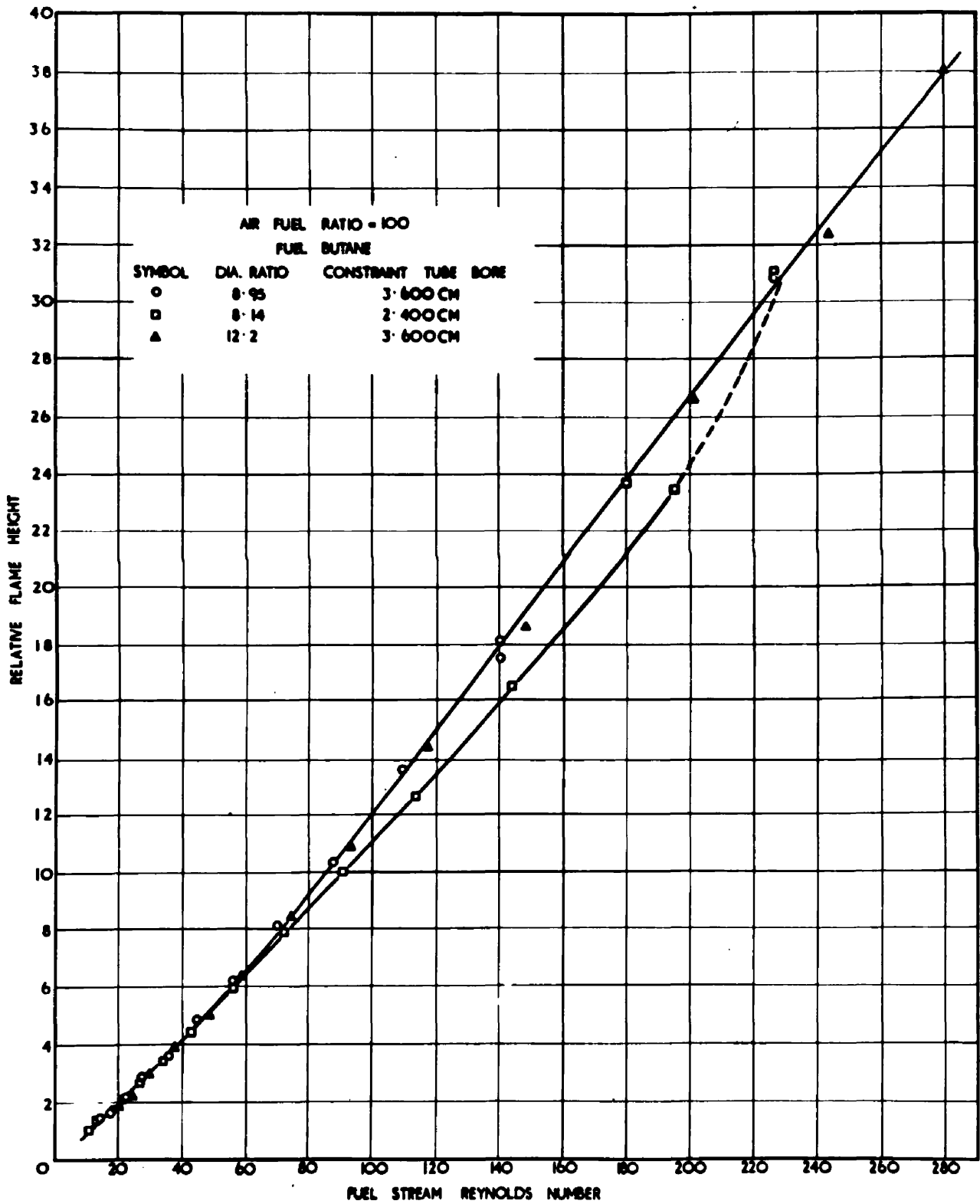


FIGURE 23

The behaviour of the relative flame height within a particular scale is essentially that of a purely radial phenomenon which is shown by the linear relationship of the relative flame height to the fuel Reynolds number. The pronounced effect of scale upon the coefficient of the Reynolds number in this relationship is an anomaly which has not been resolved.

Figure 24 shows the reduced flame height as a function of the air-fuel ratio, for the same diameter ratios and scale as those of Figure 23, at fuel Reynolds numbers of 50 and 90. These results show even more strikingly the effect of the diameter ratio on the reduced flame height. In these results the asymptotic value of the reduced flame height is essentially attained at an air-fuel ratio of 100.

In order to assess the effect of the density ratio upon the characteristic curves different fuels were used in the burner consisting of the 0.874 cm. bore fuel supply tube within the 2.400 cm. bore constraint tube.

The relative flame heights as a function of fuel Reynolds number for butane, propane and methane along with a single point at a fuel Reynolds number of 50 for ethane are presented in the graph of Figure 25. These curves show a distinct dependence upon the fuel. The experiment in which butane was diluted with nitrogen indicates that this dependence can neither be an effect of the velocity ratio nor the density ratio, since the nitrogen reduced the butane-air density ratio of 2.07 to a density ratio of 1.2. Thus, this effect is probably of a chemical nature. The behaviour of the methane is anomalous in that the other three fuels follow a pattern of decreasing slopes as the number of carbon atoms in the

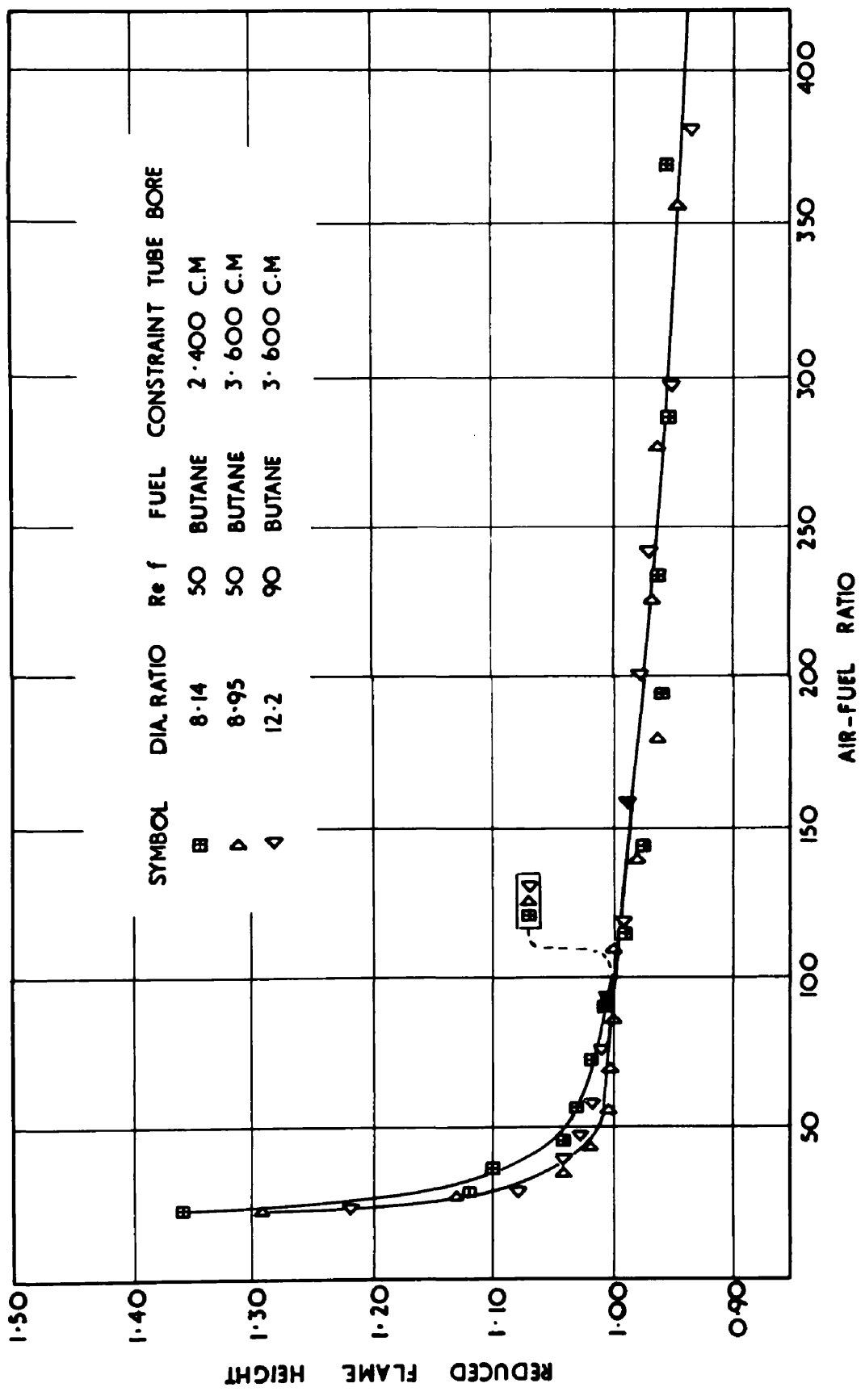


FIGURE 24

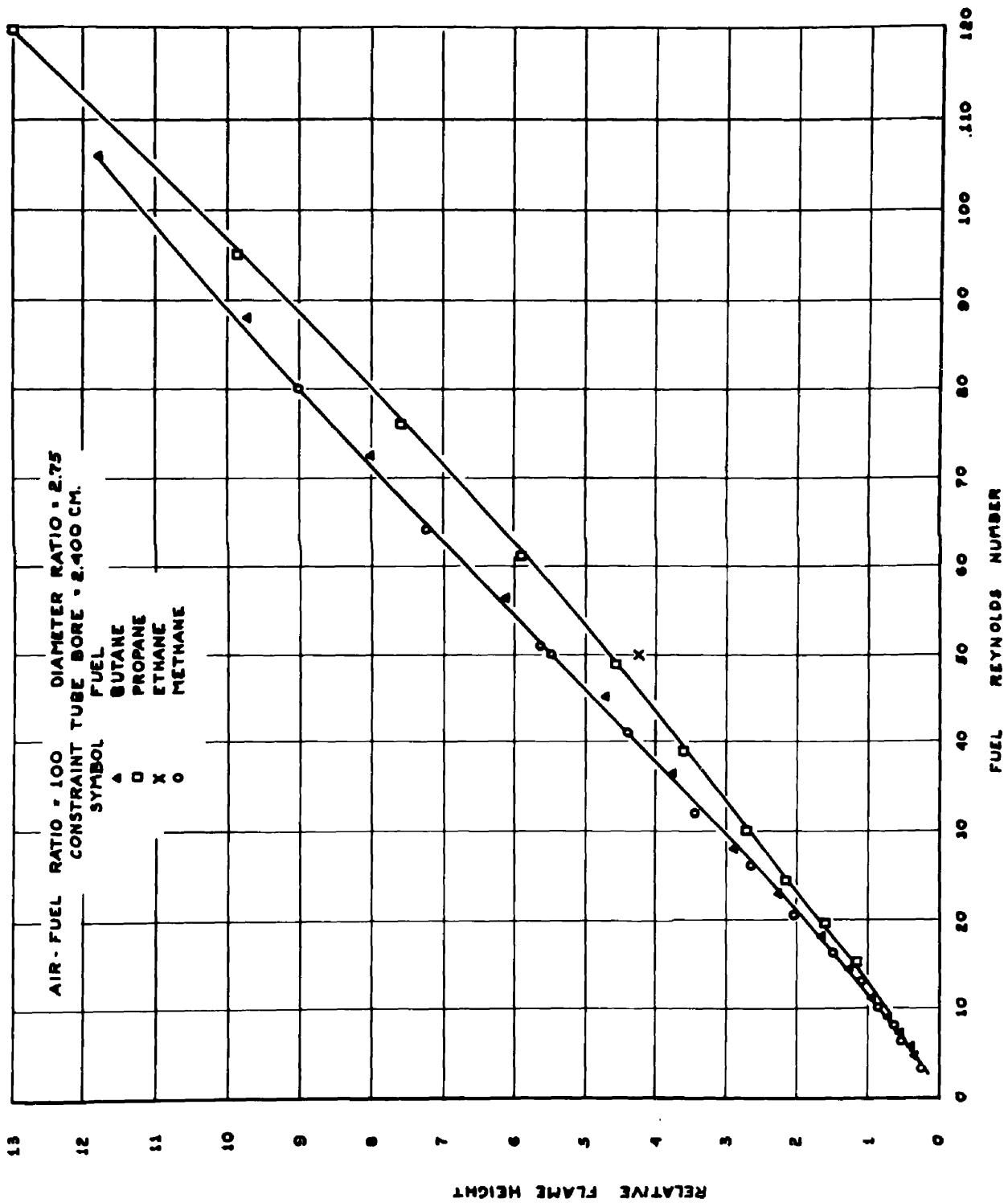


FIGURE 25

molecule is decreased, the exception being methane for which the slope is coincident with that of butane. There are two characteristics of the fuel that change proportionally with the number of carbon atoms in the molecule. The ratio of hydrogen atoms to carbon atoms increases with a decreasing number of carbon atoms and the viscosity of the gas decreases with a decreasing number of carbon atoms. One feature which indicates that the density ratio might have an effect upon these results is the anomalous behaviour of methane and the fact that it is the only gas of those employed for which the density is less than that of air.

The reduced flame heights as a function of air-fuel ratio for the four fuels used in this burner are presented in Figure 26. These results indicate a slight dependence of the reduced flame height upon the density ratio. Thus, either the ratio of the density of the air to the density of the fuel or the velocity ratio has a parametric effect upon the reduced flame height such that the asymptotic value of the reduced flame height is more nearly attained at an air-fuel ratio of 100, the larger the density ratio. The same effect was observed to be a result of either the diameter ratio or the velocity ratio in a previous set of experiments. The velocity ratio is altered in the same manner by increasing either the diameter ratio or the density ratio so that an effect which is observed as a result of increasing either of these directly controlled variables is probably the result of the common secondary variable, the velocity ratio.

It is to be expected that any variation which changes the velocity ratio will have an effect upon the behaviour of the reduced flame height as a function of the air-fuel ratio, since varying the air-fuel ratio alters

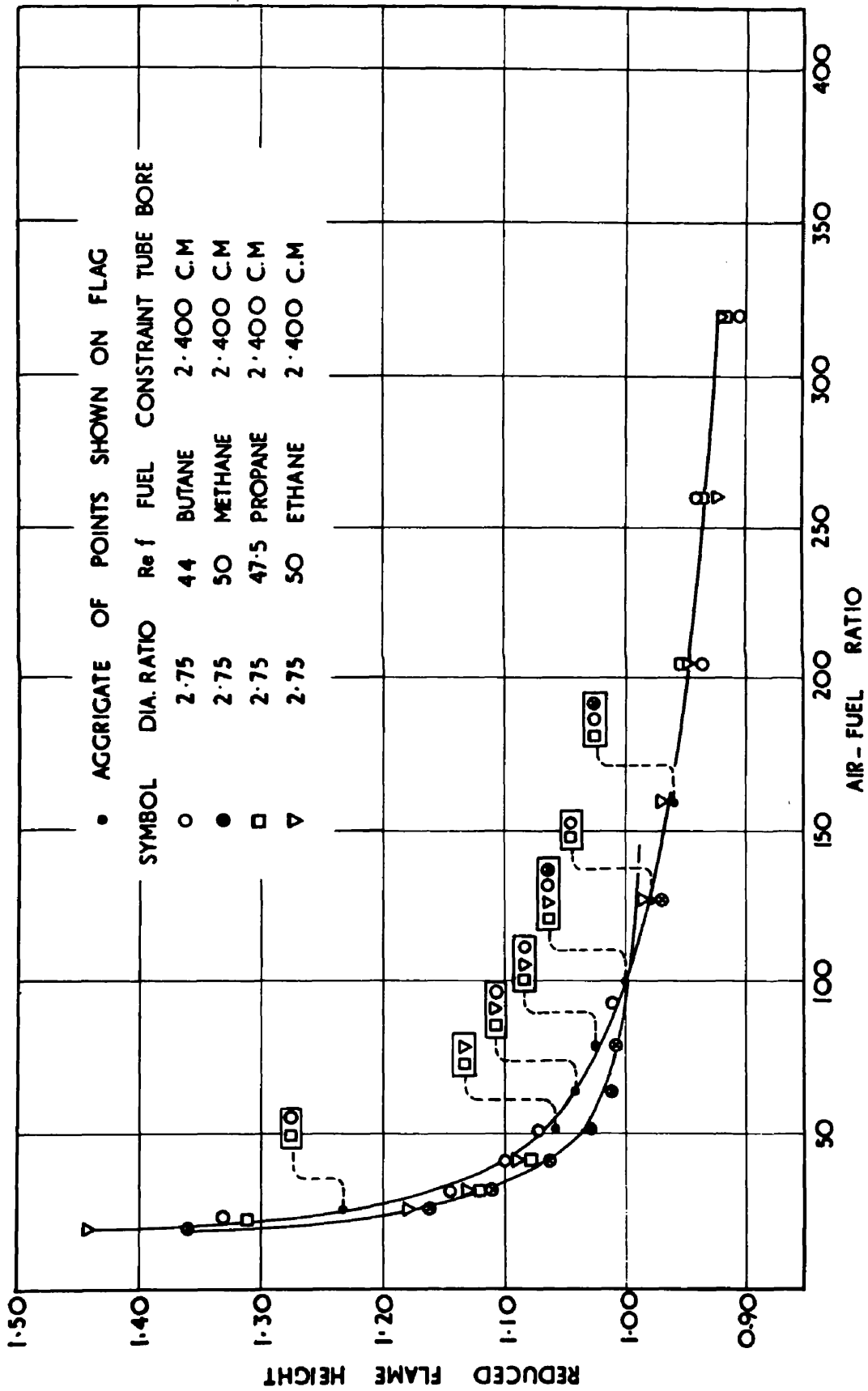


FIGURE 26

the velocity ratio as well as the amount of oxygen available to the reaction. The surprising feature of these results is that the effects of changing the velocity ratio by means of the diameter ratio are opposite to the effects of changing the velocity ratio by means of the air-fuel ratio. That is, if the effects of varying the air-fuel ratio were solely due to the change in the velocity ratio and the air-fuel ratio of 100 was one quarter the asymptotic air-fuel ratio, then doubling the diameter ratio would result in the air-fuel ratio of 100 being one sixteenth the asymptotic air-fuel ratio. However, when the air-fuel ratio of 100 is one quarter the asymptotic air-fuel ratio doubling the diameter ratio results in the air-fuel ratio of 100 becoming about one half the asymptotic air-fuel ratio.

The parametric effect of the form of the velocity profiles upon the principal variables is the most difficult to assess as this must be done by comparing different experiments in which several parameters might be varied. It has been established that the approach velocity profiles of the flow system used by Barr differ slightly from the fully developed axially symmetrical approach velocity profiles of this study. It is also known that the approach velocity profiles of the author's preliminary experiments using the 0.83 cm. bore constraint tube differ considerably from these fully developed flows. It is possible, therefore, to compare the results from these three sets of experiments in which the scale and the diameter ratio of the two tubes were nearly matched, but the shapes of the velocity profiles were different.

The relative flame heights as a function of the fuel Reynolds number for these three experiments are presented in Figure 27. The fact

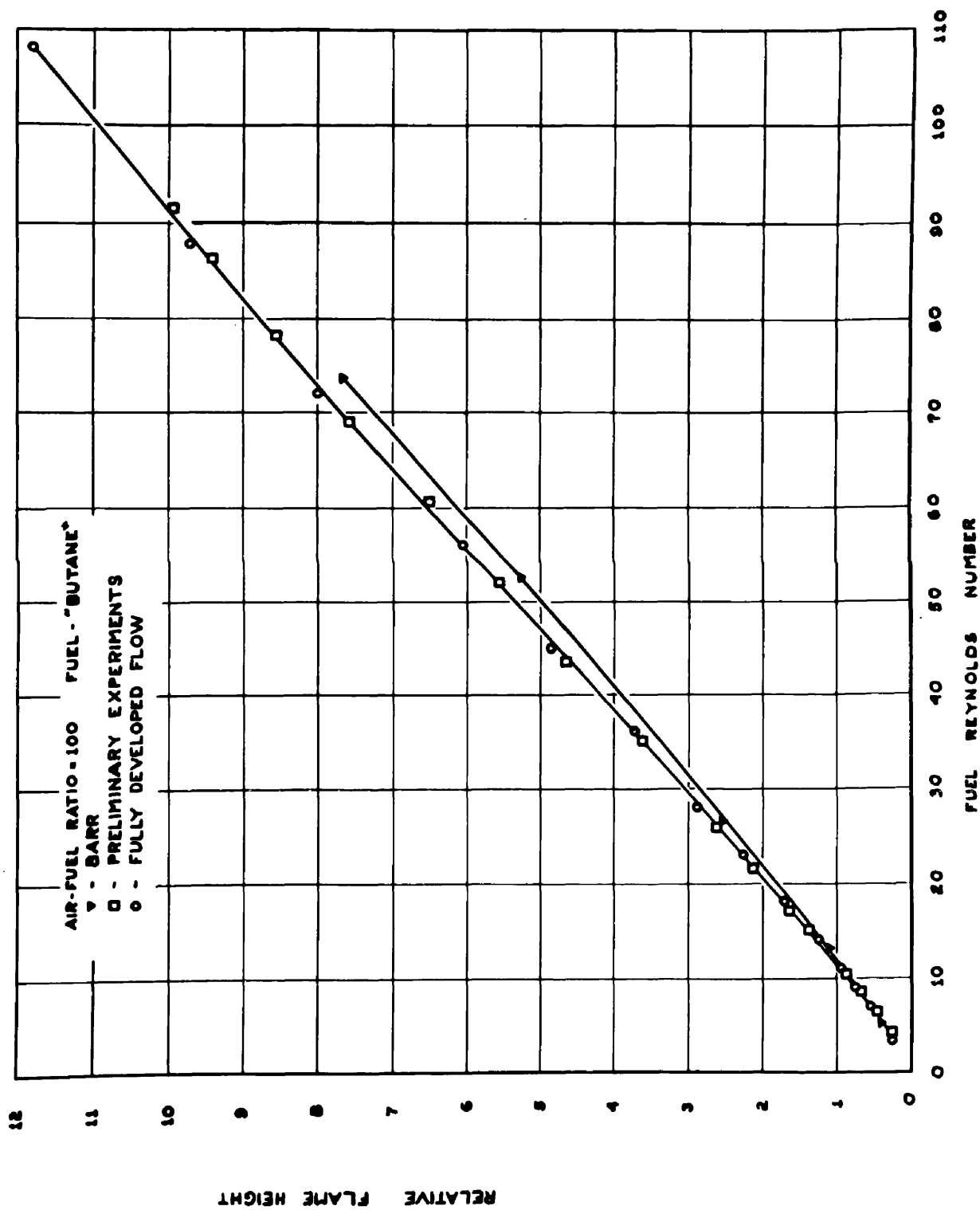


FIGURE 27

that the results from Barr lie below those results from the fully developed flows is consistent with the 10% difference in the scales between the two experiments. Since the results from the 0.83 cm. burner of the preliminary experiments are at the same scale as the results from Barr it can be deduced that the difference between these results is due to the difference in the velocity profiles, so that there appears to be some dependence of the relative flame heights upon the form of the approach velocity profiles.

The reduced flame heights as a function of the air-fuel ratio for the same three experiments are presented in Figure 28. The shape of the velocity profiles have a very decided effect upon these characteristic curves. The more severe the velocity gradient within the air stream at the wall of the fuel supply tube, the further the reduced flame height at an air-fuel ratio of 100 is removed from the asymptotic value.

The reduced flame height, therefore, appears to be sensitive, to some extent, to all of the dynamic variables. However, before any deductions can be formed concerning the effect of the variables upon the reduced flame height curve, the problem of the existence of an asymptote to this curve must be resolved. The constant velocity solutions of the diffusion equations indicate that the flame height will be increased as the flow velocity is increased and the study of momentum exchange indicates that the velocities within the fuel portion of the flow stream will be increased as the air-fuel ratio is increased at a constant fuel Reynolds number. Thus, from these considerations the flame height should be increased rather than decreased as a result of increasing the air-fuel ratio. The asymptote could be the result of this effect being counter-

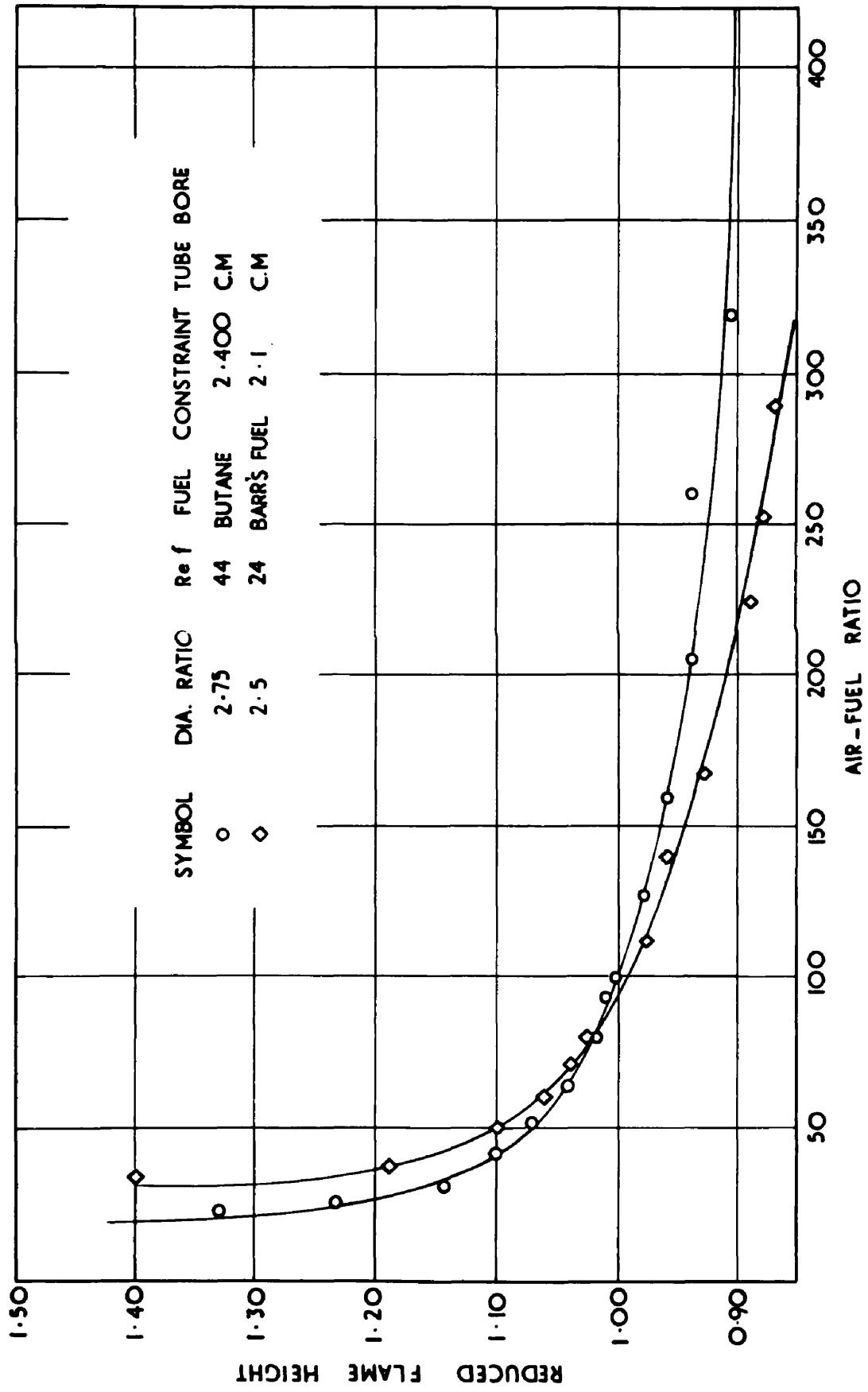


FIGURE 28

balanced by the increase in the amount of oxygen available to the flame, but there is not sufficient evidence to clearly verify this possibility.

The relative flame height as a function of the fuel Reynolds number at a constant air-fuel ratio is essentially independent of the dynamic parameters of diameter ratio, velocity ratio, and density ratio; and is slightly dependent upon the scale of the system, the chemistry of the fuel and the form of the velocity profiles.

The equation which describes the curve of the common points of Figure 20 is:

$$\frac{y}{B} = 0.113 \text{ Re}_f - \frac{2.64}{6.76 + \left(\frac{\text{Re}_f - 30}{10}\right)^2} \dots\dots\dots 8.1$$

where (y) is the flame height, (B) is the bore of the fuel supply tube and (Re<sub>f</sub>) is the fuel Reynolds number. The results of the preliminary experiments for the 0.28 cm. bore fuel supply tube system all lie on this curve when the Reynolds numbers are recalculated according to the flow correlations of Chapter 5. This equation is dominated by the linear coefficient of the Reynolds number, which indicates that the controlling mechanism of these flames is a purely radial molecular transport phenomenon. From the behaviour of the reduced flame height results it would appear that this relationship is particularly valid where the reduced flame height has attained its asymptotic value.

The non-linear behaviour of the relative flame height at high fuel Reynolds numbers, at an air-fuel ratio of 100, appears to be a result of the shift of the smoke point to the air-fuel ratios approaching 100 as the Reynolds numbers are increased. If the above relationship (equation 8.1)

is strictly applicable to the case of the asymptotic value of the reduced flame height, then when the whole reduced flame height curve is moved to higher air-fuel ratios along with its right hand asymptote (the smoke point) it can be expected that the relative flame height at an intermediate air-fuel ratio will be increased to some value greater than that given by the above relationship.

Thus, although according to equation 8.1 the relative flame height divided by the Reynolds number has been established as a particular position within the region of the fluid dynamic development space  $z/R(Re)$ , a second variable (the reduced flame height) which appears to respond to the complex physico-chemical processes within the flame has been bared as a primary ponderable of these systems.

CHAPTER 9

MULTIPLE SPECIES INTERDIFFUSION

Any complex physico-chemical mechanism which occurs within the flame must be a manifestation of intermolecular collisions and molecular transport. The several rate terms applied to gaseous processes are simply descriptive of the particular manifestation of concern such as the coefficient of diffusion, the coefficient of viscosity and the coefficient of heat conduction.

The enclosed laminar diffusion flames are dominated by some such mechanism since the flame height is essentially proportional to the fuel Reynolds number. The Reynolds number, by virtue of being written in terms of one of these coefficients of transport manifestation, is representative of molecular transport effects. The results reported in Chapter 7 indicate that the difference between the height of anchored flames and the height to the stoichiometric fuel concentration at the centreline cannot be completely attributed to the effect of temperature upon the coefficient of diffusion. This then leads to the possibility that the inadequacy of the Burke and Schumann solution lies in the assumption of a two gas system.

In order to evaluate this question a simplified concept of multiple species interdiffusion with chemical reaction was devised, based on the concept of self diffusion.

Each of the gases involved has a different coefficient of self diffusion which is proportional to the kinematic viscosity of that gas. This relationship introduces a point which has been the cause of some debate.

The dynamic viscosity of the gas is independent of the pressure so that the kinematic viscosity, which is the ratio of the dynamic viscosity to the density, will be dependent upon the density of the gas. As a consequence, the coefficient of self diffusion will be dependent upon the density of the gas. In the Ficks law form of the diffusion equation this would give the impression that the coefficient of diffusion was dependent upon the local concentration of the gas; whereas, within the concept of self diffusion, the density used to determine the kinematic viscosity should be the thermodynamic density, that is the density of the gas at the total pressure and temperature of the mixture. This is a fundamental point in determining the coefficients for the process of multiple species interdiffusion.

The fundamental diffusion equations are always written for a two gas process, that is, a process in which the gas of concern diffuses into a second gas. If the second gas is considered as a hypothetical medium which consists of massless force centres whose frequency of distribution is that of any gas at the conditions of pressure and temperature applicable to the field, then the frequency and nature of the collisions will be the same as those for self diffusion, and the concentration term of the diffusion equation becomes the local density of the gas of concern. If all of the other gases in the system are considered to exhibit the properties of the hypothetical gas with respect to each gas of concern in turn, then each of the gases can be considered separately as behaving according to the description of self diffusion.

Then, in an axially symmetrical system where axial diffusion can be neglected and the coefficient of diffusion is constant for all radii,

the diffusion equation for any species (i) can be written in terms of the local densities as:

$$r \frac{d\rho_i}{dt} = D_i \frac{\partial}{\partial r} \left( r \frac{\partial \rho_i}{\partial r} \right) \dots\dots\dots 9.1$$

where ( $\rho_i$ ) is the local density of the species, (r) is a general radius, (t) is time, and ( $D_i$ ) is the coefficient of self diffusion of the species.

If the radius of the constraint tube is assumed to be constant and, as employed by Burke and Schumann, the velocity is assumed to be constant in both the radial and axial directions, then equation 9.1 can be rewritten in terms of this constant velocity (v) and the density gradient in the axial (z) direction as

$$rv \frac{d\rho_i}{dz} = D_i \frac{\partial}{\partial r} \left( r \frac{\partial \rho_i}{\partial r} \right) \dots\dots\dots 9.2$$

The total derivative of density includes sources and sinks.

When this source term is separated from the total derivative, the coefficient of diffusion is written in terms of the kinematic viscosity and equation 9.2 is rearranged it becomes:

$$v \frac{\partial \rho_i}{\partial z} = vS_i + \frac{1.4}{r} \frac{\mu_i}{\rho_{ri}} \frac{\partial}{\partial r} \left( r \frac{\partial \rho_i}{\partial r} \right) \dots\dots\dots 9.3$$

where ( $+S_i$ ) is the linear rate of generation of the species in units of density per length, ( $\mu_i$ ) is the dynamic viscosity of the species and ( $\rho_{ri}$ ) is the density of the species at the conditions of pressure and temperature of the interdiffusion. This equation is applicable to each species separately, and the equations for the various species are interconnected by the requirement that the sum of the generation and consumption of species throughout all of the species, in terms of density, must be zero.

In order to bring these several equations of the form of equation 9.3 into a dimensionless form the density or the viscosity of each species is divided by the average density or viscosity across the cross section at the tip of the fuel supply tube, and the lengths (r and z) are divided by the radius of the constraint tube. The dimensionless form of equation 9.3, where the dimensionless form of a variable is denoted by a prime, is:

$$\frac{\partial \rho'_i}{\partial (z'/Re)} = (Re) S'_i + \frac{1.4}{r'} \frac{\mu'_i}{\rho'_{ri}} \frac{\partial}{\partial r'} \left( r' \frac{\partial \rho'_i}{\partial r'} \right) \dots\dots 9.4$$

These equations can then be treated by computer techniques by considering each species separately, with its own coefficient of diffusion. The method of introducing reaction into the problem is dependent upon a property of finite difference techniques and the mean value theorem of the calculus. Over some sufficiently small distance along the axis the radial rate of molecular transport, that is the left hand term of equation 9.4, will be constant. At the reaction surface the transport to the surface over this small interval will be equal to the rate of consumption of the species, as the radial rate of transport through the surface must be zero due to the reaction. From this characteristic it is possible to determine the quantity of a species which would have entered into the reaction throughout this interval by considering the diffusion processes to have been active in transporting this species into a small volume across the reaction surface from the source of the species. This quantity of the species and the appropriate quantity of its opposing reagent can then be removed from the small volume and reentered into the same volume as the species or species which result from the chemical reaction.

As a preliminary test of the set-up of this problem for the computer and the use of the viscosity-diffusivity relationship, the boundary of stoichiometric concentration for air and methane interdiffusion was determined for a diameter ratio of 10 so that these results could be compared with the evaluation in Appendix II of the Burke and Schumann solution. This system was treated, however, as a three gas system with the oxygen and nitrogen of the air diffusing separately. The results of this calculation agreed very well with the graphical solution of the Burke and Schumann method for determining the same boundary.

The case of the interdiffusion of methane and air with reaction was then treated in which the mixture of water vapour and carbon-dioxide produced from the reaction was considered as a single gas. The flame profile from these calculations is shown in Figure 29. This method of calculation permits the determination of the mass of fuel at any axial position as well as determining the flame boundaries, so that the fraction of initial fuel which has been consumed between the tip of the fuel supply tube and various positions along the flame is also noted on this figure. Surprisingly, having regard to the severe concentration gradients introduced by the reaction, the results from the solution with reaction indicate a flame boundary quantitatively almost identical with that of the Burke and Schumann solution.

Figures 30, 31, 32 and 33 are density distributions along the flow of the various species within the system. Smith and Gordon<sup>(10)</sup> experimentally determined the distribution of all identifiable species at three positions along the axis of an open diffusion flame of methane in air.

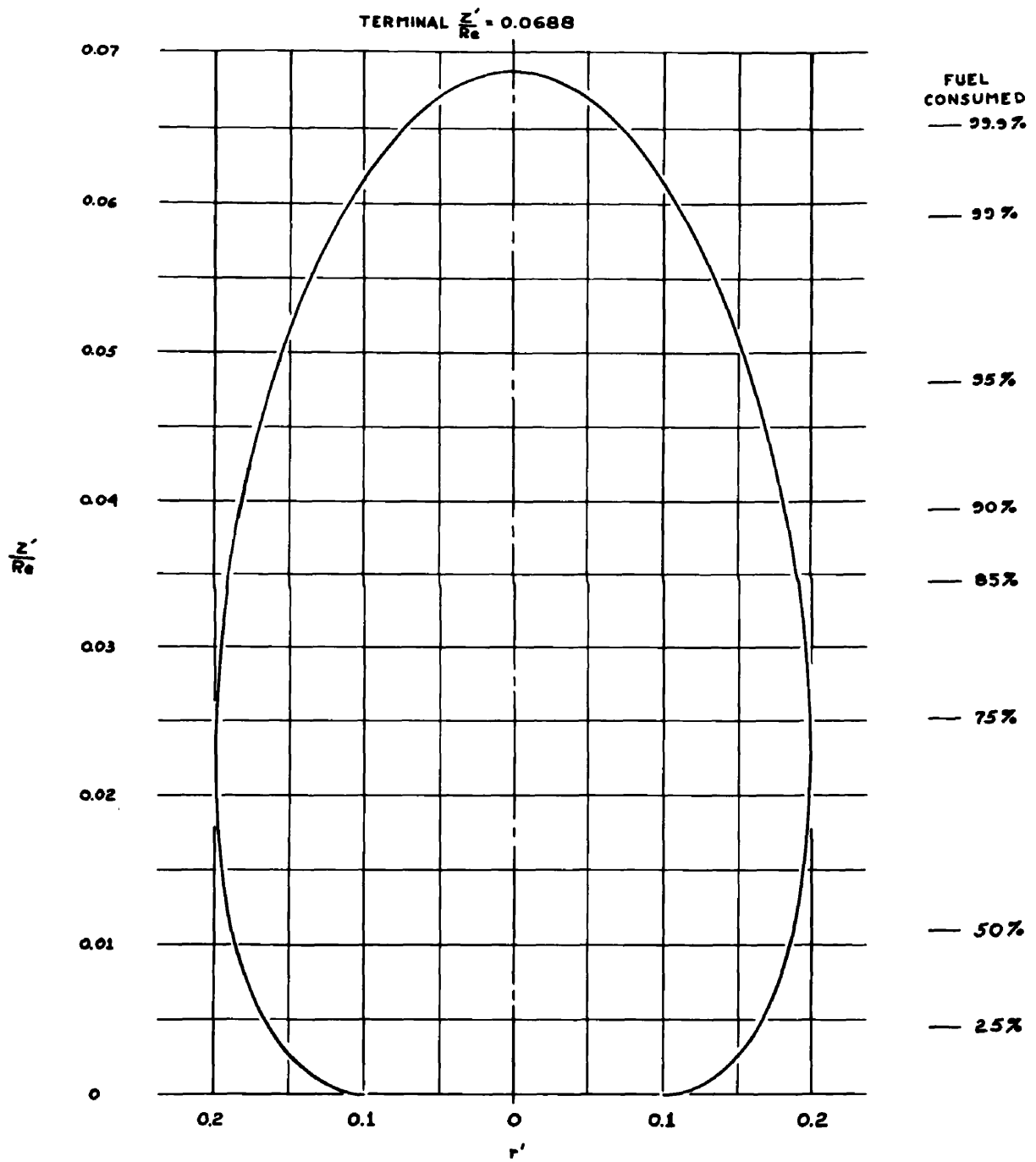


FIGURE 29

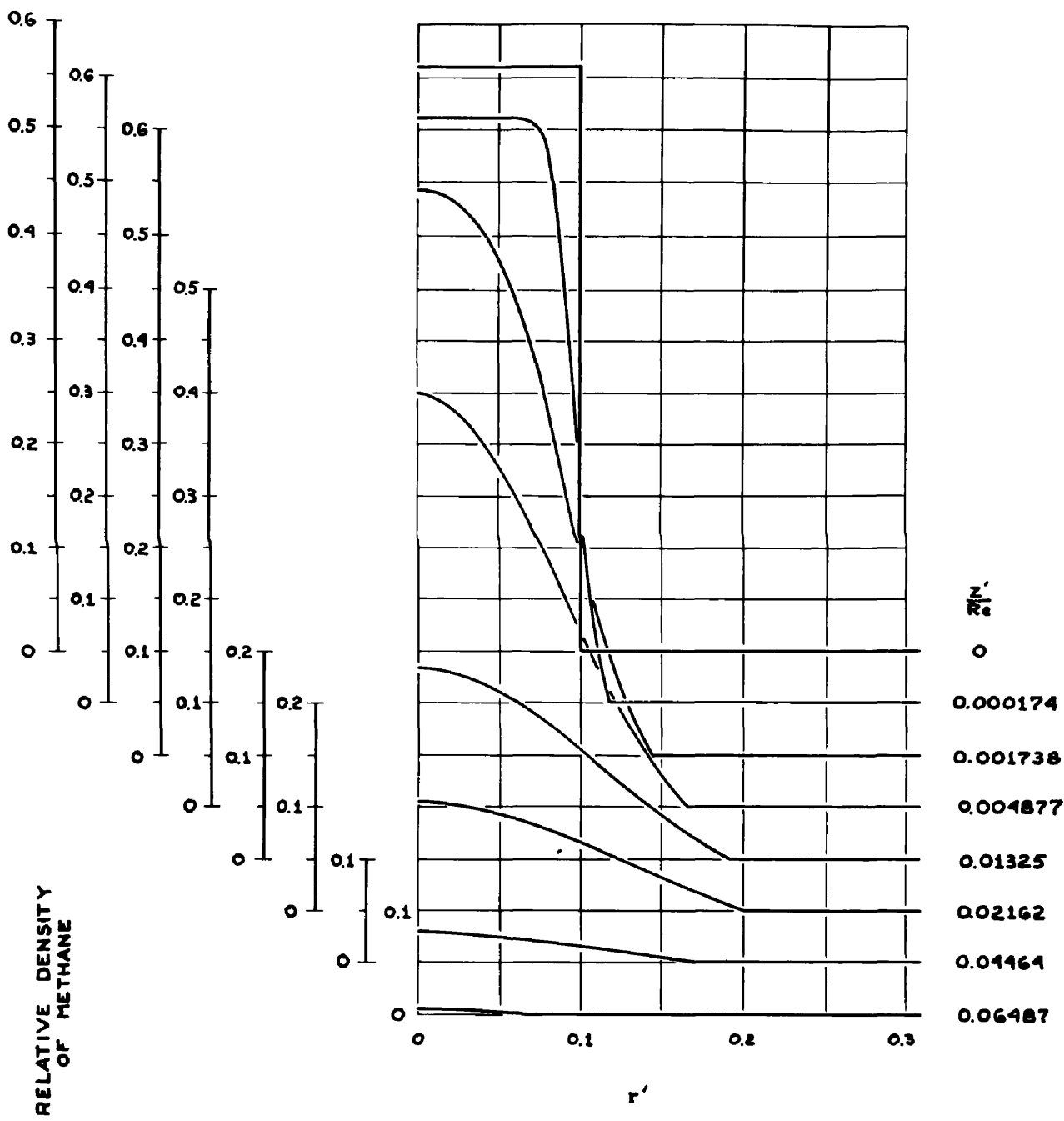


FIGURE 30

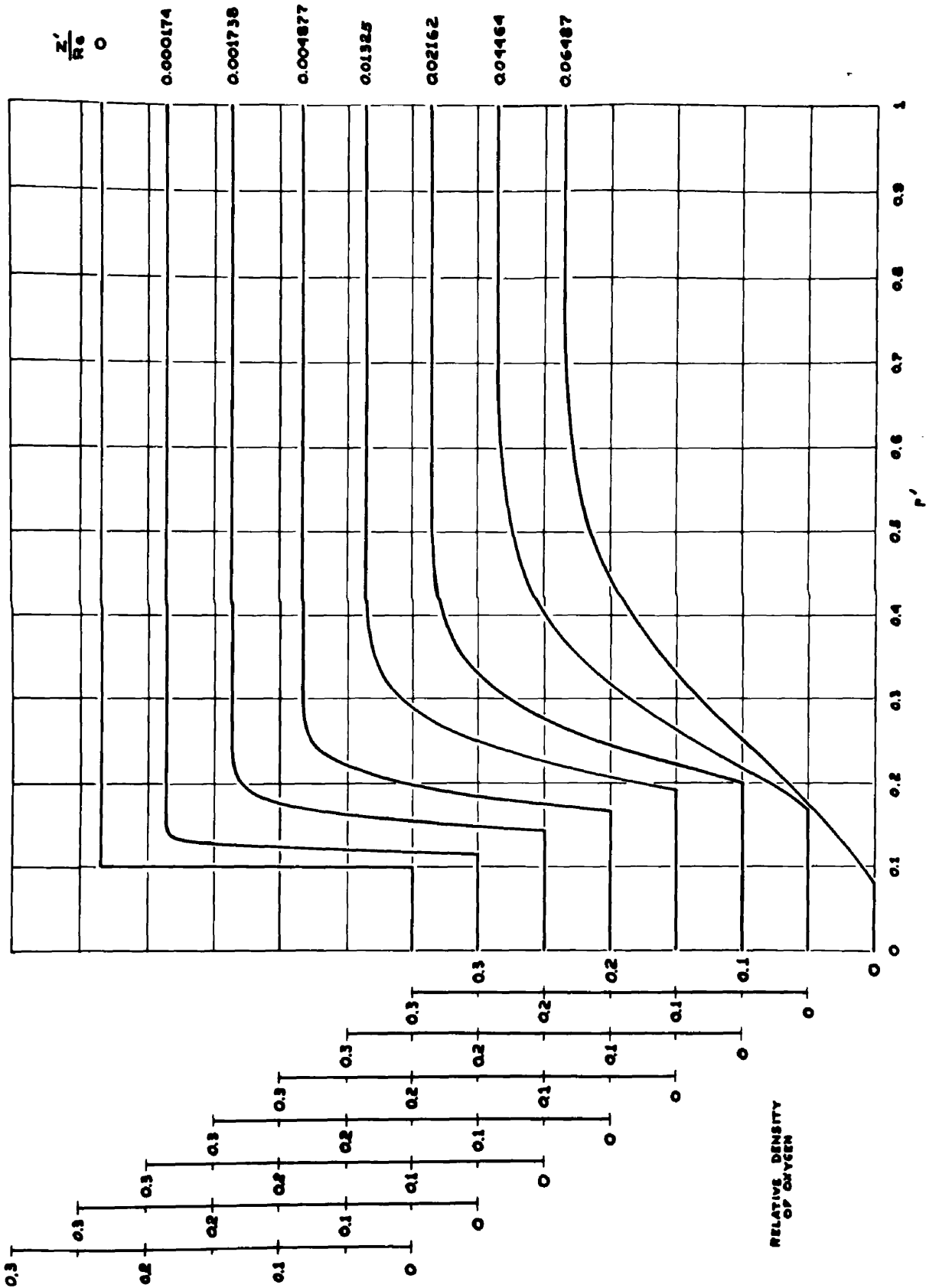


FIGURE 31

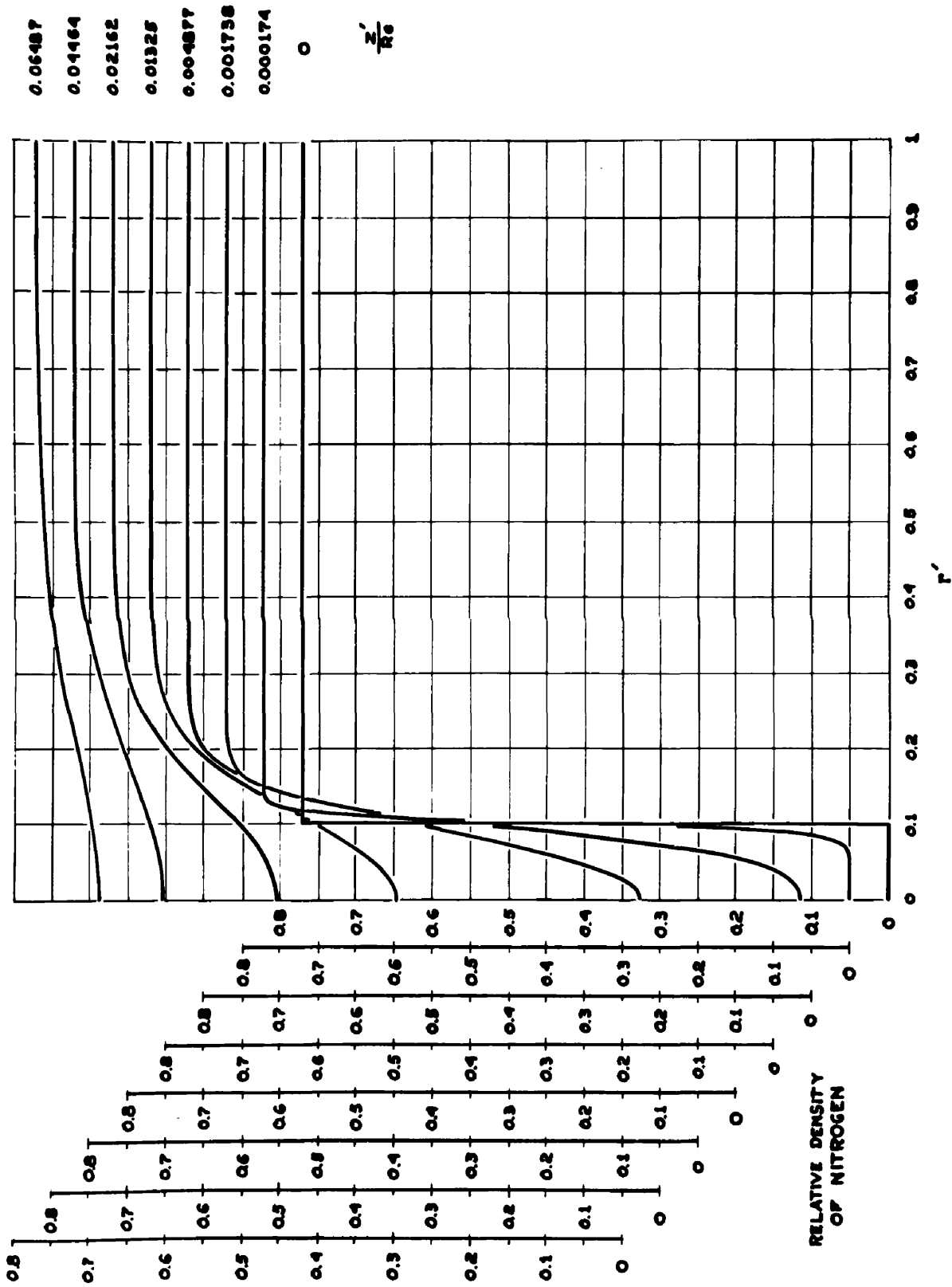


FIGURE 32

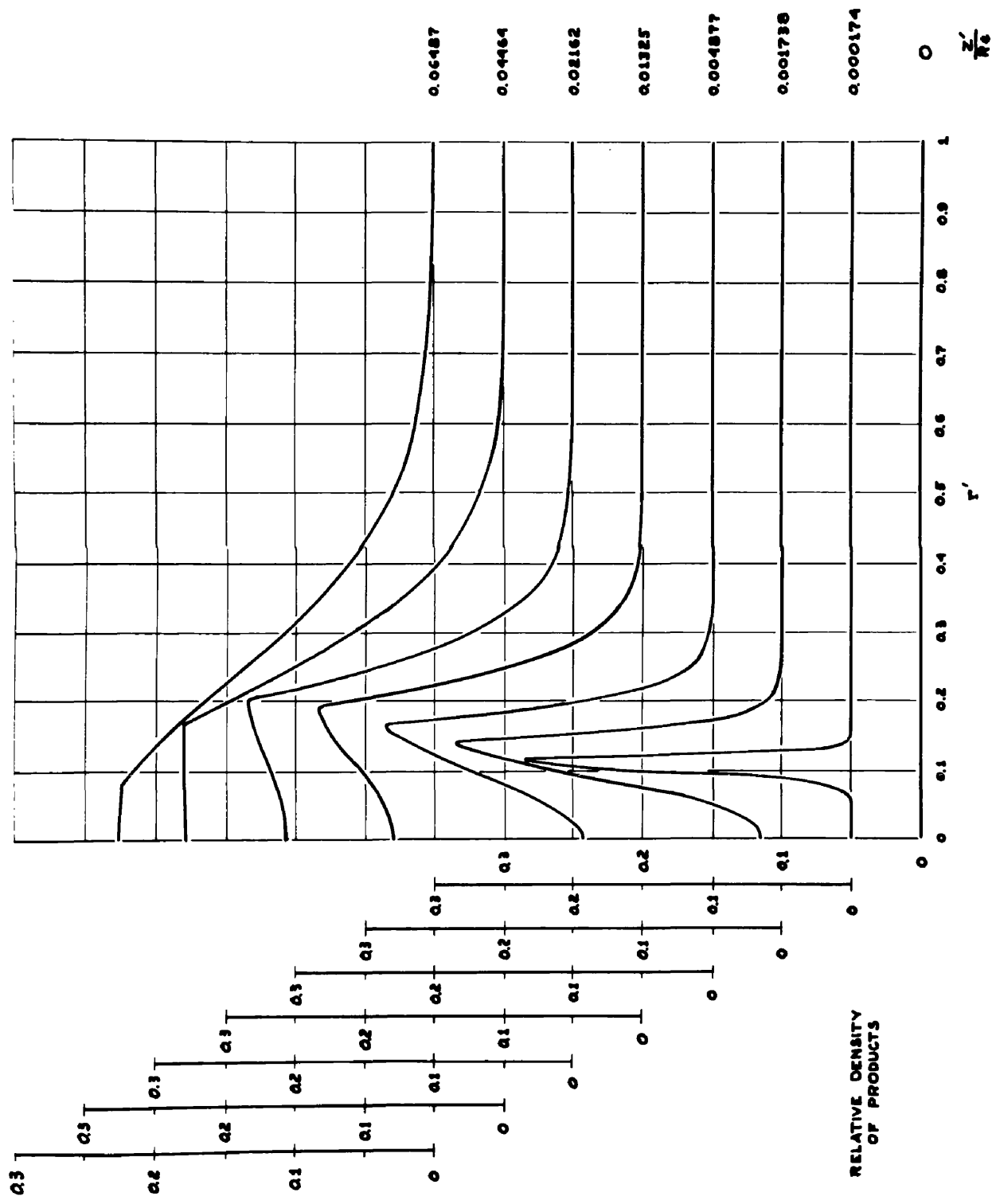


FIGURE 33

When the methane distribution at one of these positions is selected as a reference and matched to the same distribution of Figure 30, the remaining experimental profiles match the theoretical profiles at corresponding positions along the axis. This result indicates that the fuel in the central portion of the flow essentially remains intact, and only undergoes the pyrolysis reactions in the neighbourhood of the flame surface itself.

Although this solution is quantitatively as poor a representation of the terminal flame height as that of Burke and Schumann, the excellent agreement at a relative scale with the results of Smith and Gordon suggest that the shortcoming is a scale factor.

There is still the possibility, then, that the deviation from the experimental results is due to the effect of temperature upon the coefficients of diffusion. This method offers a potential means of investigating these effects, since the heat conduction equation is of the same form as the diffusion equation. Therefore, the temperature of the gases can be treated as simply another species which is diffusing at its own rate. It is then simple enough to introduce the characteristics of the temperature dependence of the coefficient of dynamic viscosity into the computer techniques. It is possible that the system with a variable coefficient of diffusion will not satisfy the conservation of mass condition, so that a secondary test for this condition is advisable.

This method is successful enough that it could as well be employed to examine various proposals of intermediate reactions, which could then be checked against actual measurements of the type made by Smith and Gordon.

CHAPTER 10

CONCLUSIONS

The studies which are the subject of this thesis arose from the question posed by Barr<sup>(2)</sup> concerning the effect of the momentum exchange processes upon the enclosed laminar diffusion flame.

In the process of examining the fundamental equations which apply to such flames it was established that the axial length ( $z$ ) must appear in the group  $z/R(Re)$  in the solution of any or all of the controlling equations when axial transport phenomenon can be ignored. This is well illustrated in Appendix I by the dimensionless form of the momentum equation, one of the controlling equations. From this, it follows that the experimental observation of the flame height being described by  $z/R(Re)$  equal to a constant cannot support any particular solution of some, or one, of these equations, and quantitative agreement between the theoretical and experimental coefficients of this  $z/R(Re)$  relationship is necessary to verify a theoretical solution.

The attainment of an axially symmetrical system, which is usually a requirement in the solution of equations in a cylindrical coordinate system, was found to be one of the most difficult conditions to satisfy experimentally. It was therefore necessary to make reservations concerning the experimental results of Barr and the preliminary experimental results of the author pending verification with a flow system which satisfied these conditions. There is an indication that departure from this condition does influence the results.

It was found experimentally that the simplification of no radial pressure gradients, which made a particular method of treatment of the

Navier-Stokes equations possible, was not applicable to the flame development region where the initial velocity distributions were those of concentric fully developed flows. The condition of no radial pressure gradients was later found to be permitted by the Navier-Stokes equations when there are established radial components to the velocities at the initial plane of the transition. However, the radial pressure gradients observed experimentally are necessary in the initial stages of transition when the flow entering this transition is without radial velocity components.

The restricted studies of the velocity profiles in the transition region indicate that there is a 'memory' of the initial velocity profiles, that is the form of the initial velocity profiles is reflected in the subsequent profiles. The 'horns' on the flame profiles near the smoke point indicate that there is this 'memory' of the initial velocity profiles, even in systems where there are large accelerations due to the energy release within the flame.

The use of published property values to evaluate the Reynolds numbers of commercial fuels can lead to errors greater than any average experimental errors. The method of determining the relative Reynolds numbers of the various fuels employed in this study can be improved considerably, but some such direct experimental method is necessary if a valid correlation of results is desired.

Of the many forms the flame within an enclosed system can assume, the stable premixed double cone is the most interesting. This flame appears to be associated with a stable toroidal flow pattern at a short

distance above the tip of the fuel supply tube, and the processes of material transport in such a mixing system are a potential field of study in themselves.

The floating laminar flame, which is only possible in an axially symmetrical system, indicates that the dynamic transition length from the concentric fully developed approach profiles is of the same order of magnitude as that from an initially constant velocity profile. These flames are a potential tool for an extended study of the relative cold interdiffusion of various fuels and oxidants. At the same time they can be employed to study the burning velocity, since such flames, when near the tip of the constraint tube, can be readily extinguished and the velocity of flow at the point of equilibrium can be directly measured. These flames appear particularly attractive for burning velocity studies, since the flame itself is remote from any heat sinks, and the event of the burning velocity exceeding the flow velocity results in a standard diffusion flame rather than the dangerous 'flash-back' of premixed burners.

The experimental observation of the terminal flame height being represented by a constant value of  $z/R(Re)$  for dynamically similar experiments establishes that the molecular transport processes can be considered as purely radial. The principal variable for the conditions of dynamic similarity is the air-fuel ratio, and all of the other dynamic variables have an influence upon the curves of flame height as a function of the air-fuel ratio. The effect of several of these variables is opposite to that which would be indicated by the behaviour of the flame height as a function of the air-fuel ratio. One of the most striking of these effects is the effect of the chemistry of the system. This effect has brought

the laminar diffusion flame the 'whole circle'; whereas, at one time these flames were abandoned by the Chemist as being adequately described by the diffusion process, the study of the molecular transport effects has brought the problem back to being, at least partially, one of a chemical nature.

The method of multiple species interdiffusion does not provide a quantitative improvement over the Burke and Schumann solution when the room temperature properties are employed to determine the coefficients of the equations. However, the degree of flexibility introduced by this method makes it possible to extend such investigations to include the effects of variable coefficients and internal equilibrium reactions.

BIBLIOGRAPHY

1. BURKE, S.P.                      Diffusion Flames, Industrial and Engineering  
SCHUMANN, T.E.W.                Chemistry, Vol. 20, No. 10, 1928.
2. BARR, J.                         Diffusion Flames, Their Structure and  
                                      Stability. A thesis submitted to the  
                                      University of Glasgow, 1954.  

Summaries of the thesis are reported as follows:-

  - (a) Diffusion Flames, Fourth Symposium of Combustion,  
1953, page 765.
  - (b) Length of Cylindrical Laminar Diffusion Flames,  
Fuel, Vol. 33, No. 1, 1954.
3. GOUDIE, G.O.                    Unpublished experiments at the University  
                                      of Glasgow, 1956.
4. HAWTHORNE, W.R.,                Diffusion in Laminar Flame Jets, Third  
HOTTEL, H.C.,                      Symposium of Combustion, 1949.
5. WOHL, K.,                        Diffusion Flames. Third Symposium of  
GAZLEY, C.                         Combustion, 1949  
KAPP, N.M.
6. GAYDON, A.G.,                    Flames, their structure, radiation and  
WOLFHARD, H.G.                    temperature. Chapman and Hall, Ltd. London,  
                                      Second edition, 1960.
7. SHAPIRO, A.H.                    Friction Factor in the Laminar Entry Region of  
SIEGEL, R.                         a Smooth Tube. Proc. of the 2nd U.S. Congress  
KLINE, S.J.                         of Applied Mechanics, 1954.
8. CHAPMAN, S.                      The Mathematical Theory of Non-uniform Gases,  
COWLING, T.G.                      Cambridge, at the University Press, 1939.
9. HATTORI, H.                        Stability of Diffusion Flames. Proc. of the  
TAKEUCHI, K.,                       eighth Japanese Congress for Applied Mechanics,  
YOSHIZAWA, K.                      1958.  
HIRAMOTO, T.  
HOSHINO, T.
10. SMITH, S.R.,                     The Methane Diffusion Flame, Journal of  
GORDON, A.S.                       Physical Chemistry, Vol. 60, 1956.

APPENDIX I

The complex set of simultaneous differential equations known as the Navier-Stokes equations describe the conditions of conservation of momentum and conservation of mass which must apply to any element of fluid in a flow system. Several particular analytic solutions of these equations have been accomplished after considerable simplification.

Subsequent to the solution of the Navier-Stokes equations by Hagen and Poiseuille, it was discovered that the fluid entering a straight tube underwent a transition from a potential flow state (that mode of flow described by the simplified Bernoulli form of the energy equation only) to the viscous flow state described by the Hagen-Poiseuille solution. As a consequence, the mode of flow described by the Hagen-Poiseuille solution is now referred to in the literature as the fully developed flow condition, and considerable effort has been devoted to attempts to describe the transition from the potential flow state to the fully developed flow state.

In this transition region the magnitude and the direction of the velocity vectors is continually changing; the magnitude of the pressure gradient vectors is continually changing; and the angle subtended between these two vectors is continually changing, thus precluding the possibility of an algebraic solution. Experimental evidence indicates, however, that there are no radial components to the pressure gradient vectors.

The applicable set of Navier-Stokes equations for an axially symmetrical system are:

$$\rho r v \frac{\partial v}{\partial z} + \rho r u \frac{\partial v}{\partial r} - r \frac{\partial p}{\partial z} + \frac{\partial}{\partial r} \left( \lambda r \frac{\partial v}{\partial r} \right) = r v \frac{d\rho}{dt} \quad \dots \text{la}$$

$$\rho r v \frac{\partial u}{\partial z} + \rho r u \frac{\partial u}{\partial r} - r \frac{\partial p}{\partial r} + \frac{\partial}{\partial r} \left( \lambda r \frac{\partial u}{\partial r} \right) = r u \frac{d\rho}{dt} \quad \dots \text{lb}$$

With the associated equation for the conservation of mass:

$$\frac{\partial}{\partial z} (\rho r v) + \frac{\partial}{\partial r} (\rho r u) = 0 \quad \dots \text{2}$$

where

$\lambda$  = the viscosity of the fluid,

$v$  = the velocity in the 'z' direction (the coordinate along the axis of the tube),

$u$  = the velocity in the radial direction,

$r$  = a general radius, assuming the value 'R' at the wall of the tube,

$\rho$  = the density of the fluid,

$p$  = the local pressure,

$t$  = time.

The boundary conditions to be applied to these equations for the development section are:

The conditions do not vary with time.

The density of the fluid is constant.

The viscosity of the fluid is constant.

The cross sectional area of the tube is constant.

All velocities at the wall of the tube are zero (the fluid is viscous).

As a result of the constant area condition the fully developed state is represented by the velocity 'u' becoming zero, and the velocity 'v'

at any radius remaining constant with 'z'.

The Von Mises transform, viz.,

$$\left. \frac{\partial \omega}{\partial z} \right)_r = -\rho u r \quad \dots 3a$$

$$\left. \frac{\partial \omega}{\partial r} \right)_z = \rho v r \quad \dots 3b$$

satisfies the conservation of mass equation with an identity by defining a stream function ' $\omega$ '.

When the Von Mises transform, the condition of steady state and the condition of no radial pressure gradients are applied to the equations 1a and 1b they become:

$$\left. \frac{\partial \omega}{\partial r} \right)_z \left. \frac{\partial v}{\partial z} \right)_r - \left. \frac{\partial \omega}{\partial z} \right)_r \left. \frac{\partial v}{\partial r} \right)_z = r \frac{dp}{dz} - \frac{\partial}{\partial r} \left( \gamma r \frac{\partial v}{\partial r} \right)_z \quad \dots 4a$$

$$\left. \frac{\partial \omega}{\partial r} \right)_z \left. \frac{\partial u}{\partial z} \right)_r - \left. \frac{\partial \omega}{\partial z} \right)_r \left. \frac{\partial u}{\partial r} \right)_z = -\frac{\partial}{\partial r} \left( \gamma r \frac{\partial u}{\partial r} \right)_z \quad \dots 4b$$

The left hand terms of the equations 4a and 4b are respectively the Jacobians in the variables,  $\omega$ , v, z and r; and  $\omega$ , u, z and r. One of the identities of the Jacobian (J) of the set of variables  $\omega$ , x, z and r is the relationship:

$$J = - \left. \frac{\partial x}{\partial z} \right)_\omega \left. \frac{\partial \omega}{\partial r} \right)_z$$

which reduces the equations 4a and 4b to:

$$\left. \frac{\partial v}{\partial z} \right)_\omega = \frac{\partial}{\partial \omega} \left( \gamma v r^2 \rho \frac{\partial v}{\partial \omega} \right)_z - \frac{1}{\rho v} \frac{dp}{dz} \quad \dots 5a$$

$$\left. \frac{\partial u}{\partial z} \right)_\omega = \frac{\partial}{\partial \omega} \left( \gamma v r^2 \rho \frac{\partial u}{\partial \omega} \right)_z \quad \dots 5b$$

At any particular 'z' equation 3b is integrable and as a result of the constant area condition results in:

$$\int_0^R \rho v r dr = \frac{1}{2} \rho v_1 R^2 \quad \dots 6$$

where  $v_1$  is the average velocity across the cross section.

This relationship provides a form of the conservation of mass equation in terms of the velocity 'v' only, so that the transition can then be treated by equations in terms of 'v' (equations 5a and 6) and those equations in terms of 'u' (equations 3a and 5b) can be neglected.

If, however, the 'u' velocity fields determined from equation 2, corresponding to two adjacent 'v' velocity fields satisfying equations 5a and 6, do not satisfy equation 5b, the non-zero residue from equation 5b must represent a radial pressure gradient term, which is in contradiction to the initial assumptions.

For any particular value of 'z' there is one, and only one value of  $dp/dz$  which will provide a subsequent 'v' velocity profile which satisfies equation 6 and is connected to the 'v' velocity profile at 'z' by equation 5a for all values of ' $\omega$ '. Thus, for some interval  $\Delta z$ , sufficiently small for the mean value theorem to be applicable, a convergent iterative procedure can be established to determine the unique value of  $dp/dz$  over this interval.

This iterative method for the determination of the pressure gradient can be used when the transition is treated by the numerical method of finite differences. In order to have a range of validity to a solution by numerical methods the problem must be treated in a dimensionless form.

If the notation ( $x'$ ) is used to denote the dimensionless form of a variable the following definitions may be set down:

$$\begin{aligned} r &= r'R \\ z &= z'R \\ v &= v'v_1 \\ u &= u'v_1 \\ p &= p'2\rho v_1^2 \\ \omega &= \omega' \rho v_1 R^2 \end{aligned}$$

In their dimensionless forms equations 5a and 6 are:

$$\frac{1}{2} \frac{\partial v'}{\partial (z'/Re)} \Big|_{\omega'} = \frac{\partial}{\partial \omega'} \left( v' (r')^2 \frac{\partial v'}{\partial \omega'} \right) \Big|_{\frac{z'}{Re}} - \frac{1}{v'} \frac{dp'}{d(\frac{z'}{Re})} \dots\dots\dots 7$$

$$\int_0^1 v' r' dr' = \frac{1}{2} \dots\dots 8$$

It is convenient, however, to express equation 8 in terms of the transform space ( $\omega'$ ), which also provides a means of evaluating ( $r'$ )<sup>2</sup> for the numerical evaluation of equation 7, thus:

$$(r')^2 = \sum_0^{\omega'} \Delta (r')^2$$

where  $\Delta (r')^2$  is determined by:

$$\Delta \omega' = \int_{\omega'_1}^{\omega'_2} \bar{v}' r' dr' = \frac{1}{2} \bar{v}' \Delta (r')^2 \text{ or } \Delta (r')^2 = \frac{2\Delta \omega'}{\bar{v}'}$$

where ( $\bar{v}'$ ) is the average dimensionless velocity over the interval  $\Delta \omega'$ .

In the difference form of the transform variable  $\omega'$  equation 8 becomes:

$$\sum_{i=1}^{i=n} \frac{2\Delta\omega'_i}{\bar{v}'_i} = 1 \quad \dots 9$$

where (n) is the number of  $\Delta\omega'$  intervals between  $\omega' = 0$  and  $\omega' = 1/2$ .

In order to satisfy the boundary condition that  $v'$  at the wall is equal to zero,  $\bar{v}'$  over the interval adjacent to the wall must be  $1/2$  when the value of  $v'$  at all other  $\omega'$  is one, which forces all the other velocities  $v'$  to be greater than one to satisfy equation 9. This, then, establishes a minimum core velocity for which the iterative method is applicable and which will be dependent upon the size of the intervals chosen for the  $\omega'$  coordinate.

An approximate method must be used in the region between the initial constant velocity across the cross section and that region where the iterative method can be used. Insomuch as the velocity  $v'$  at the wall is zero, and the velocity  $v'$  at a small distance  $\delta$  from the wall, no matter how finely the space is divided, is the mean velocity of the stream, the whole of the curvature of the velocity profile must take place within the distance  $\delta$  in the initial stages of development. A semi-boundary layer approach was prompted by this situation, but rather than assuming a shape to the curve of the velocity profile between the wall and the constant velocity section, a curvature was assumed only for a small element of mass flow adjacent to the wall, the curvature of the remainder of the velocity profile being determined from equation 7. In order to determine the velocity gradient in the  $z'$  direction at a distance  $\delta$  from the wall a synthetic 'slip' velocity was assumed at the wall. This velocity was

determined from equation 9 as that velocity which results in a mean velocity over the interval  $\delta$  which satisfies equation 9. The velocity profile over this interval  $\delta$  was assumed to be a hyperbola passing through zero at the wall, and having the same slope as the calculated velocity profile at the distance  $\delta$  from the wall, this eventually reduces to a linear velocity gradient which is of the form used in the finite difference method. The pressure gradient was then assumed to be twice the velocity gradient at the wall determined from this hyperbola. In order to avoid confusion this method is referred to as the boundary film method.

#### NUMERICAL METHODS

The method of finite differences is based on the mean value theorem of the calculus and assumes that the variables and all of their derivatives can be represented by some 'mean' value over the finite interval chosen for the independent variable. This assumed property is the exact condition of the mean value theorem provided the interval is sufficiently small. Problems are then typically treated by assigning a fixed interval size to all independent variables. The problem set forth herein is such that the gradients of the dependent variables assume all values between zero and near infinity for various values of the independent variables, and it was thus advisable on the basis of computer size and speed to devise a variable interval size along the direction of both independent variables.

This variable interval size made it possible to determine the errors introduced by assuming linear gradients of the dependent variables where the errors are a function of the interval size, by comparing the calculated gradients with the analytic gradients for the fully developed

flow case. The error in the pressure gradient term was found to be  $4\Delta\omega'/\Delta r'$ , and the error in the viscous stress term of equation 7 was found to be  $1/\sqrt{1+(\Delta v'/v')^2}$  where both of these factors are multipliers of the calculated terms.

The finite difference method provides an exact solution to the equations employed if, on altering the interval size, the numerical results are not altered. This test was employed on the 'boundary film' method for both co-ordinates. Alternate interval sizes in the 'z' direction were employed at several places along the development path without any changes in the results. Since the variation in the velocity profile occurs in the region adjacent to the wall, and the variation in the ' $\omega$ ' direction was such that the intervals were made smaller as the wall was approached, the elements adjacent to the wall were altered in size without altering those near the centreline of the tube. This alteration produced some interesting results, in that all the boundary film results were identical provided the velocity at the distance  $\delta$  from the wall was in excess of a given value, after which deviation from this initial coincident behaviour followed a pattern related to the velocity at the distance  $\delta$  from the wall. These results emphasised that the velocity profiles obtained by this method, to be used in initiating the successive approximation method, could only be approximate.

The method of successive approximations deals with a system described by an analytically exact set of equations rather than an approximate set of equations. The successive approximations are carried out for each finite increment taken along the axis until the pressure gradient for the increment converges to an exact value. This is

accomplished by (a) assuming that the pressure gradient is that due to the velocity gradient at the wall; (b) calculating from equation 7 the resultant velocity profile; (c) calculating the error in the integral of equation 9; and (d) correcting the assumed pressure gradient by this error factor. The procedure is repeated with this new pressure gradient as the assumed pressure gradient until the integral equation 9 is satisfied within the accuracy of the computer. This method resolves, therefore, to a finite difference solution for a succession of velocity profiles with a successive approximation solution for the pressure gradient, the second unknown, at each increment of the finite difference procedure.

The path of development, that is the sequence of values assumed by all of the variables as the (z) direction is traversed, will be dependent upon the initial velocity profile chosen and the location chosen for this profile. However, as the fully developed state is approached, the various paths must become coincident as they are identical from the point of complete development onward. If various velocity profiles, only slightly different from the desired profile, are chosen at some point along the development path, then, the paths of development from these profiles will become coincident with the path of the desired profile quite rapidly. Thus, if several different intermediate velocity profiles are assumed, and at some point the paths of development from these assumed profiles become coincident, the coincident path is that of the ideal development.

The successive approximations method was tested with three different intermediate velocity profiles (the approximate profiles being obtained from the results of the boundary film calculations). In all

cases the paths converge to a common path within a decade (for example in  $z'/Re$  increasing from  $10^{-9}$  to  $10^{-8}$ ) and remained on this common path three to four decades, when the calculations were terminated. One of the initial profiles was that for a finer ' $\omega$ ' grid to test the validity of the finite difference method for this grid size. The common path for the different grid sizes both verifies the finite difference method as a valid method, and verifies the common path as the desired development path.

The result of all the calculations is shown in Figure 34 of the pressure gradient as a function of the axial distance ( $z$ ). In this region of the development the pressure gradient is the most sensitive variable in the system. The various departures from a common path of the results from the boundary film method can be clearly seen. The fact that the common path of convergence of the successive approximation method is the extension of the common path of the boundary film method indicates that the initial approximations of the boundary film provide a valid solution and, further, suggest the equation of this path, common to the two methods, as the means of obtaining the initial velocity profiles for the successive approximations method.

----- BOUNDARY FILM  
——— SUCCESSIVE APPROXIMATION

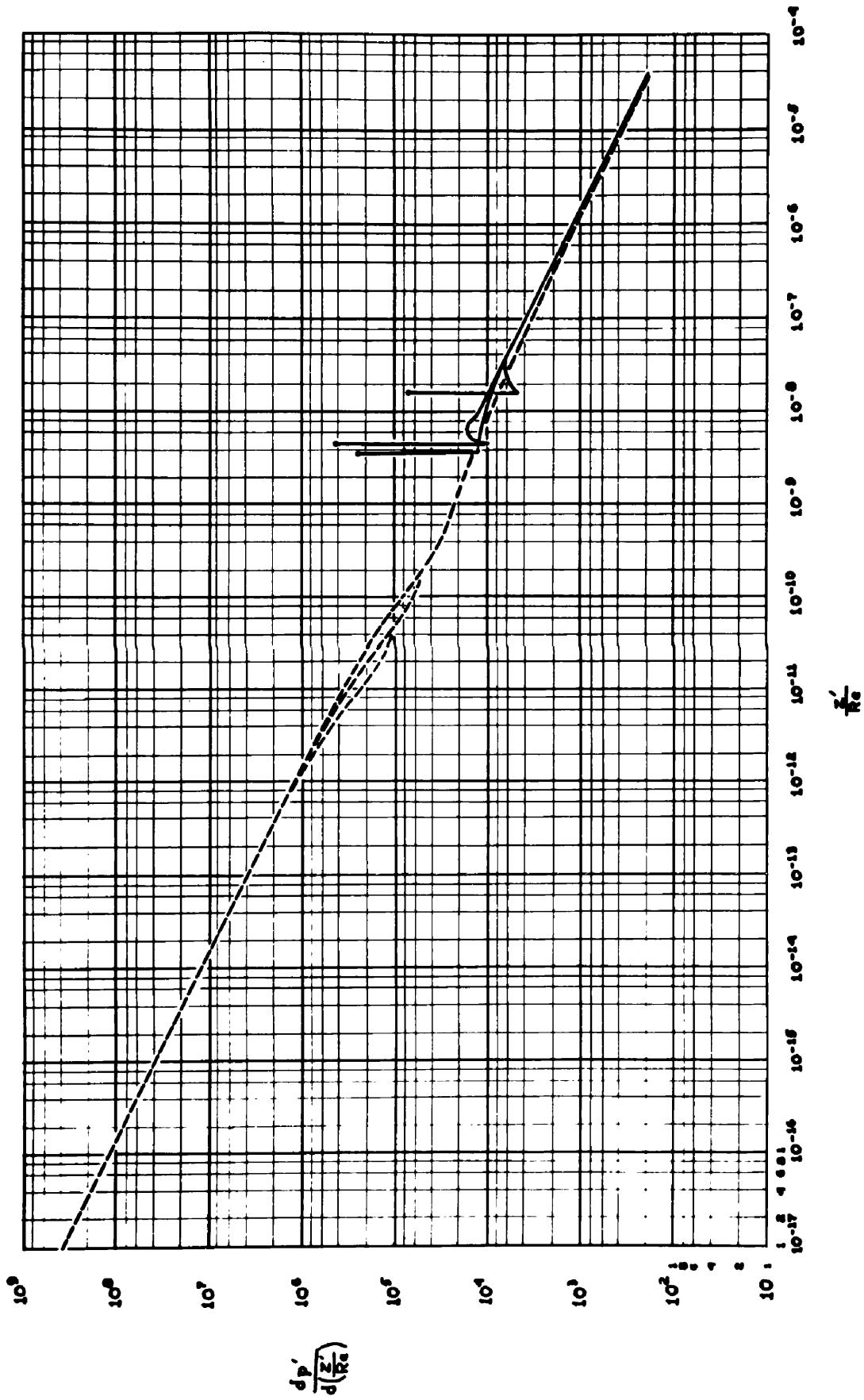


FIGURE 34